1986

Pullout and creep of geosynthetics in a soil matrix.

Newman, R. Scott.

PULLOUT AND CREEP OF GEOSYNTHETICS IN A SOIL MATRIX

A Special Research Problem

Presented to

The Faculty of the School of Civil Engineering

by

R. Scott Newman

In Partial Fulfillment

of the Requirements for the Degree

Master of Science in Civil Engineering

December 1986

GEORGIA INSTITUTE OF TECHNOLOGY
A UNIT OF THE UNIVERSITY SYSTEM OF GEORGIA
SCHOOL OF CIVIL ENGINEERING
ATLANTA, GEORGIA 30332

PULLOUT AND CREEP OF GEOSYNTHETICS IN A SOIL MATRIX

A Special Research Problem

Submitted to:

The Georgia Institute of Technology

Department of Civil Engineering

in partial fulfillment of the requirements

for a Master of Science Degree

in Civil Engineering

R. Scott Newman

December 1986

ABSTRACT

Factors influencing the creep and confined tensile strength of geosynthetics in soil are evaluated. State-of-the-art, current practices and methods used to evaluate confined creep and tensile strength are investigated. A Large-Scale Pullout / Creep Device, which improves upon previous instrumentation, is designed and results of analyses are presented. A complete laboratory analysis of the soil media is presented to further quantify results.

ACKNOWLEDGEMENTS

A successful project is rarely the work of one person. This research project has been no exception. In the course of this investigation several people played key roles. Although my words here cannot do justice for all the hard work put forth, I do want to acknowledge the assistance and offer my heartiest thanks.

Both my undergraduate and graduate studies could not have been completed without the constant praise and encouragement provided to me from my parents.

To Mr. Ken Thomas, engineering technician, and Mr. S. Scott, Machinist, Ken's insight into the practical side of the project led to an improved and more streamlined device. Further, he was always available and willing to lend a hand. Scotty provided expert machining of the various components for the device. The precice fabrication of the pullout box led to smooth and successful operation.

To Gary Risse and Ken Whitehead, research assistants, Gary assisted with the development of the device and provided superb engineering assistance. Ken provided the electronics knowledge required to coordinate the data aquisition system. His time and diligence resulted in the system coming on line when needed.

To Dr. Neil Williams for sharing with me his invaluable experience in the field of geotechnical engineering, his time and thorough review of this paper.

To Dr. Q. Robnett, who provided his insight on the operation of the device and offered constructive changes.

To Dr. R.C. Bachus for providing a thorough review of the manuscript which served to markedly increase the value of the paper.

Professor George Sowers has been a source of constant inspiration for the students at Georgia Tech. His lectures were a constant source of enjoyment as they provided me with certain tools from which I was able to improve my engineering skills.

To all of the graduate students, who didn't allow me to loose my sense of humor and, in the thick of it all, made sure I knew that it was going to get much worse.

To the U.S. Navy, for providing me this opportunity.

Finally, to my wife, Kimiko and my two sons, Joseph and Eric, without whom this year, and my life, would be much less.

TABLE OF CONTENTS

LIST OF FIGURES

LIST OF TABLES

INTRODUCTION

Scope and Objectives

The purpose of this research investigation is to design and fabricate a Large Scale Pullout/Creep Device (LSPCD) to isolate and evaluate the parameters which affect the restrained pullout and creep properties of extensible earth reinforcement. The analyses presented in this report focus on the interaction of a polyester geogrid material in a cohesionless soil under a variety of boundary conditions.

A review of existing equipment and methodology is presented for constrained tensile strength and constrained tensile creep analyses. The analytical methodology for the LSPCD is presented for both types of analyses. Evaluation of geosynthetic strain is discussed and several alternatives for equipment design are evaluated in the investigation.

Terminology

The evaluation of control, index and performance properties of geosynthetics requires a wide variety of equipment designed specifically for the application. New test methods are developed and existing methods revised

almost on a daily basis. For these reasons, it is imperative to define the terminology used in the report. The following definitions are based on the most recent usage in current literature.

The term geosynthetics refers to the broad spectrum of materials which, when used in conjunction with soil or rock materials, improve the newly formed composite system. Geosynthetics are further divided into three areas; geomembranes, geotextiles and geogrids.

A geomembrane, according to the American Society of Testing and Materials (ASTM), is defined as: "Any impermeable membrane used with foundation, soil, rock, earth, or any other geotechnical engineering-related material, as an integral part of a man-made project structure or system." Geomembranes, due to their low permativity and high resistance to deterioration, may be used in conjunction with natural materials to improve the performance of waste containment facilities.

Geotextiles refer to a knitted, woven or non-woven permeable textile used with foundation, soil, rock earth or any other geotechnical engineering-related material, as an integral part of a man-made project, structure or system (Christopher and Holtz, 1984).

Geogrids are materials which include webs, nets and formed plastic sheets, used in an application where reinforcement of the soil structure is desired.

The ability of a geosynthetic to perform is a function of its mechanical and chemical properties. A variety of test methods have been devised to define these properties. Unfortunately, the influence of test method significantly affects the property being analyzed. Three approaches are used in geosynthetic property analysis; control tests, index tests and design or performance tests.

Control tests are used by manufacturers to help ensure that the minimum roll properties are achieved or surpassed. Common control tests would be density and thickness determinations, specific gravity and in some cases unconfined tensile tests may be performed. As no standard procedures exist for control testing, comparisons of data between manufacturers is extremely difficult. Consequently, control test data are used to evaluate uniformity and consistency of the geosynthetic and should not be used in actual design.

Index tests are used to evaluate material properties under controlled laboratory conditions. Unconfined tensile strength and tension creep analyses

are index tests which may be performed for several geosynthetics under identical testing conditions. These analyses may be compared to evaluate the relative performance of these geosynthetics. However, the boundary conditions used to perform index tests do not approximate field conditions. Consequently, index test values are not appropriate for design. To properly account for soil-geosynthetic interaction, design or performance tests must be utilized.

In design or performance tests, the geosynthetic is tested under conditions which simulate field condi'ions. Soil type, confinement and loading conditions, and complex stress transfer mechanisms which may exist between the soil and reinforcement are duplicated by the performance tests. The mechanisms of this load transfer are not well understood and may vary between geosynthetics. Since performance tests allow conditions of the load transfer mechanisms to be modeled, the results of the analyses may be used in design.

A geosynthetic structure may fail by internal or external means. External failure results from the overall instability of the structure. Possible failure mechanisms for a retaining structure are those due to sliding, overturning or insufficient bearing capacity.

In foundation applications external failure would refer to bearing capacity failure. These mechanisms may be analyzed using conventional approaches. Three possible internal failure modes exist for geosynthetic reinforced structures; creep, pullout or rupture.

Polymeric materials and soils exhibit time dependent behavior. The time dependent deformation of a specimen under constant tensile stress is termed creep. In comparison to soils, geosynthetics are highly susceptible to creep. Fortunately, the confinement of the geosynthetic by soil reduces creep effects. Confined tensile creep is the creep of a material constrained by a frictional medium.

If an increasing load is applied to a geosynthetic confined by soil, the geosynthetic will eventually fail. The failure will be by either pullout, rupture or a combination of the two.

If the frictional forces and passive resistance are insufficient to constrain the geosynthetic, and the forces developed within the geosynthetic are less than those required for failure, the geosynthetic will slide along the soil interface. This sliding is termed pullout. Sliding may also occur along some weak plane within the soil matrix. In this failure mode, also

termed pullout, the geosynthetic is of sufficient strength to withstand the imposed load and is of such geometry to arrest the soil matrix forcing the soil to yield at a location removed from the soil-geosynthetic interface. However, if the geosynthetic is sufficiently anchored, and the stresses within the geosynthetic exceed the confined tensile strength of the material, the geosynthetic will fail. Such failure is termed rupture.

Confined tensile strength is defined as the tensile strength of the geosynthetic while constrained in a frictional media.

Background

The efforts of man to improve soil conditions to his advantage are well documented. Early efforts such as the use of reeds for adobe bricks and roadway stabilization have been in use for centuries and are in fact still extensively used in South America, Southeast Asia and many developing nations (Christoper and Holtz, 1984).

Henri Vidal (1978), who pioneered the use of reinforced earth in the 1960's, brought to the forefront the advantages of tension reinforcement to improve

substandard soil conditions. Vidal began by placing alternating layers of pine needles within sand. The slope of the composite structure was observed to be noticeably steeper than the pile of sand without the pine needles. These simple observations led to more complex investigations and finally to the patent of what Vidal termed "reinforced earth".

The concept of reinforced earth consists of four primary elements:

1. A soil backfill which provides the overburden pressure, the compression resistance and shear strength;
2. Tensile reinforcing strips which form a pseudo coherent material with the soil to resist tensile stresses;
3. Facing elements at boundaries which prevent ravelling; and,
4. Mechanical connections between reinforcements and facing elements (Lee, 1978).

One of the major concerns with reinforced earth relates to the long term durability of the metal strips.

The recent gain in popularity of geosynthetics in the construction industry comes as no surprize. In several applications geosynthetics have proven their ability to substantially improve upon existing soil

conditions at a site. Geosynthetics can be used in a variety of situations and have been found to be reliable, durable and easy to install. Figure 1-1 details some common reinforcement applications for geotextiles. Unfortunately, as with most engineering materials, adequate testing lags behind application.

Due to the lack of performance test data, engineers have been forced to utilize the results of index tests in the design of geosynthetic reinforced structures. Index tests provide relative comparisons between geotextiles yet provide very little information regarding the in-soil performance. As a result of the lack of in-soil data and the fact that there exists very little long-term field data, designs have typically been somewhat overconservative or based on simple (hopefully conservative) designs. As will be discussed, the influence of soil on the performance of the geosynthetic is significant. It stands to reason that to properly evaluate soil-geosynthetic interaction in-soil tests must be performed under conditions which simulate field conditions.

Creep, the slow continuous deformation of a material under conditions of constant stress, is a phenomena of great interest in all engineering materials. Creep behavior of geosynthetics has been the

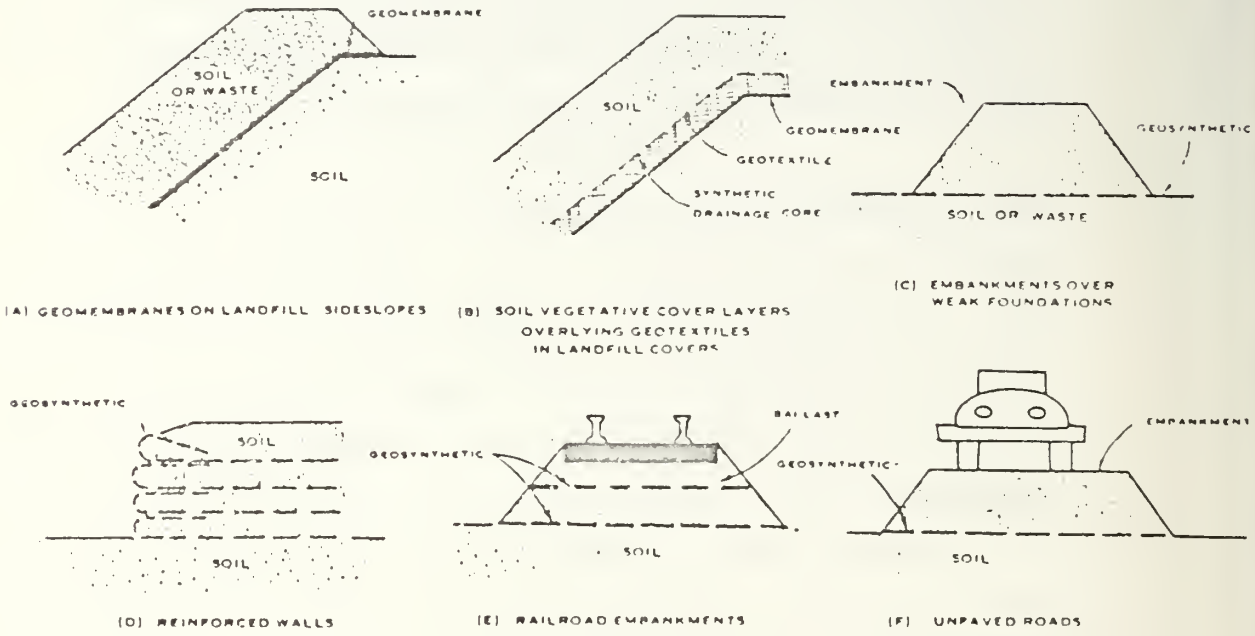

FIGURE 1. COMMON EXAMPLES OF THE APPLICATION OF INTERFACE FRICTION PROPERTIES FOR THE DESIGN OF GEOSYNTHETICS IN ENGINEERING WORKS

Figure 1-1. Common Reinforcement Applications.
(After Williams and Houlihan, 1987).

subject of particular attention (Coleman and Knox, 1957, Findley et al, 1976, Holtz et al, 1982, Onaran and Findley, 1965 and Shrestha and Bell, 1982). In certain applications such as the reinforcement of embankments for hazardous wastes or retaining wall reinforcement, catastrophic results may follow should the structures be designed without regard to creep as a design parameter. On the other hand, excessive conservatism reduces the cost effectiveness of geosynthetic reinforcement and may make other design alternatives appear more attractive. As the analytical methods improve, more accurate design data will lead to improved design methods and a better understanding of the mechanics of the soil/geosynthetic interaction. This in turn will provide the basis for less conservative, more cost effective use of geosynthetics in engineering works.

FACTORS INFLUENCING PULLOUT AND CREEP OF GEOSYNTHETICS IN A SOIL MATRIX

Introduction

Creep of geosynthetics in a soil matrix is a complex process involving both the interaction of the soil and geosynthetic at the interface and the transfer of shear stress to both the soil and the geosynthetic. Since soils are composed of discreet particles, particle reorientations occur under the sustained loads (Williams, 1986).

Along the plane of maximum shear stress in the soil, bond strengths vary due to the nature of the particle contacts. Shear stresses are typically mobilized along an area of weak bonds followed by a transfer of load to the stronger bonds. The progressive nature of this shear stress distribution results in the process of creep (Christensen, et al, 1964). Mitchell (1964) postulated that the change of creep rate with time may be attributed to changes within the soil structure for a given soil.

Total creep strain can be divided into two components, volumetric creep and deviatoric creep. Volumetric creep, or secondary compression, results from a hydrostatic stress condition under drained conditions. When shear stresses are imposed on the specimen deviatoric

strains may develop. If the shear stresses are less than those required for yield to occur, the material will deform as a function of time. The strain at constant deviatoric stress is the deviatoric creep. In the design of geosynthetic reinforced structures, changes in shape or deflection and deformation of the structure are functions of the deviatoric creep of the system (Williams, 1986).

The factors which influence creep or the deformation phenomena of soils at subfailure stress conditions also influence the failure of the soil at larger stresses (Mitchell, 1964). Analysis of deformation or equilibrium conditions at a state of stress just below failure is termed limiting equilibrium analysis and extremely important in civil engineering design. In addition, with the knowledge of the stress state which produces failure, creep analyses may be performed. The creep analyses are performed at specified stress levels, where the stress level is defined as a percentage of that stress required to produce failure.

The most common relationship used to describe the failure envelope in soils is the Mohr-Coulomb theory which states that:

$$\tau_f = c + \sigma_f * \tan\phi \qquad (2.1)$$

where: τ_f - shear stress at failure (FL^{-2}),

c - cohesion intercept (FL^{-2}),

σ_f - normal stress (FL^{-2}) and,

ϕ - angle of internal friction (-)

The equation is an approximation of the yield function for soils and may be in terms of either total or effective stresses.

A more complete form of equation (2.1) has been suggested by Mitchell (1976) to be of the form:

$$\text{Shearing Resistance} = F(e,\phi,C,\sigma',H,T,\varepsilon,\dot{\varepsilon},S) \qquad (2.2)$$

where:

e - void ratio

C - composition

H - stress history

T - temperature

ε - strain

$\dot{\varepsilon}$ - strain rate

S - structure

The introduction of a polymeric material into the soil structure results in additional factors which must be considered in the analysis of the system. These additional factors are summarized in Table 2-1.

TABLE 2-1

FACTORS INFLUENCING PULLOUT AND CREEP
OF GEOSYNTHETICS IN A SOIL MATRIX

SOIL CHARACTERISTICS

- Angle of internal friction
- Void ratio / Relative density
- Stress state
- Soil structure
- Stress History

GEOSYNTHETIC CHARACTERISTICS

- Geosynthetic type
- Interface friction angle
- Adhesion
- Tension Elastic Modulus
- Surface roughness
- Geometry and Construction
- Confined Tensile Strength

EXTERNAL FACTORS

- Temperature
- Ground Water
- Time
- Construction methods
- Ultraviolet exposure
- Chemical degradation

Soil Characteristics

Void Ratio / Relative Density

The void ratio of a soil is defined as the ratio between the volume of voids (Vv) and the volume of solids (Vs), expressed as:

$$e = Vv/Vs \qquad (2.3)$$

Void ratio is strongly influenced by particle size distribution and shape. Terzaghi (1960)* hypothesized that shear force is directly proportional to the area of contact between soil particles. Since creep may be viewed as deformation under stress states less than those that produce failure, contact area would appear to have a proportionate affect on creep behavior. Figure 2-1 demonstrates the effect of contact area.

The effect of void ratio on angle of internal friction for a concrete sand is shown in Figure 2-2. As void ratio is reduced, interparticle contacts between the

*Actually introduced in his 1925 publication, Erdbaumechanik, which marked the first systematic treatment of soil mechanics and its applications to foundation engineering and related fields of civil engineering.

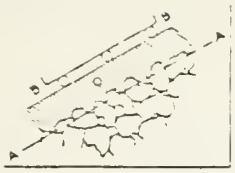

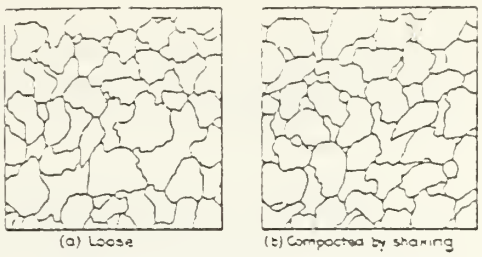

FIG. 2. LOOSE AND COMPACT STRUCTURE OF SAND
(Diagrams traced from aluminum disc apparatus)

Figure 2-1. Particle packing and void ratio (after Terzaghi, (1960).

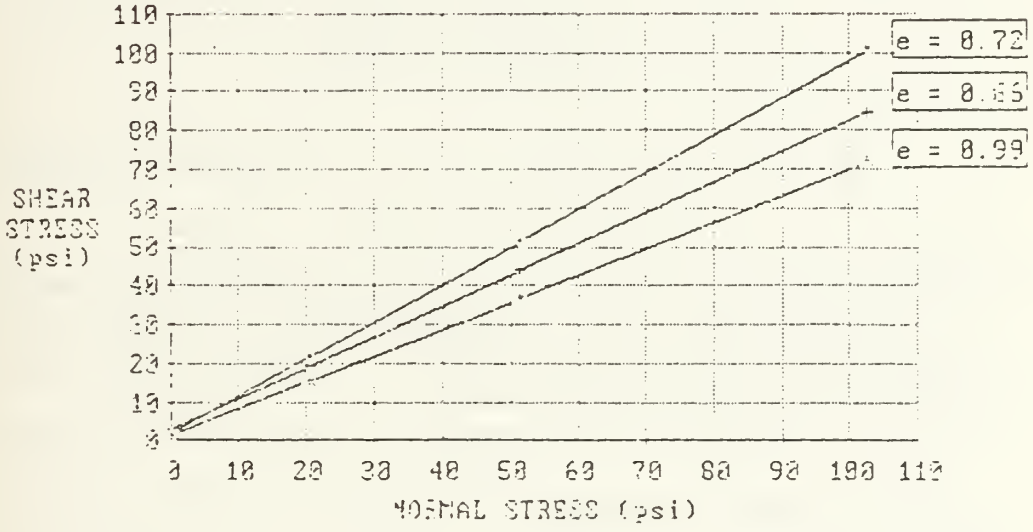

Figure 2-2. Effect of void ratio on friction angle and shear stress for a concrete sand.

soil particles increase. This results in higher strengths for the specimens at lower void ratios.

The relative density, Dr, is frequently used to characterize the density of a granular soil:

$$D_r = \frac{e_{max} - e}{e_{max} - e_{min}} \quad (100\%) \qquad (2.4)$$

where: e_{min} - void ratio of soil in densest state

e_{max} - void ratio of soil in loosest state

e - in-place void ratio

Evaluation and control of the void ratio is a major factor both in design and creep analyses. In order to sustain repeatable results in creep testing the soil should be placed and compacted in a uniform manner to assure uniform distribution of the soil.

Angle of Internal Friction

The angle of internal friction or friction angle, ϕ, occurs from the interparticle shear resistance inherent to soils. The angle of internal friction integrates all those factors of resistance to grain displacements:

distortion, crushing, shifting, rolling, sliding, and dilation, and those factors which depend on the soil mineral, the particle angularity, roughness, sphericity, gradation and relative density (Sowers, 1979).

Rowe (1962) concluded that throughout most of the range of void ratios, three components contributed to the strength of granular materials: 1) strength mobilized by frictional resistance or basic mineral friction; 2) strength required to rearrange and reorient soil particles; and 3) strength developed by energy required to cause expansion or dilation of the material. Figure 2-3 displays how these three factors relate to relative density, void ratio and friction angle.

The friction angle describes a limiting condition for the soil at a given stress state. The interface friction angle, designated δ, which is the frictional resistance to deformation at the soil/geosynthetic interface, is related to the angle of internal friction of the soil. In creep investigations a specimen is loaded to a specified stress level, followed by the observation of strains and strain rates. Stress level is a specific percentage of the stress required to produce failure given similar boundary conditions.

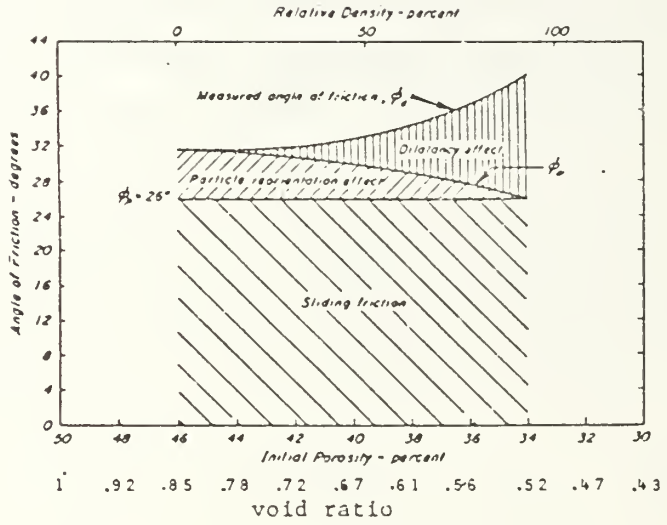

Figure 2-3. The three components contributing to the strength of granular materials (after Rowe, 1962).

Soil Structure

Soil structure includes the combined effects of fabric, composition and interparticle forces.

Fabric refers to the arrangement of particles, particle groups and pore spaces within the soil. In soils, particles vary in size. Gradation of a soil mass is a quantitative evaluation of the variety of particle sizes. In the case of well graded soils, or those which have a smooth distribution of sizes within some range, the trend will be towards higher densities and lower void ratios than soils with uniform gradation (i.e. particles all nearly the same size). The most common method for determining particle size for granular materials is by sieve analysis (ASTM D4220-63). Meta-stable structures, which result from certain depositional situations for granular soils can have very high void ratios (Holtz and Kovaks, 1981). In compacted soils, a meta-stable structure would not be encountered.

Composition refers to the mineralogy of a soil and is a major factor in determining the shape, the texture and susceptibility to weathering of a granular soil (Lambe and Whitman, 1969).

Angularity refers to the degree of sharpness of the

edges and corners of a particle. Since dense sands dilate during shear (Casagrande, 1940), angularity will result in an interlocking of the soil particles amplifying the frictional characteristics of dense and loose sands. Rounded particles will reduce shear strength and, all other factors being equal, will result in more creep than a matrix composed of angular particles.

For most granular soils, interparticle forces play only a minor role in behavior. Exceptions are found in extremely fine quartz dust and the micas (Lambe and Whitman, 1969).

Duplication of soil structure in experimental investigations will lead to more reliable predictions of field response. This may be accomplished by following standard procedures of compaction and control of moisture conditions, which can be repeated from test to test.

Stress State

The effective stress, which is the difference between the the total stress and the neutral stress, represents that part of the total stress which produces measurable effects such as compaction or an increase in shearing resistance (Terzaghi, 1948). Skempton (1960) pointed out that this was actually a close approximation which produced little error

even in partially saturated soils.

As a soil structure is loaded the pore water initially takes on all of the load resulting in an increase in pore pressure. If drainage is allowed the pore water escapes from the imposed pressure and the soil gradually supports more of the load. These analyses are frequently accomplished in a triaxial chamber.

In the testing of geosynthetics in soils it is important to simulate both the field drainage and stress conditions.

Geosynthetic Characteristics

Geosynthetic Type

Soil reinforcement by polymeric materials is primarily accomplished through the use of geotextiles and geogrids.

Geotextiles are generally classified by their manufacturing process. The three main geotextile types are woven, nonwoven and knitted. Polyesters, both woven and nonwoven, are commonly used in reinforcement applications.

Woven geotextiles are composed of two sets of

parallel yarns interlaced to form a planar structure. The weave pattern is generated by the method in which the two sets of yarns are interlaced.

Nonwoven geotextiles are formed from fibers arranged in an oriented or random pattern to form a planar structure. The fibers are bonded by chemical, thermal or mechanical means.

Knitted geotextiles, which are formed by the interlocking of a series of loops into a planar structure, are infrequently used in reinforcement applications.

Geogrids are manufactured by two different methods of polyester, polypropylene or polyethylene polymers. These geogrids are typically produced by a drawing technique. This is accomplished by first extruding the polymer in a molten form through a die, and mechanically stretching the material as it cools. This results in orientations of the hydrocarbon chains within the structure. This orientation results in increased tensile strength and improved ductility of the thermally extruded polymers.

Geogrids may be produced by two-dimensional elongation of perforated sheets. This process results in a planar material with strands oriented in the machine direction and ribs oriented in the cross direction. The

junctions of the strands and ribs are called joints.

An alternative method is to overlap strands of extruded polymer in perpendicular directions and bond the two strands by heat welding or interweaving. Junction strengths are generally appreciably lower than than the junction strengths of the geogrids produced by the two-dimensional elongation processes.

The magnitude of the shear strength developed at the soil/geosynthetic interface is a function of the degree of interlocking between the soil and the geosynthetic. Geogrids, due to their open nature, result in high shear resistance due to the development of passive resistance during deformation. Strength of the junctions is critical since very little shear resistance is developed along the smooth polymer face. Specimen geometry, therefore, plays a significant role in interaction behavior (Christopher and Holtz, 1984).

Interface Friction Angle / Adhesion

Friction along the interface between soil particles and a geosynthetic develops in a manner similar to the development of friction in granular media. This frictional resistance is termed interface friction. Figure 2-4 displays some common mechanisms for the development of friction

a. Deformation at the interface

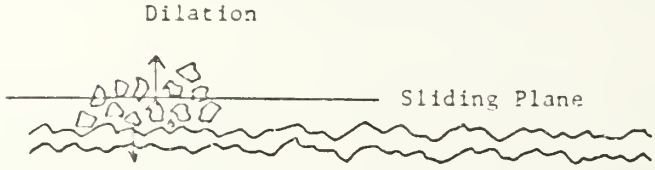

b. Dilation

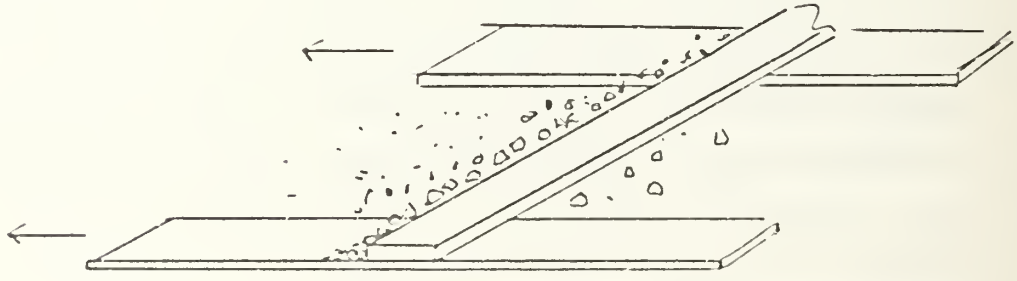

c. Passive Resistance

Figure 2-4. Shear mechanisms of confined geosynthetics

between geosynthetics and soil particles. The effects of specimen geometry and surface roughness are apparent.

As Vidal discovered in his early experiments, a pseudo-cohesion develops within the reinforced soil mass (Vidal, 1978). The interface friction angle and cohesion for a geosynthetic can be determined by measuring the shear resistance at different values of normal stress in a manner similar to the direct shear test for soils. The maximum shear stress is plotted against normal stress as shown in Figure 2-5. This results in the Mohr envelope of failure for the reinforced system. The angle produced by this failure envelope is termed the interface friction angle, δ, and the shear stress intercept, the adhesion, a.

Tensile Elastic Modulus

The stress strain relations for polymeric material are often nonlinear and highly dependant on the boundary conditions and the strain rate. Three different means are used to obtain various geosynthetic moduli; initial tangent, offset and secant (Christopher and Holtz, 1984). The tensile elastic modulus, regardless of the method used in its definition, provides an indication of geosynthetic strength. To properly account for the effects of soil confinement the results from confined tensile tests should be utilized.

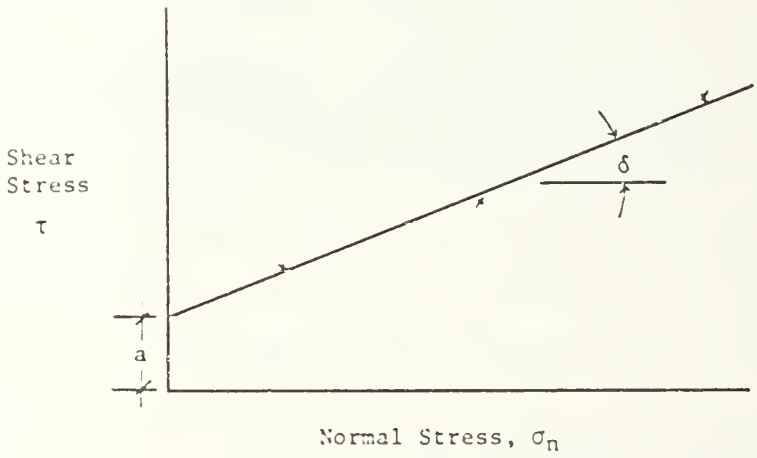

Figure 2-5. Failure envelope for geosynthetic reinforced soils.

Confined Tensile Strength

The effects of interface friction provide for increased moduli and strengths when compared to isolation tests (Bell and Hicks, 1980). Both the confinement provided by the soil and the frictional resistance result in these increased strength properties. The composite system, comprised of the soil and the geosynthetic, acts as one. The geosynthetic "binds" to the soil through friction and interlocking mechanisms and therefore draws upon the relatively high compressive strength of the soil and the geosynthetic provides a transfer mechanism for the tensile forces created in the structure. The confined tensile strength may be determined by several methods including, direct shear tests, pullout tests and triaxial tests.

External Factors

The soil-geosynthetic system may be strongly influenced by external factors. Environmental concerns include ground water and its movement, surface water and erosion, animal burrows, plant and tree growth, temperature, ultraviolet exposure and chemical degradation. The effect of most of these factors will result in increased deflections as a result of the decreased area of influence of the geosynthetic; a transfer of stress to those areas which are less effected by the environmental factors and; if left

unchecked these factors may result in structural failure. Further, since creep by definition is time dependent, the designed lifespan of the structure is also of concern. Improper construction practices will also severely affect the adequacy of the structure.

Temperature

According to ASTM test procedures, testing on geosynthetics is specified to be carried out at 21 ± 02 °C. Creep tests performed in this range are typically conservative since most soil temperatures fall well below 21 °C. In cold regions, where soil temperatures fall substantially below 21 °C, geosynthetics may become less flexible and more brittle. At temperatures above the specified range, a reduction in modulus and tensile strength may be expected (Bonaparte et al, 1984). Therefore, when extreme temperatures may be expected, the analyses should be performed at temperatures representative of field conditions. In addition, in those instances where actual conditions are known, tests could be modified to account for even slight temperature variations.

Ground Water

Because the geosynthetic is an inclusion within the soil matrix, water will tend to flow along the

soil/geosynthetic interface. In addition, seepage forces may result in localized damage and possibly collapse of the structure. If hydrostatic pressures develop with the corresponding reduction of effective stress, catastrophic failure may occur from the loss of friction at the interface of the soil and geosynthetic. Seepage forces may disturb the soil particle distribution in the area around the geosynthetic and result in a corresponding reduction in the interface friction. As discussed, the area along the interface is an area of high shear stress within the soil. The deliterious effects of seepage forces and flow can be minimized through proper allowances for drainage in design, however, it is normally impractable to prevent all flow from occuring within the structure.

Ultraviolet Exposure

The polymers used in geosynthetic fabrication are subject to degradation when exposed to ultraviolet (UV) radiation. Of the common polymers, polypropylene and polyethylene have the poorest UV stability while polyester has a greater resistance (Bell and Hicks, 1980). The UV radiation may result from natural sunlight or warehouse fluorescent lighting. Since geosynthetics are normally covered with soils, UV degradation is not a concern unless protection is not provided while in storage (on the project site or in a warehouse), or the material is left exposed

after any construction sequence. Stability of the fabrics may be increased by the addition of carbon black to the material during the extrusion process. Chemical stabilizers are less frequently used to inhibit UV degredation.

Chemical Degradation

Most of the polymers associated with geosynthetics are highly resistant to degradation in the normal chemical environment found in soils. However, in unusual situations such as those found in hazardous waste containment facilities or locations where the pore water is extremely acidic or basic, special evaluations must be made to determine the effects of these conditions. To ensure compatability of the geosynthetic expected to be exposed to a particular chemical the EPA 9090 test is commonly conducted. This test involves the immersion of geosynthetic specimens in baths surrounded by the particular leachate. The baths are set at temperatures of 22 °F and 50 °F. The two specimens are tested at the end of 30, 60, 90 and 120 days for weight, thickness, tensile strength, tear strength and seam strength.

Construction Methods

Material placement errors and damage as a result of poor construction practice and the lack of adequate quality

control may result in unexpected deflections within the reinforced structure.

Relatively few contractors have gained substantial competence in the construction of geosynthetic reinforced structures. Therefore, close supervision by design engineers is imperative until the materials become more common in the construction industry.

Factors of safety are commonly employed both to insure against unknowns of soil geosynthetic response and to circumvent damage and minor placement errors inherent in the construction of the structure. In soil reinforcement, a factor of safety of 1.5 is commonly used. However, the use of safety factors of 1.2 to 1.4, combined with the conservative design approaches, often yields adequately safe designs.

TECHNOLOGY ASSESSMENT

Introduction

Of the factors which influence the conservative design of soil-geosynthetic structures, none is more apparent than the lack of adequate in-soil test data. Furthermore, tests need to be standardized in order to obtain repeatable results from region to region. Three international conferences have been held which have been of great assistance in exposing the lack of uniformity of testing programs and procedures throughout industry and acedemic circles. Through the use of past experimental data and apparatus designs, new equipment is developed which improves upon previous experimental methods and equipment. In addition to the type of equipment, the test conditions under which the stress strain properties are evaluated greatly influence results. Significant factors are temperature, specimen geometry, clamping procedures, specimen size and rate of loading (Christopher and Holtz, 1984).

Two basic types of equipment have been used to determine creep and strength behavior of geosynthetics in soils; the pullout test and the direct shear test. The triaxial test has been used in geotextile-soil frictional analysis only to a limited extent. These tests are depicted

in figures 3-1 and 3-2.

In the pullout test the geosynthetic is encapsulated in a soil mass under a surcharge load. The geosynthetic is pulled laterally at a constant rate of deformation until the geosynthetic fails due to rupture or until translation of the geosynthetic occurs relative to the soil mass.

The direct shear test for soils and geosynthetics is similar to the direct shear test performed on soils. In this test a layer of soil is displaced at a constant rate relative to a geosynthetic.

The triaxial test may be performed by either one of two methods (Christopher et al, 1986). The first method involves the placement of geotextile layers sandwiched between alternating layers of soil followed by testing as in a standard consolidated drained or undrained triaxial test. The second method is a modification of the pullout test. the geosynthetic is displaced in the longitudinal direction relative to the soil in a triaxial cell. Figure 3-2 shows a schematic of the two triaxial tests.

Numerical models have been developed for the creep of polymeric materials and the creep of soils but to date none have been developed for in-soil geotextile creep.

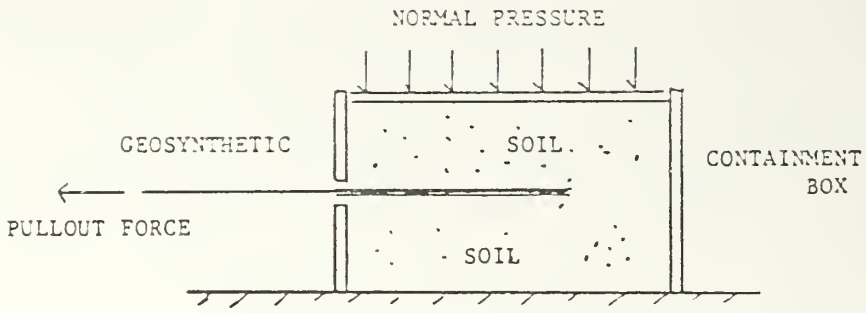

a. PULLOUT TEST DEVICE

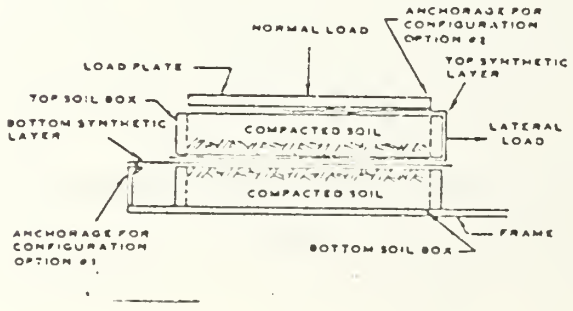

b. DIRECT SHEAR TEST DEVICE (After Williams and Houlihan, 1986)

Figure 3-1. TEST METHODS FOR DETERMINING IN-SOIL STRENGTH CHARACTERISTICS OF GEOSYNTHETICS.

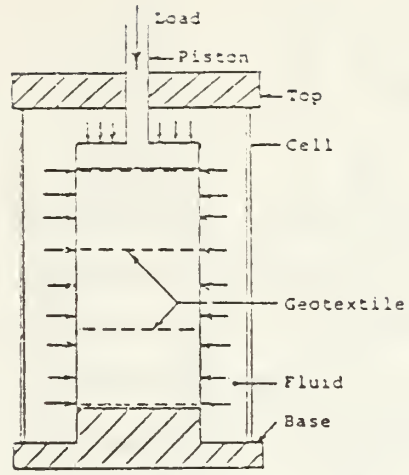

Triaxial Compression Test

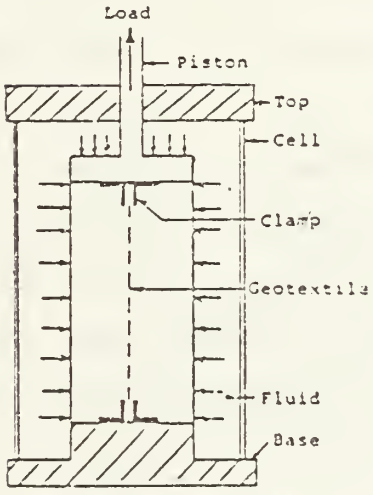

Triaxial Tensile Test

Figure 3-2. Triaxial tests modified to analyze in soil geotextile strengths (after Christopher et al., 1986).

Pullout Tests

In Soil Apparatus

McGown et al. (1982) developed an in-soil test apparatus which is actually a modification to the pullout test since the geotextile is rigidly fixed at both ends. The device allows for the measurement of strains at each end of the fabric through a set of rods which are connected to dial gauges. The schematics for the testing arrangement are shown in Figure 3-3.

One of the difficulties in the pullout test is the measurement of actual strains in the geotextile. Maximum stresses and strains typically develop in the area adjacent to the clamp. The stresses are distributed along the geotextile and reduce to zero at the free end of the specimen (Christopher and Holtz, 1984). Typically average strains are reported indicating an average over the entire gauge length, from clamp to free end. To properly account for the unequal stress / strain distribution a system must be in place to measure the distribution of strain along the length of the geosynthetic.

In the apparatus developed by McGown et al. (1982), strains are averaged over the entire gauge length. Actual strains in the geotextile are therefore probably somewhat

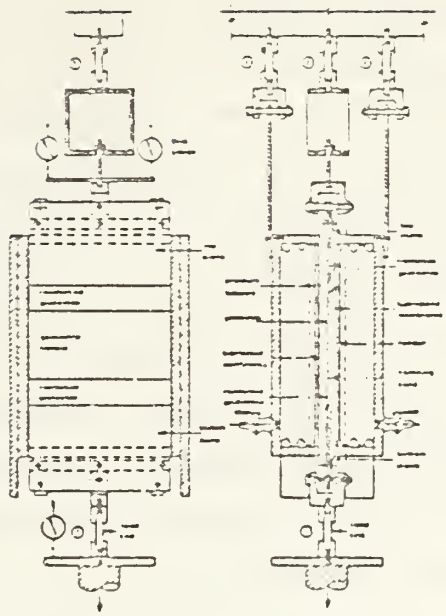

(a) Layout of the apparatus

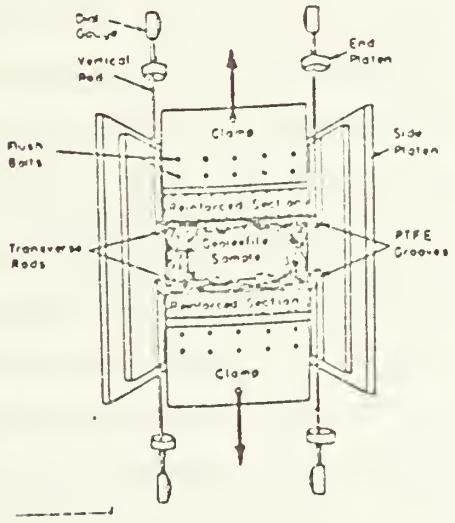

(b) Scheme for measuring extension

Figure 3-3. In Soil Test Apparatus (after McGown et al., 1982).

higher than those reported.

Further, soil cover in this apparatus was limited to 10 to 25 mm (.4 to 1 in.). Not only does this limit the type soils which could be used, the small amount of cover also imposes boundary conditions on the soil adjacent to the geotextile, possibly resulting in soil slippage. Conservative results would most likely be obtained if slippage occured since the friction between soil and geotextile is probably somewhat less than that of the internal friction of the soil.

From the testing program, McGown et al. (1982) concluded that highly structured non-wovens and composite geotextiles' strengths were significantly higher when tested in soil. Yet the wovens, with similar structural arrangements did not exhibit such a change. In fact, there was not observed to be much strength gain in the woven geotextiles. The small value of strength gain in the woven geotextile as compared to tests performed in isolation was attributed to the method in which the woven generates its strength. The researchers explained that strength of the wovens depended on the strength of the aligned tapes which were not greatly affected by embedment in the sand. Extension of this finding to other wovens should not be taken for granted however, since geometry may play an important role in other woven geotextiles.

In an effort to simplify McGown's instrumentation, El-Fermaoui and Nowatzki (1982) developed an extremely simple device.

Sample Box

El-Fermaoui and Nowatzki (1982) developed a sample box to determine in-soil strengths of geotextiles. Testing was performed on nonwoven and woven geotextiles at various confining stresses. The test, shown in Figure 3-4, fixed the one end of the fabric to obtain strength values, preventing pullout from occurring unless the specimen failed by rupture.

Because of the small size of the device, results obtained are subject to significant influence from the imposed boundary conditions. However the results, taken as comparative or index values do indicate that the effect of confining pressure is significant. Caution must be exercised in using the results from this type of test for design as failure mechanisms in the field may be substantially different than those developed in this test.

Comparisons of strength between wet and dry conditions for wovens and nonwovens were also shown. Wet woven geotextiles were shown to have a 30% reduction (at 25% strain) in strength as compared to its dry strength. This

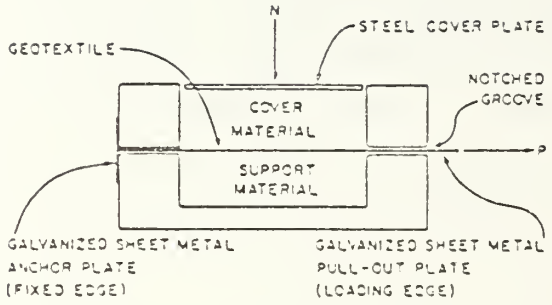

Figure 3-4. Sample Box for geotextile tensile tests (after El-Fermaoui and Nowatzki, 1982).

was attributed to the water retained on the geotextile soil interface due to the rough surface of the woven fabric resulting in slippage. Nonwovens displayed a 5% increase in observed tensile strength. A wick action resulting in an increase of effective stresses and reduction in void ratio of the soil around the geotextile may have resulted in this increase in strength. It would appear that a similar wick action would develop for the woven yet the findings of this paper indicate otherwise.

Zero Span Test

The zero span test, developed by Christopher et al. (1986), utilized surface treated clamps in order to provide simulated soil conditions. The test setup is shown in Figure 3-5. A tension test is performed under specific lateral confinement provided by the clamps.

Average strains are calculated on the geotextile. Actually, strains develop progressively from the center of the specimen to the free ends as load increases. As previously explained, actual strains are probably higher than those reported in their paper.

One problem with the test is that when the clamps move apart, an unconfined length develops in the specimen which would produce necking and premature failure of the

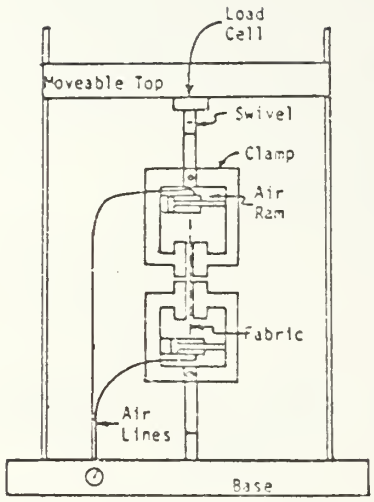

Fig. 3. Zero Span Clamp Setup

Figure 3-5. Zero Span test setup (after Christopher et al., 1986).

specimen. Failure is therefore induced in the specimen in this area of stress concentration.

The measured angle of internal friction would be expected to be less in this device since dilation effects are negated by the simulated soil clamps.

Direct Shear Tests

Soil Fabric Shear Box

A large shear device was used by Myles (1982) to assess the frictional behavior of soils and geosynthetics. The box, depicted in Figure 3-6, provided results for interface shear angles which were somewhat less than the results obtained through the small, conventional type direct shear apparatus. The larger size reduces boundary condition effects and result in more realistic values. However, soil was placed on only one side of the geotextile and the other side of the geotextile was glued to a plate.

Modified Direct Shear Device

A modified direct shear device, developed by Williams and Houlihan (1986), is shown in Figure 3-7. This device is used for the evaluation of interface friction coefficients between soils and geosynthetics (Williams and Houlihan,

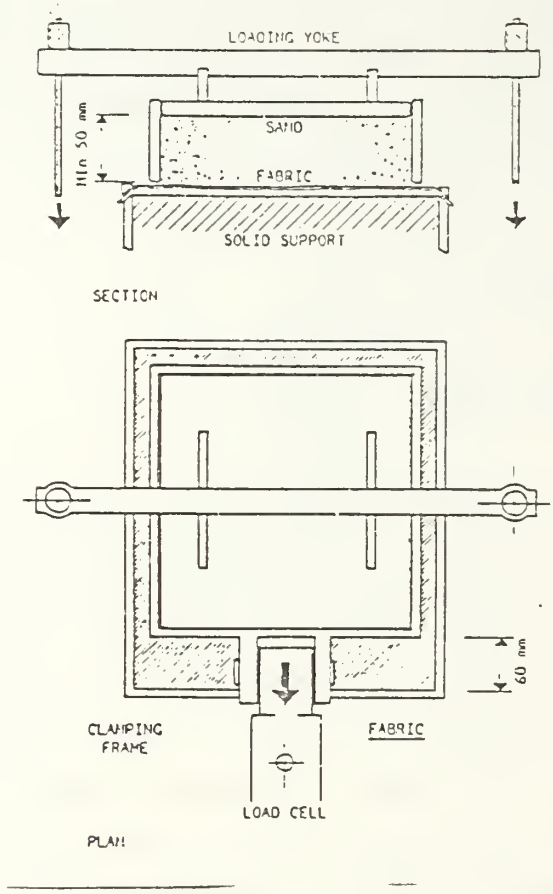

Figure 3-6. Soil Fabric Shear Box (after Myles, 1982)

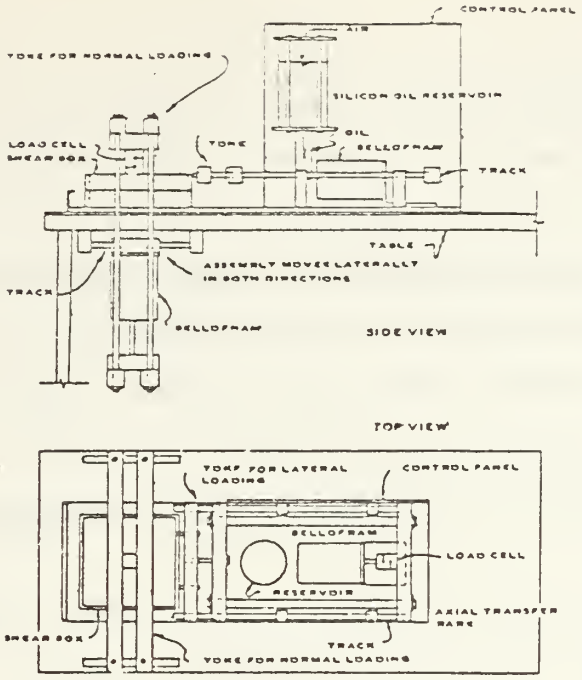

(a) Profile and plan view

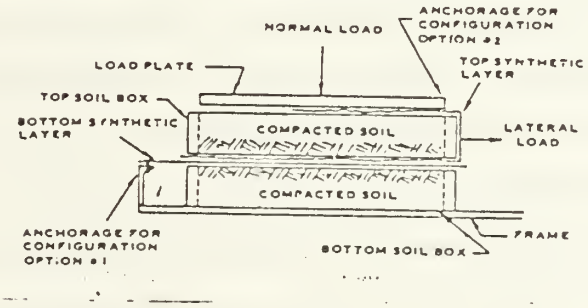

(b) Specimen configuration

Figure 3-7. Modified Direct Shear Device (after Williams and Houlihan, 1986).

1987) and between multiple layers of geosynthetics (Williams and Houlihan, 1986).

The device accomodates specimens with dimensions of 12 by 12 inches placed between soil layers of approximately 2 inches in thickness. The large specimen dimensions limit the boundary condition effects which resulted in some inaccuracy in previous analyses (Myles 1982 and Martin et al. 1984).

Triaxial Test

Holtz et al. (1982) performed triaxial tests on a concrete sand with horizontal geotextile inclusions similar to the setup as depicted in Figure 3-2. The tests were conducted on specimens 36 mm (1.42 in) in diameter and 73 mm (2.87 in) in length, providing a length to diameter ratio of 2:1. The circular geotextile disks were located at the upper and lower third points and on the top and bottom platens. All tests were consolidated-drained (CD) and principal stress difference was calculated using initial specimen cross-sectional area.

From these tests the researchers concluded that, at high relative densities for the sand (Dr = 90%), geotextile properties do not appear to greatly influence stress strain or creep behavior of reinforced samples. Further,

significantly larger axial strains and more creep were observed in the geotextile reinforced sand when compared to the unreinforced sand. The ultimate strength, deformation modulus and angle of internal friction were all increased by geotextile inclusions. These relationships are shown in Figure 3-8.

Numerical Models

Several numerical and rheological models have been developed to analyze the creep behavior of soils. Similar models have also been developed for the treatment of geosynthetic creep. However, no model has yet been developed for the two materials as a composite system. The present challenge then, is to develop a workable model which provides those constitutive relationships and a means for determining the parameters involved with an acceptable degree of accuracy and repeatability. An excellent historical review and analysis of creep behavior is found in Findley et al. (1976).

Three stages of creep have been identified, as shown in Figure 3-9 (a). The application of stress leads to a period of transient creep in which the strain rate decreases with time. This is followed by creep at a constant rate, then, depending on the material, the creep rate may accelerate to rupture. These three stages are called

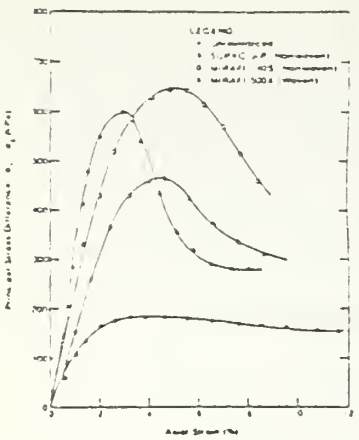

Stress-Strain Relationships for Various Reinforcement Materials (σ_3 = 35 kPa, D_r = 90%)

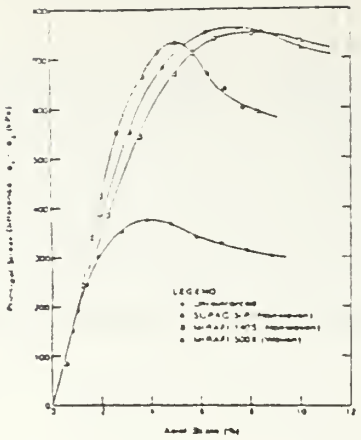

Stress-Strain Relationships for Various Reinforcement Materials (σ_3 = 69 kPa, D_r = 90%)

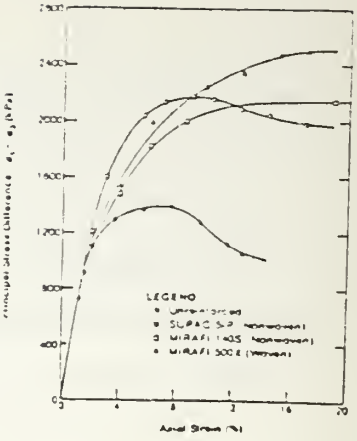

Stress-Strain Relationships for Various Reinforcement Materials (σ_3 = 276 kPa, D_r = 90%)

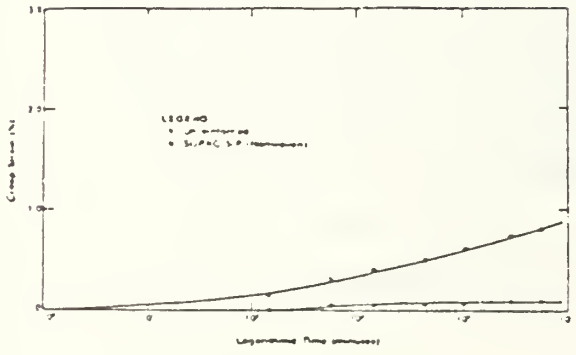

Creep Strain Relationships for Fabric-Reinforced and Unreinforced Triaxial Specimens (σ_3 = 35 kPa, D_r = 90%)

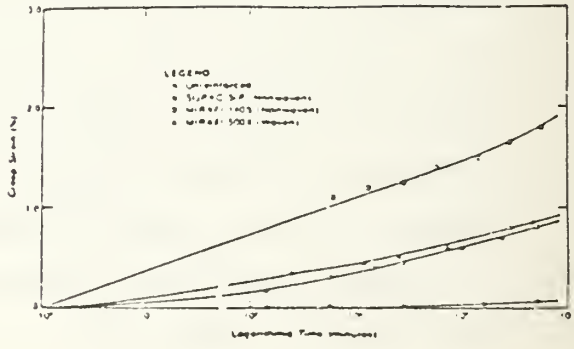

Creep Strain Relationships for Fabric-Reinforced and Unreinforced Triaxial Specimens (σ_3 = 69 kPa, D_r = 90%)

Figure 3-8. Stress strain and creep strain relationships for reinforced and unreinforced triaxial specimens (after Holtz et al., 1982).

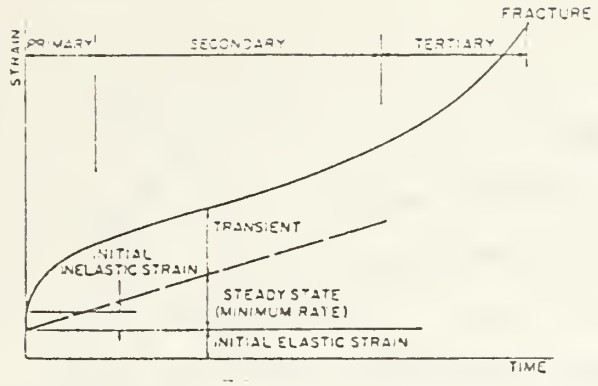

(a) The three stages of creep (after Finnie and Heller, 1959)

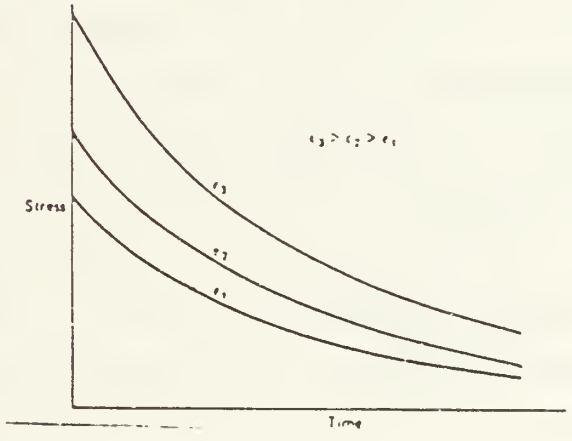

(b) Stress relaxation (after Mitchell, 1976)

Figure 3-9. The stages of creep. Stress relaxation.

primary, secondary and tertiary creep, respectively.

Under conditions of constant strain a system may "relax" to attain a more stable equilibrium condition. This results in a reduction in stress and is termed, stress relaxation. Stress relaxation effects, which are illustrated in Figures 3-9(b) and 3-10, have been studied to a lesser degree than creep and stress relaxation effects are typically ignored in design, resulting in an added degree of conservatism (Bonaparte et al, 1985).

Mitchell (1964) utilized the Rate Process Theory (Glasstone et al., 1941) to relate the shearing resistance of soils in triaxial compression to frictional and cohesive properties, effective stress, soil structure, rate of strain and temperature. By holding constant conditions of structure, strain rate and temperature, Mitchell reduced his equation to the Coulomb equation (equation 2.1). Therefore, creep can be uniquely defined by Mohr-Coulomb for various fixed conditions.

Christensen and Wu (1964) studied the creep of clays using the Rate Process Theory and compared experimental results to the Kelvin-Maxwell rheologic model depicted in Figure 3-11. The model was shown to provide good correlation between experimental data and theoretical expectations.

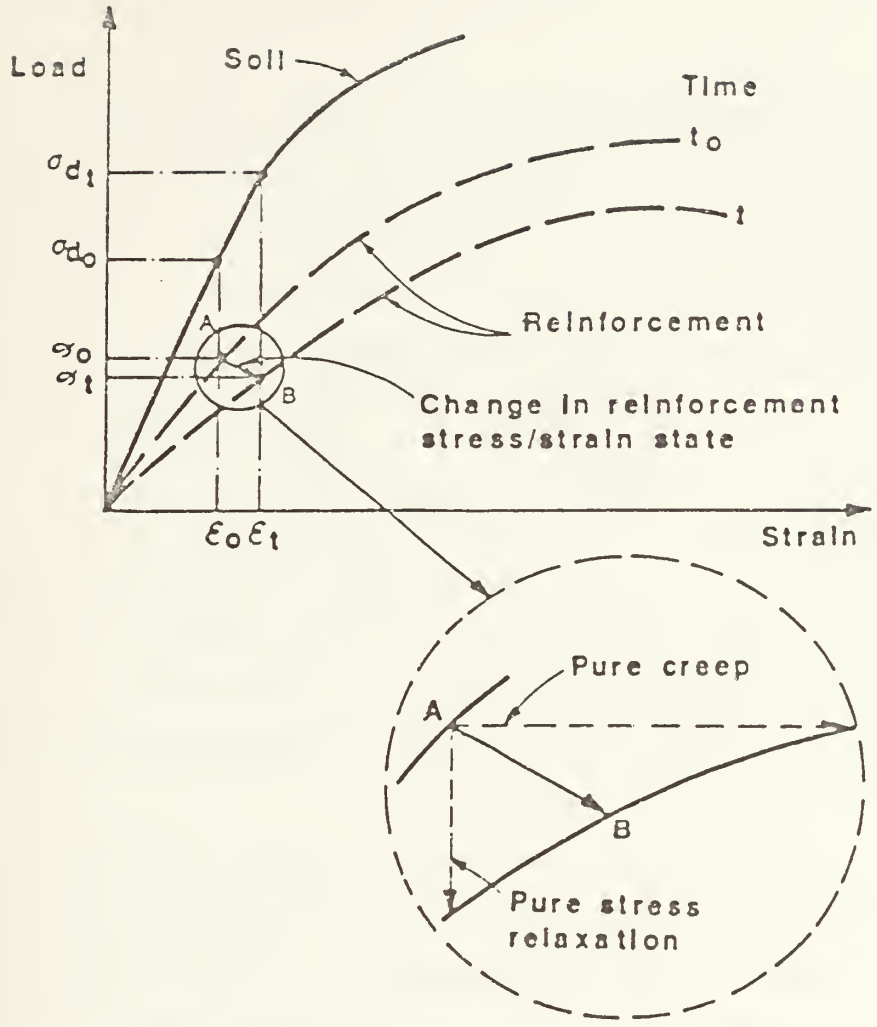

Figure 3-10. Influence of reinforcement creep and stress relaxation on strain developed under working conditions (after Bonaparte et al., 1985).

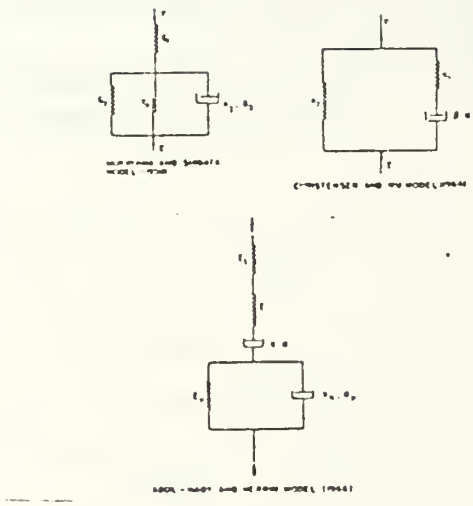

Figure 3-11. Rheological models used in the creep analysis of soils (after Singh and Mitchell, 1968).

Several other rheological models have been proposed, some of which are shown in Figure 3-11.

Singh and Mitchell (1968) stated that the primary limitation of these models is they do not properly predict the exponential dependence of creep rate and creep strain. A three parameter phenemological relationship was used to describe the stress-strain-time behavior of soils within a practical range of stress intensities.

Coleman and Knox (1957) utilized the Rate Process Theory to describe the creep behavior of partially oriented polymeric filaments such as drawn polyester fiber, rayon and cotton. A simplified rate process theory was used which yielded good agreement to experimental results.

Onaran and Findley (1965) employed a multiple integral functional relationship as a constitutive equation for nonlinear creep of a viscoelastic material under combined stress. Kernel functions involving stress terms up to third order were expressed explicitly for combined stress-creep, and experiments were performed to determine the kernel functions. Comparisons between the Multi-Integral Theory and experiment data for the polyvinyl chloride copolymer showed excellent correlation. (shown in Figure 3-12).

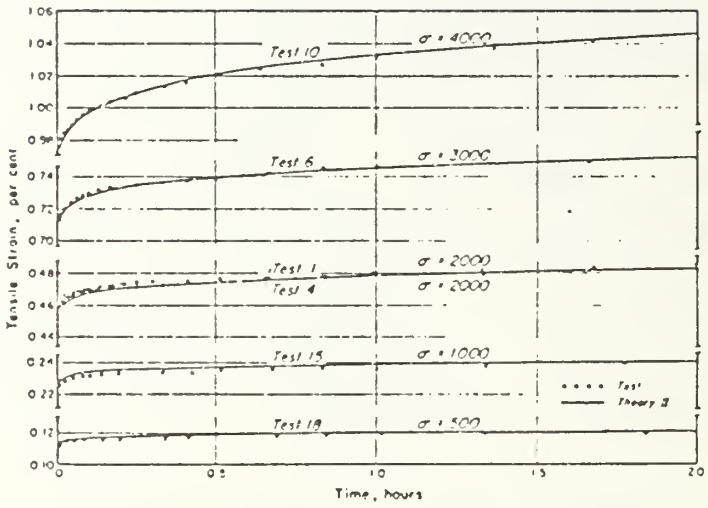

Figure 3-12. Comparisons of Multiple Integral and Hyperbolic Sine Theories to experimental data for materials subjected to pure tension (after Onaran and Findley, 1965).

Shrestha and Bell (1982) compared the creep of woven and nonwoven polyesters and polypropylenes to the Rate Process Theory and a curve fitting, three parameter equation. More reliable results were found through the use of the Rate Process Theory. Results of their work are depicted in Figure 3-13.

The development of a numerical technique is beyond the scope of this study. However, work in this direction is presently underway at the Georgia Institute of Technology.

Conclusions

Several methods exist for the analysis of confined tensile strength of geosynthetics. Many approaches lead to erroneous data due to imposed boundary condition effects of the small devices. A Large Scale Pullout / Creep Device was designed, fabricated and tested to improve upon previous equipment and methodology. The device and testing program are explained in the remainder of this paper.

Stress Levels for Creep Tests

Fabric	Geotextile Construction	Filament	Sustained Load N/cm (lbs/inch)	Load Level* %
NW-1	Nonwoven, Resin bonded	Polyester, Continuous	22 (13)	40
			44 (25)	57
NW-3	Nonwoven, Heat bonded	Polypropylene, Continuous	47 (27)	35
			86 (49)	63
NW-5	Nonwoven, Needlepunched	Polypropylene, Continuous	0.11 (2.2)**	37
			0.20 (3.8)**	57
NW-6	Nonwoven Needlepunched	Polypropylene, Staple	26 (15)	33
			46 (26)	56
W-4	Woven	Polypropylene, Monfilament	126 (72)	31
			180 (103)	44
C-1	Woven, with Needled Fap	Polypropylene, Slit Film	77 (44)	36
			117 (67)	55

*Stress level is the sustained stress as % of the maximum strength.

**Stress normalized to weight per unit area in $\frac{N/cm}{gm/m^2}$ ($\frac{lbs/inch}{oz/yd^2}$).

The laboratory room temperature and humidity were 68° to 82°F and 20% to 58% respectively.

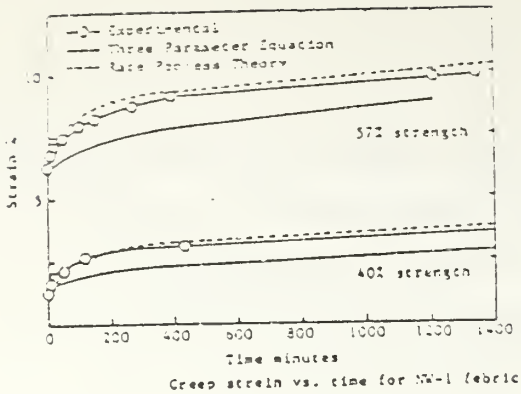

Creep strain vs. time for NW-1 fabric

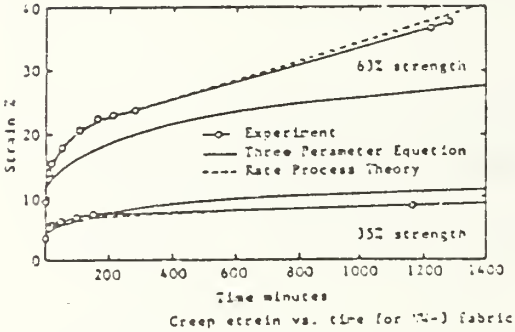

Creep strain vs. time for NW-3 fabric

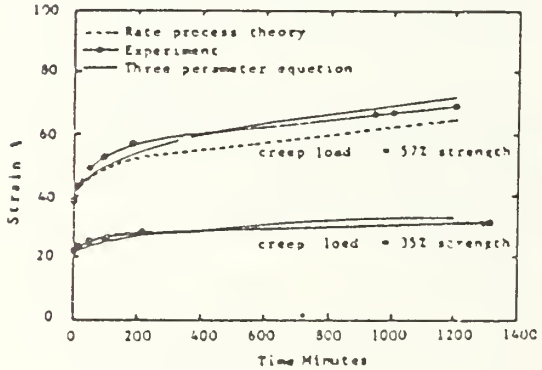

Creep strain vs time for e Fabric NW-5.

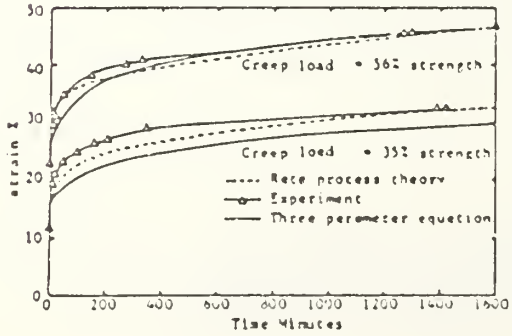

Creep strain vs time for Fabric NW-6.

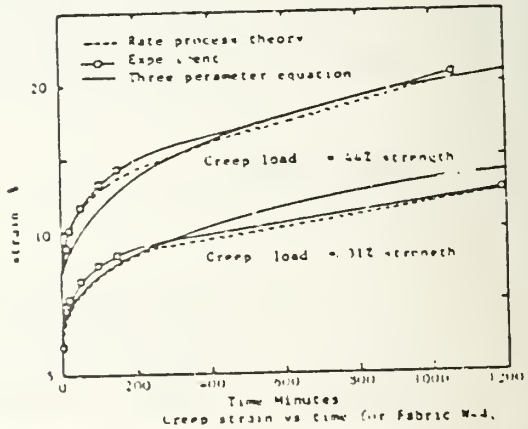

Creep strain vs time for Fabric W-4.

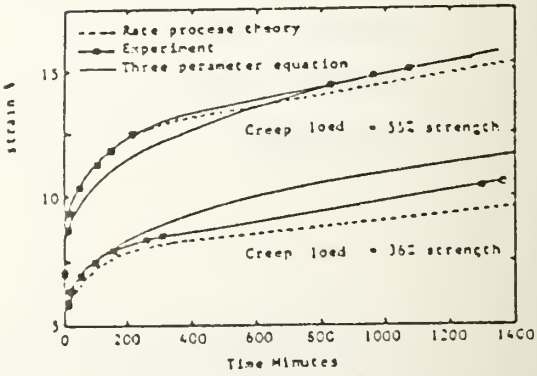

Creep strain vs time for Fabric C-1.

Figure 3-13. Creep strains vs time graphs for several different geotextiles and comparisons to Rate Process Theory and Three parameter equation (After Shrestha and Bell, 1982).

LARGE SCALE PULLOUT / CREEP DEVICE (LSPCD)

Introduction

The Large Scale Pullout / Creep Device (LSPCD) provides a means for evaluating the in-soil tensile strength and creep properties of geosynthetics. The LSPCD allows testing to be accomplished under a maximum normal stress of 14400 psf and maximum horizontal pullout load of 16330 pounds.

The LSPCD consists of a rectangular structural steel box (Figure 4-1) used to contain the soil and geosynthetic; a clamp used to transfer load from hydraulic pistons on each side of the box; and two pressure systems, one to apply a normal load to a rubber bladder on the top of the soil, and the other to apply pressure to an oil reservoir for the hydraulic pistons. A linear variable differential transformer (LVDT) with two inches of linear range is used to measure displacement of the clamp and a 25000 pound capacity load cell is used to measure force. Data acquisition for the system is accomplished through use of a PC-MATE LABMASTER (Tecmar) board which is installed in a LEADING EDGE Model D (IBM compatible) computer. The device is housed inside an environmentally controlled room enabling control of temperature and humidity. Figure 4-1 is a view of the interrelation of all of the components. Figure 4-2 is a

detail of the container assembly which includes the box, the hydraulic pistons and the clamping arrangement. A photograph of these features is provided in Figure 4-2P.

A complete listing of vendors, materials and costs for the fabrication of the LSPCD is provided in Appendix C.

Container Structural Features

The containment box is constructed of standard structural steel members and steel plate. The interior of the box measures 54 inches by 19 inches. This length allows for adequate anchorage of the geosynthetic within the soil. Bolted connections were used throughout to facilitate fabrication in the machine shop and subsequent reconstruction and placement in the environmental room. A325 bolts were used throughout. All steel members were primed with Pratt and Lambert Tech-gard E155 red oxide primer and painted with E148 maintenance gloss enamel.

The bottom plate is a 58 by 24 by 1/2 inch steel plate with 11/16-inch diameter drilled holes on 6 inch centers around the edges to attach the channel steel walls. A 1/2 inch spacer is used to support the plate bottom on the environmental room floor as the bolt heads protrude through the plate. Steel strips, 1 by 1/2 by 16 inches, are welded to the interior bottom of the box on 12" centers to prevent

the plate from becoming a shear interface for the soil. Details of the top and bottom plates are shown in Figure 4-3.

The side panels consist of two standard C 8 by 18.7 channel sections stacked one atop the other to provide a 16 inch deep wall. Bolt holes are again drilled on 6 inch centers to match the bottom plate and center flanges. Flange connections are used to connect the end channels. Details for the walls are shown in Figure 4-4.

End panels consist of two C 6 by 10.5 channel sections which are bolted to the top and bottom plates of the box and connected to the side panel sections. The 4 inch gap between the two channels is closed by two plates which are slotted with a 1/2 inch slot for adjustment of the gap. Adjacent to the front bottom adjustment plate a HDPE 100 mil (GUNDLE 100 mil) lining is placed which is cut slightly taller than the front adjustment plate. This prevents the reinforced section of the specimen from rubbing against the hard steel plate and minimizes the amount of soil lost through the gap during tests. The rear panels are slotted to provide the ability to further secure the free end of the geosynthetic should this be desired. These features are detailed in Figure 4-4.

The top plate is used to provide confinement for the

rubber bladder which imparts the normal load to the geosynthetic. A 3/8 inch-18 threaded hole accepts the high pressure gas line for application of pressure. The plate is 1/2 inch steel, reinforced on 6 inch centers with L 3 1/2 by 2 1/2 by 1/4 inch angle iron. The angle iron is welded using a 4 inch fillet weld per 12 inches of length. Using ultimate strengths for the steel and a factor of safety of four, this design allows a working pressure of 140 psi. The limiting factor however, is the surface between the plate and the rubber membrane which, not being a machined edge, allows highly pressurized gas to escape through microscopic imperfections in the steel. The top lid has been tested to 100 psi with unnoticable leakage when bolted to the frame at 105 $\pm$ 05 foot-pounds.

Pressure Systems

As discussed previously, a rubber bladder is used to apply normal load to the geosynthetic. This load is transferred through the soil which covers the geosynthetic. The membrane is a 24 by 58 by 1/8 inch thick sheet of industrial grade neoprene rubber. Cork cutters were used to place holes to match the top plate. A standard 2250 psi nitrogen tank provides pressure to the system. An OXWELD #998355 non-bleeding regulator allows adjustment of outlet pressures from 0 - 900 psi. The regulator was further fitted with a 0 - 15 psi gauge to accurately measure low pressures.

Calibration for the pressure gauge used is provided in Appendix B. A high pressure 3/8 inch hose was used for the connection.

A separate nitrogen tank is used to supply pressure to a hydraulic oil reservoir which in turn, applies this pressure to the hydraulic cylinders. A SMITH #H1883-580 regulator allows outlet pressures from 0 - 1500 psi. Two 3/8 inch hydraulic hoses extend from the reservoir to the hydraulic cylinders. The reservoir doubles as a pressure vessel and is constructed of a 10 inch diameter schedule 40 pipe constrained by 3/4 inch end platens which are recessed to accept the pipe and 1/8-inch diameter neoprene O-rings. Eight 5/8 inch threaded bars clamp the assembly. The nuts are torqued to 40 ft-lbs. Using a safety factor of four, the pressure vessel is rated at a maximum pressure of 650 psi. The vessel was tested to 650 psi by first filling with water and then pressurizing the system. The two pressure system schematics are shown in Figure 4-5. Specific details of the oil reservoir are shown in Figure 4-6.

Hydraulic Cylinders

The hydraulic cylinders are placed on each side of the box to provide pullout force to the geosynthetic. The DAYTON model Z196A hydraulic cylinders are 4 inch bore diameter cylinders with 16 inches of maximum stroke.

Technical specifications are provided in Appendix D. The cylinders are attached to the longitudinal wall flanges and end webs by a rear brace and front bracket which affix the cylinders to the box. The front bracket is a stabilizing bracket which aligns the cylinder and results in parallel extension of the tandem cylinders. The rear brace provides resistance to the force created by extrusion of the geosynthetic. These brackets are shown in Figure 4-7.

Clamp Assembly

The Clamp was designed to provide a thin profile extending into the containment box. A single compression load cell was incorporated in the assembly to measure lateral loads at the clamp.

The clamp consists of a primary yoke, which provides attachment to the load cell and connects the two hydraulic rams, and a secondary yoke, which connects the clamping plates with two steel bars and holds the load cell button. The LVDT brace is attached to the clamping plates, which secure steel plates to the epoxy reinforced geosynthetic. These components and their interrelation are shown in Figure 4-2.

The primary yoke is constructed with two C 6 by 8.2 channels welded back to back with 3/4 inch spacers. The

flanges are cut away as shown in Figure 4-8 to accept the hydraulic ram clevis. The front of the clamp is machined to provide a smooth surface for the load cell mounting plate which is made of cold rolled steel and machined to a surface tolerance of .0002 in/in. The mounting plate distributes the load over the primary yoke.

The secondary yoke consists of two C 3 by 4.1 channel sections back to back, separated by 1/2 inch spacers. This yoke has 11/16-inch diameter holes drilled in each end to connect the bars which transfer load to the clamping plates. The bars are drilled with holes at various lengths to facilitate clamp setup during testing. The load cell button is machined to match the curvature of the load cell pressure plate. The button is bolted through the center of the secondary yoke. These components are shown in Figure 4-8.

Clamping of the epoxy reinforced geosynthetic is accomplished through the use of two C 4 by 5.4 sections. The reinforced geosynthetic is sandwiched between two sheets of 16 gauge sheet metal or stainless steel which is then bolted in between the two channel sections. The LVDT brace is attached to one of the center bolts. These details are shown in Figure 4-9. A photograph of the clamp assembly is provided in Figure 4-9P.

The potential weak link in the clamp system design is the reinforced section of the geosynthetic. Epoxy resin is used to provide a stiff section resistant to deformation and creep. Technical specifications for the MAGNABOND 2014 epoxy resin and a 346 curing agent are provided in Appendix D.

Data Acquisition System

The Data Aquisition System (DAS) utilizes a PC-Mate Lab Master board to retrieve analog data; a BASIC program "DATA2.BAS" to process the data and tabulate the results; a LEADING EDGE Model D computer and printer; a DC power supply and amplifier to supply power and amplify response of the load cell; and a signal conditioner to amplify the LVDT signal. The interrelationship of these components is shown in Figure 4-10.

The PC-Mate Lab Master board consists of a mother board which fits into a slot in the computer. The switches on the mother board are set to one of several addresses in accordance with the board installation procedures. Figure 4-11 indicates the switch setting for this setup and shows the switch setting for the address of 784. The daughter board is then connected to the mother board via a 40 pin wire.

The daughter board is kept remote from the computer in order to accurately convert the analog to digital data away from computer interference. Because of the low operating voltage of the load cell, a NEFF model 122 DC amplifier and SORESEN model GRD 60-5/30-1 DC power supply were used to boost the signal to the daughter board.

The LVDT signal conditioning unit provides an AC voltage supply to the LVDT and amplifies the resulting analog signal. The analog signal from the LVDT is sent via cable to the daughter board of the DAS.

Load Cell

Compression loads are measured using an INTERFACE model 1221 load cell and the DAS described above. The load cell specifications and factory calibration are provided in Appendix D. Calibration for the acquisition system is provided in Appendix B.

LVDT

The linear variable differential transformer (LVDT) is used to accurately measure displacement. The device is set up for either of two LVDT's; one is a 1000 HR SCHAEVITZ AC LVDT which is used for pullout tests and has 2 inches of total linear range; the other, a 3000 HR model for long term

creep analyses, which has a 6 inch total linear range. Test and inspection data along with linearity calibration curves are provided in Appendix D for both LVDT's.

Environmental Room

The environmental room is an insulated chamber in which temperature can be closely controlled. The room was tested at 70 °F for one week and did not vary by more than ± .2 °F. The room is a LAB-LINE instrument model 1766AUX H. Humidity, which may also be controlled by the environmental room, was not monitored during this investigation.

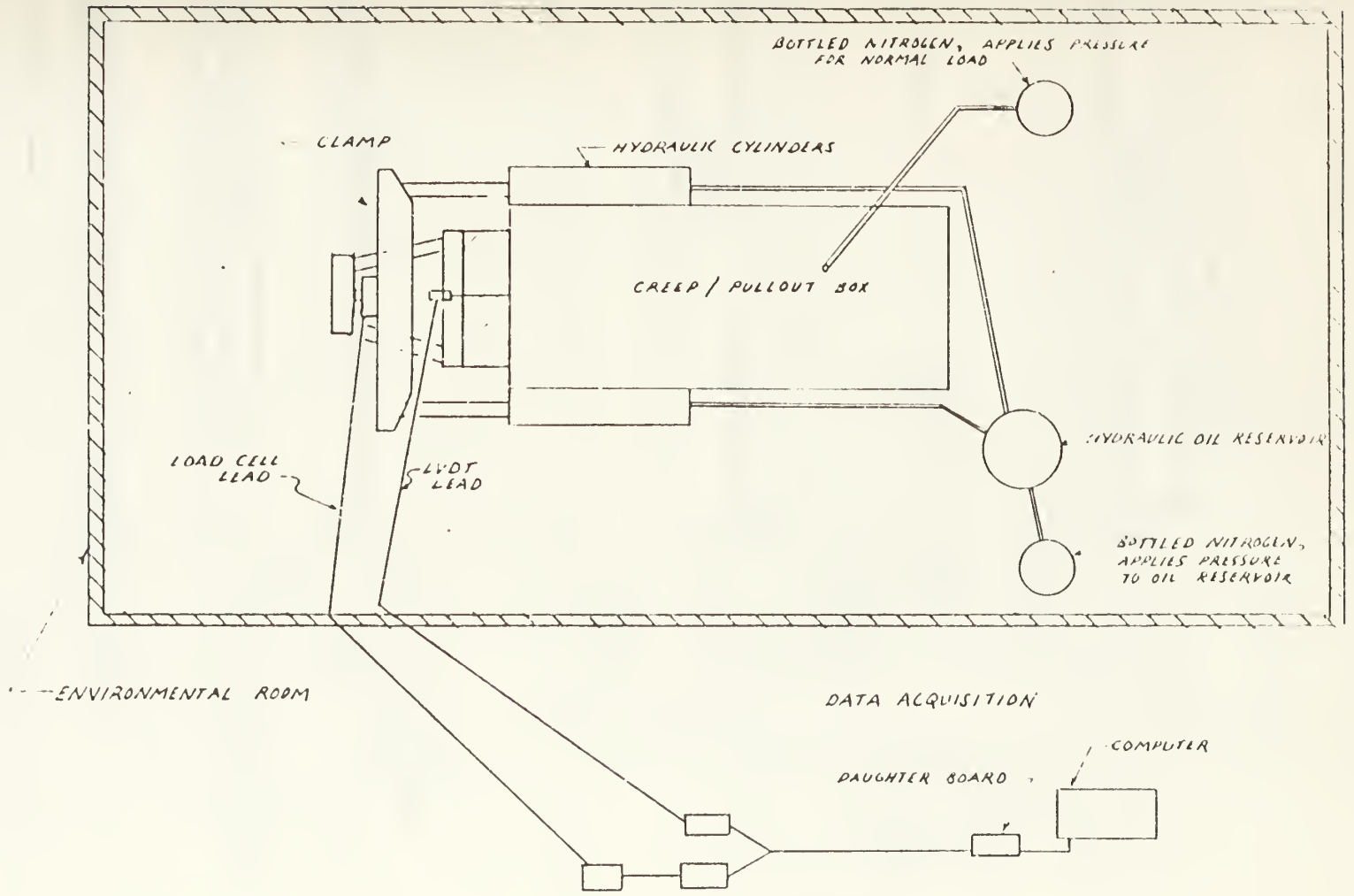

FIGURE 4-1 COMPONENT LAYOUT

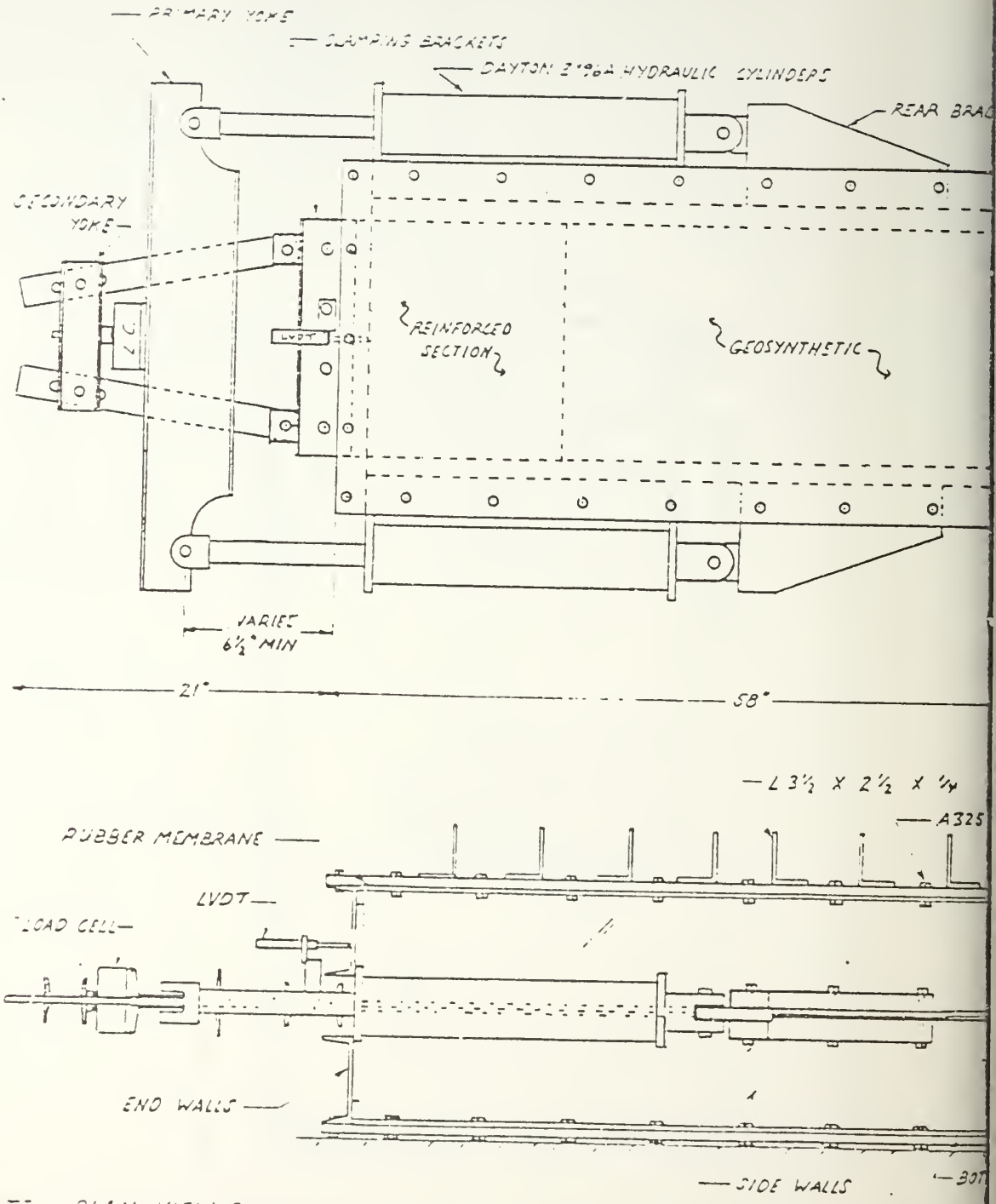

FIGURE 4-2 GENERAL DETAILS

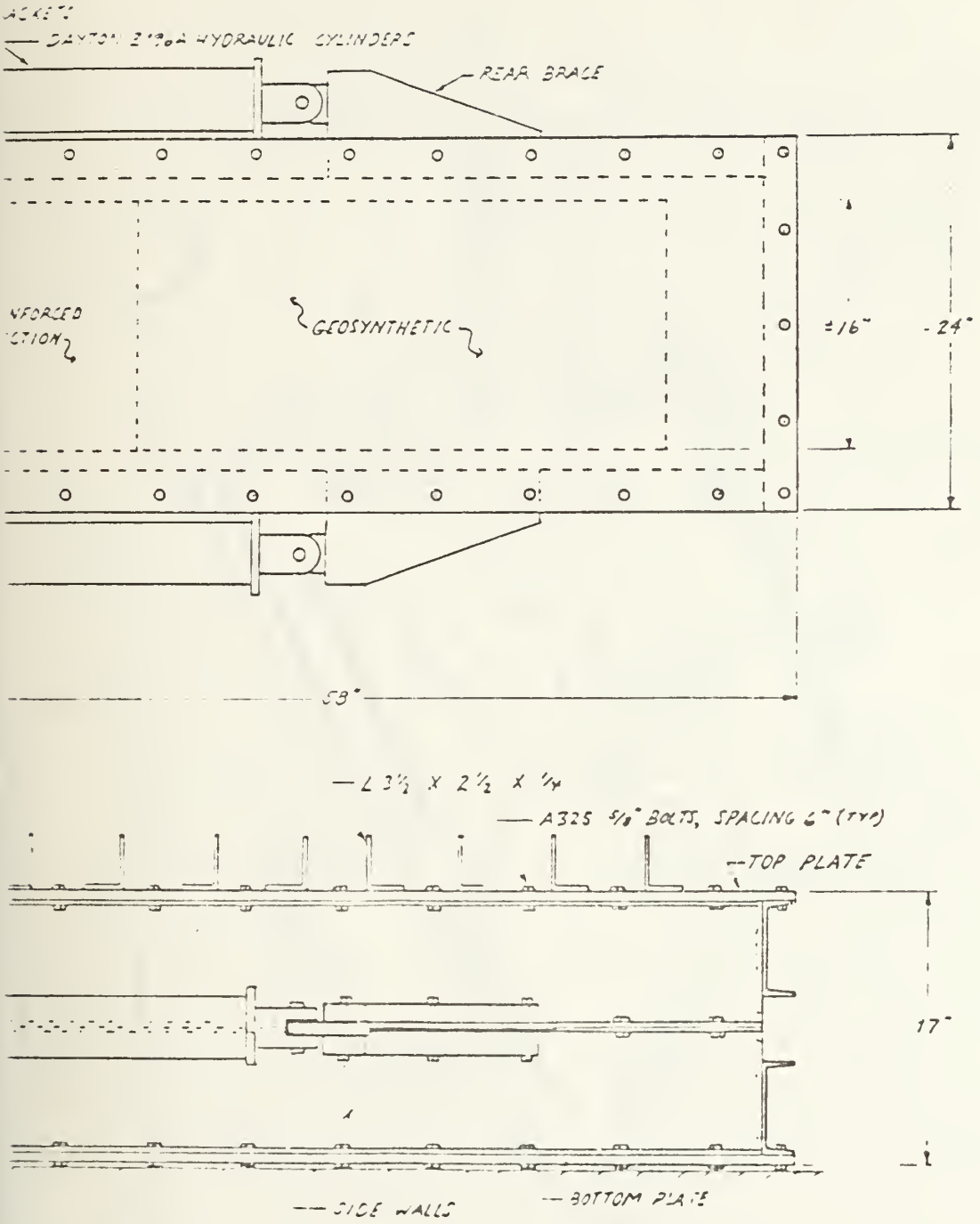

SCALE 1:10

-2 GENERAL DETAILS

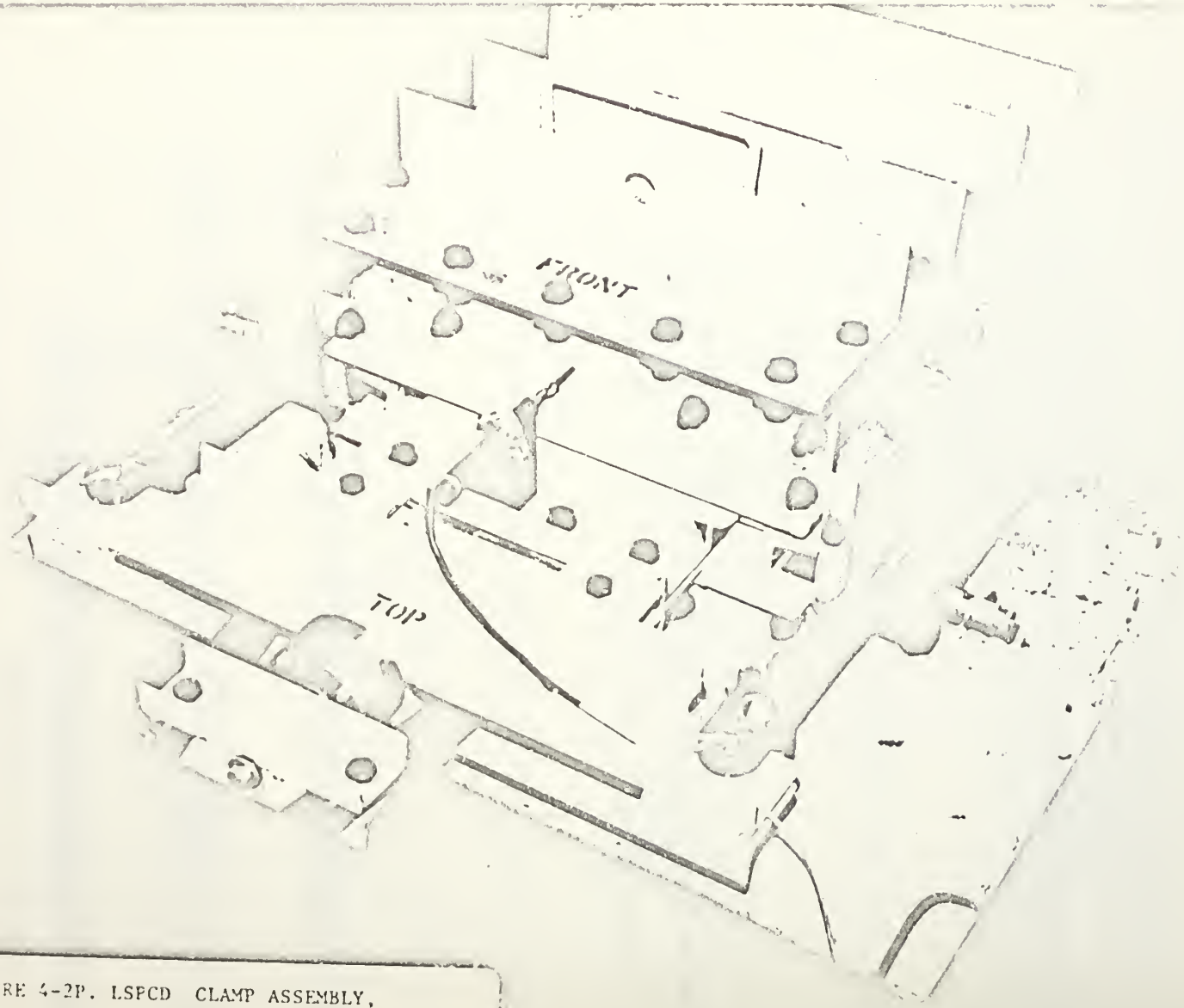

FIGURE 4-2P. LSPCD CLAMP ASSEMBLY, CONTAINMENT BOX AND HYDRAULIC RAMS

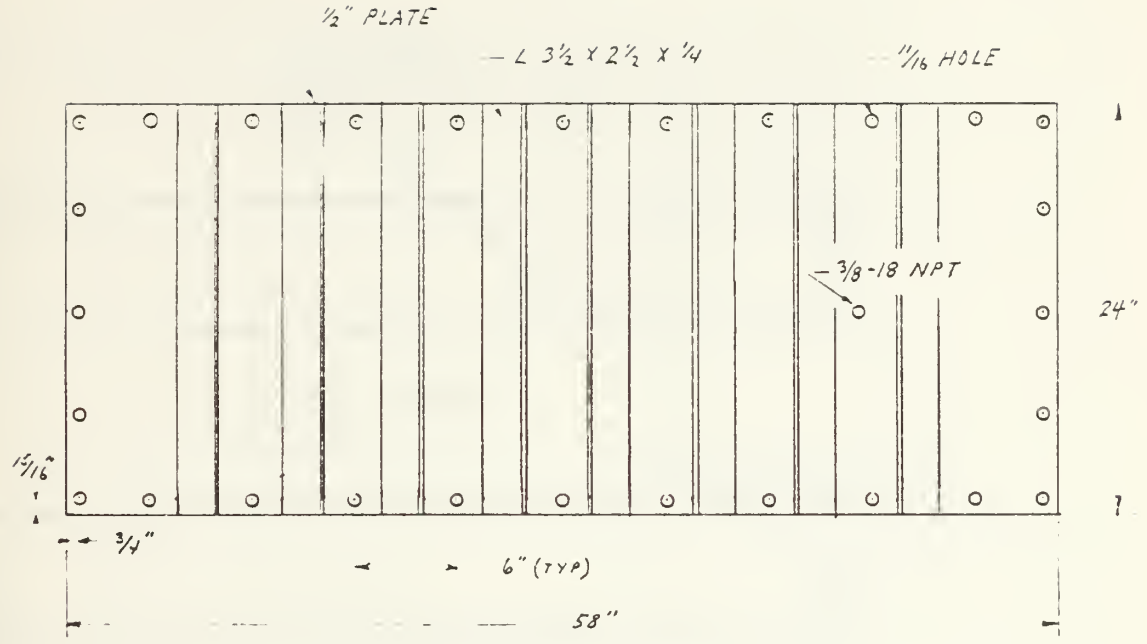

TOP PLATE

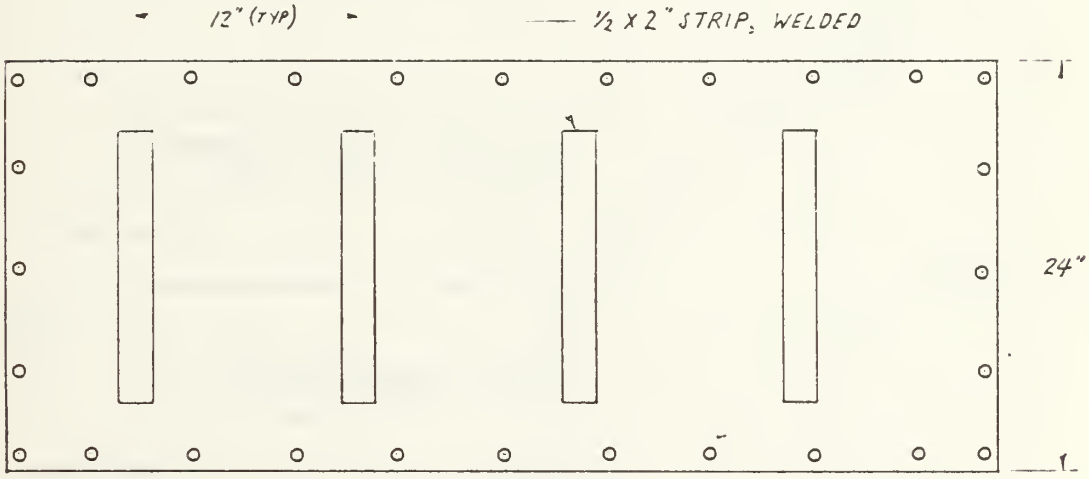

BOTTOM PLATE

FIGURE 4-3 TOP AND BOTTOM PLATES

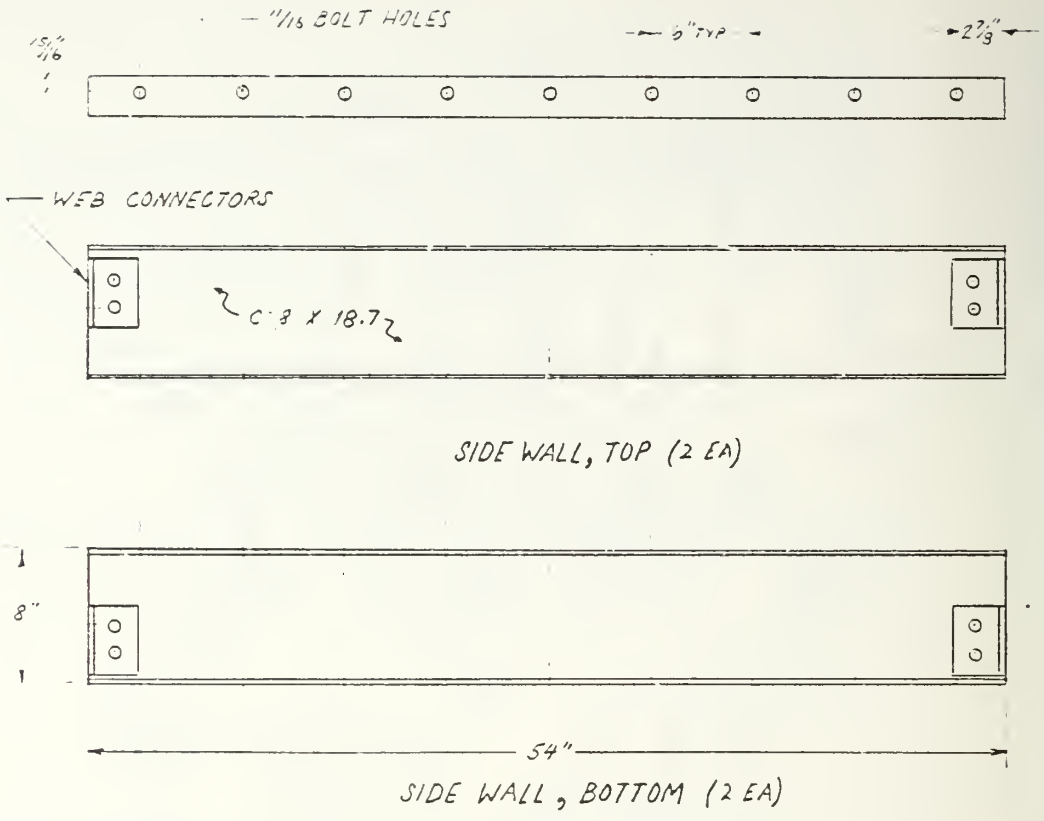

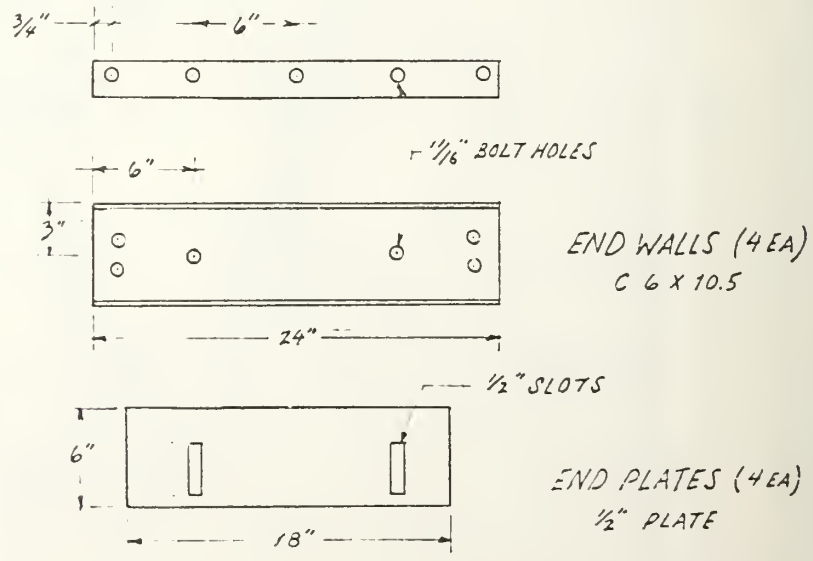

FIGURE 4-4. SIDE AND END WALLS

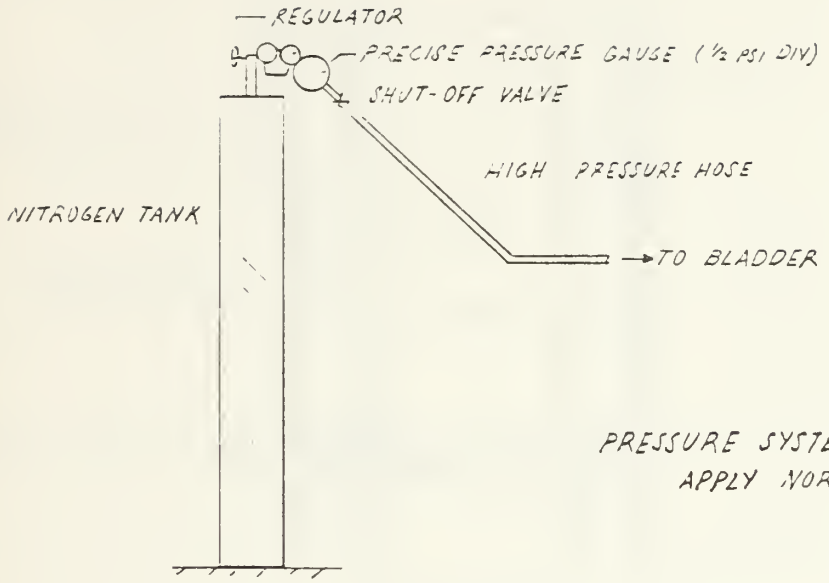

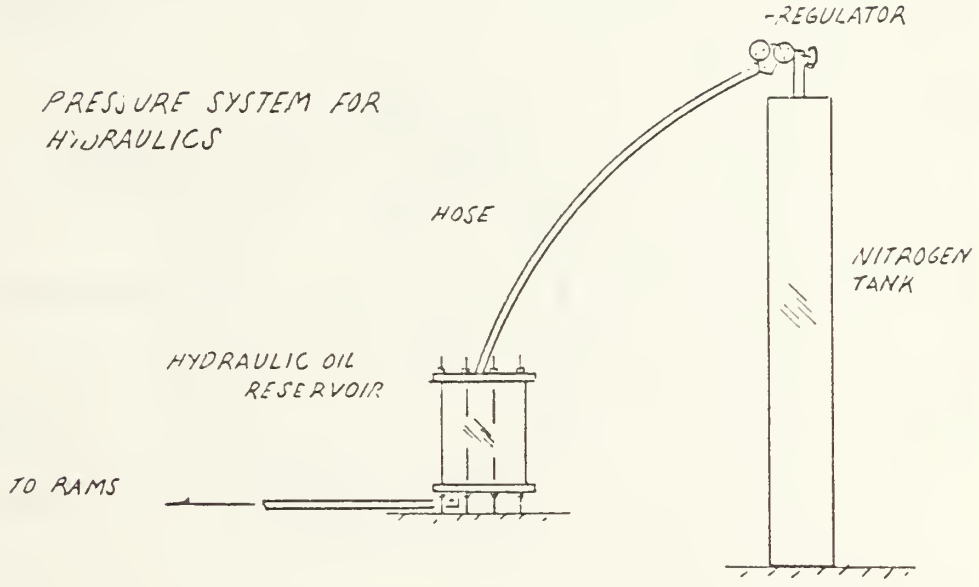

FIGURE 4-5. PRESSURE SYSTEMS

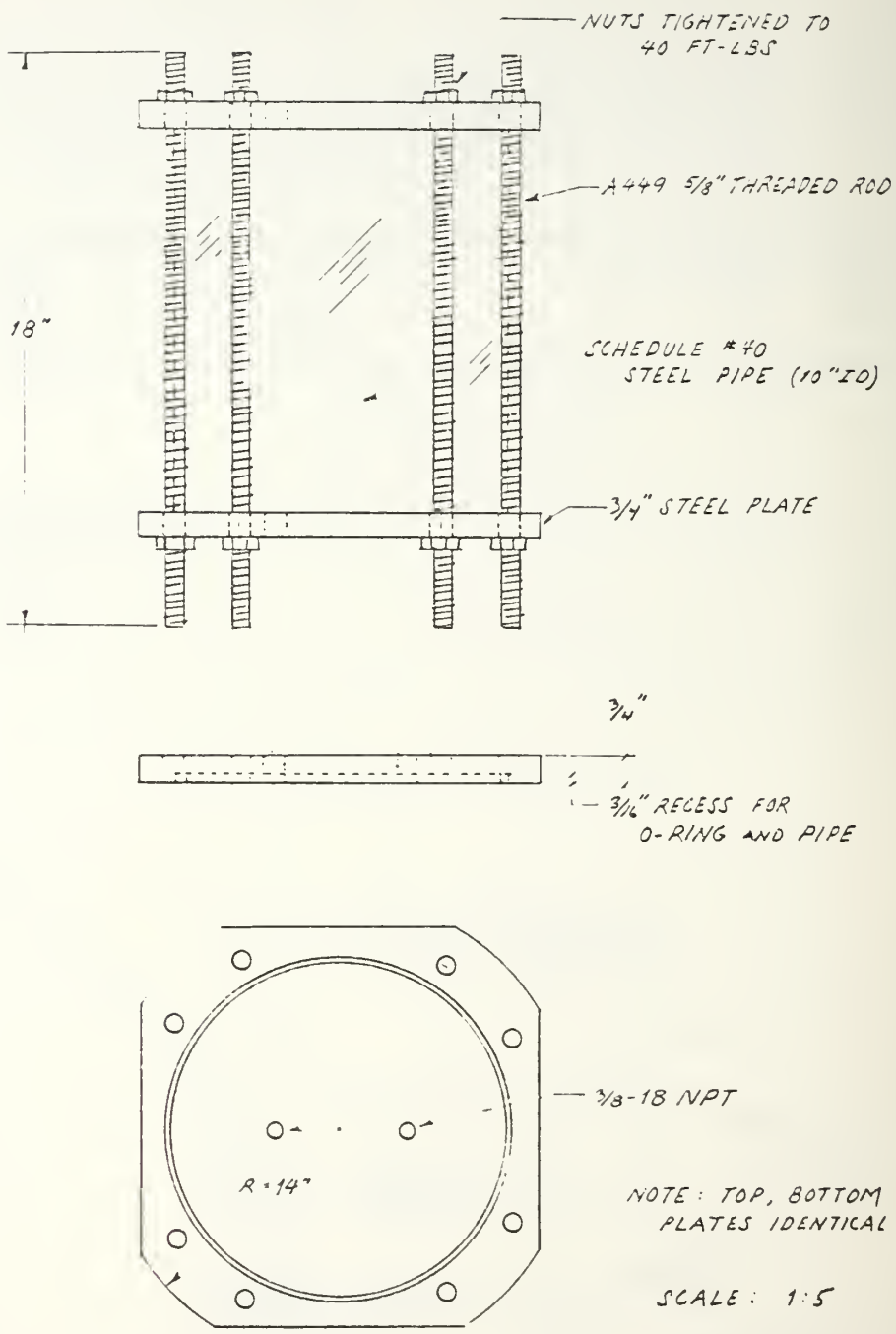

FIGURE 4-6. OIL RESERVOIR

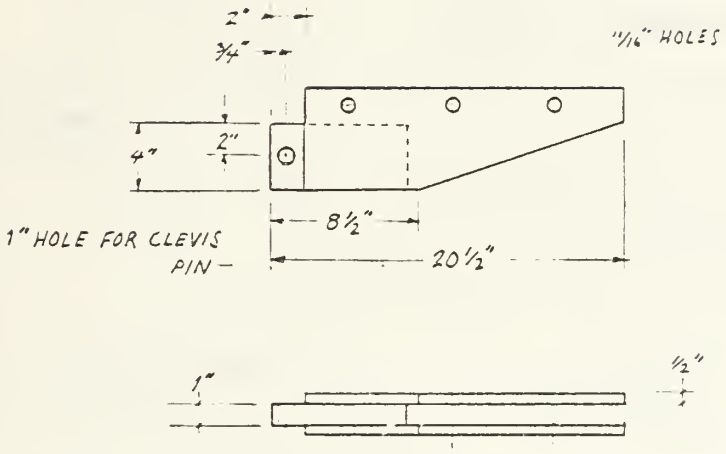

REAR BRACE (2 EA)

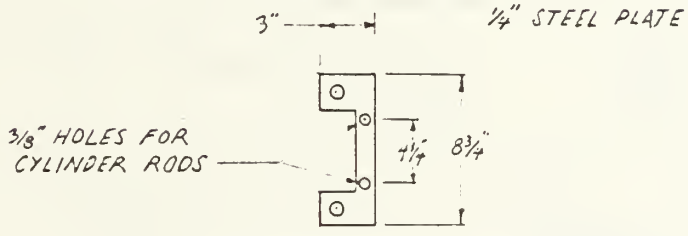

FRONT BRACKET (2 EA)

FIGURE 4-7. CYLINDER BRACKETS

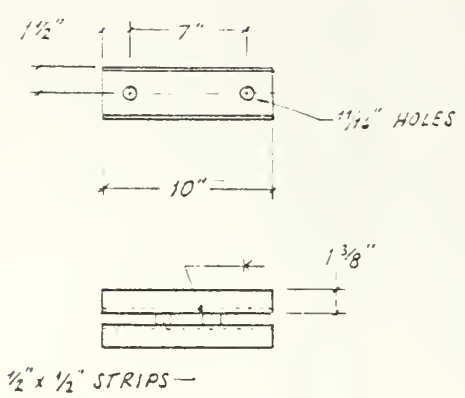

SECONDARY 'YOKE'
C 3 x 4.1

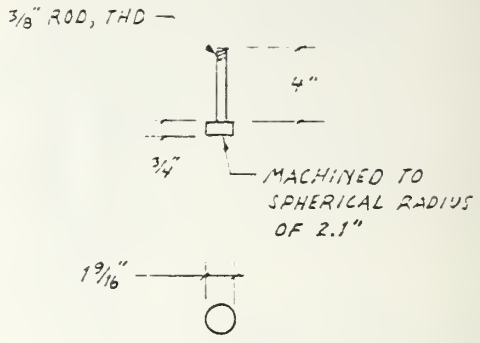

LOAD BUTTON

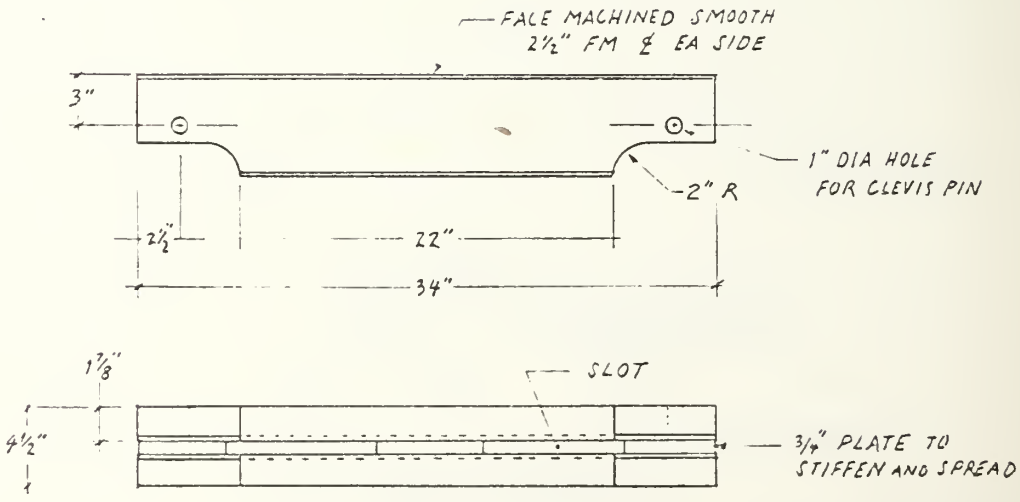

PRIMARY YOKE
C 6 X 8.2

FIGURE 4-8. CLAMP, YOKE DETAILS

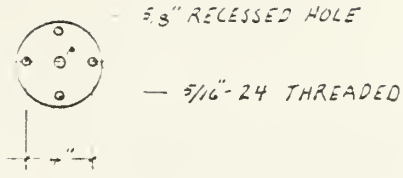

LOAD CELL MOUNTING PLATE

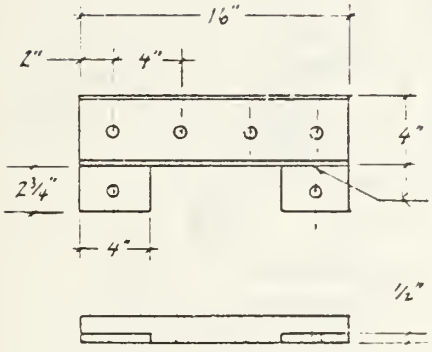

CLAMPS (2 EA)
C 4 X 5.4

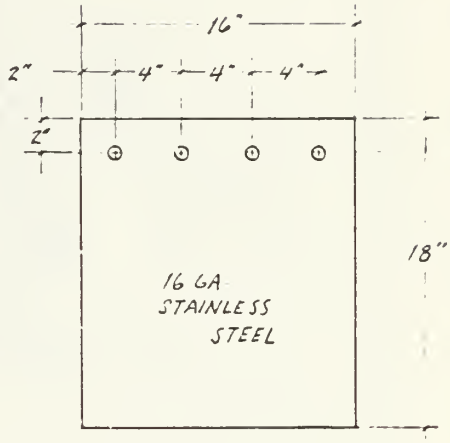

COVER PLATES (2 EA)

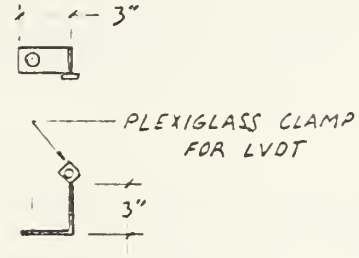

LVDT CLAMP

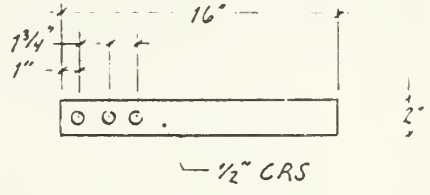

BARS

FIGURE 4-9. CLAMP DETAILS

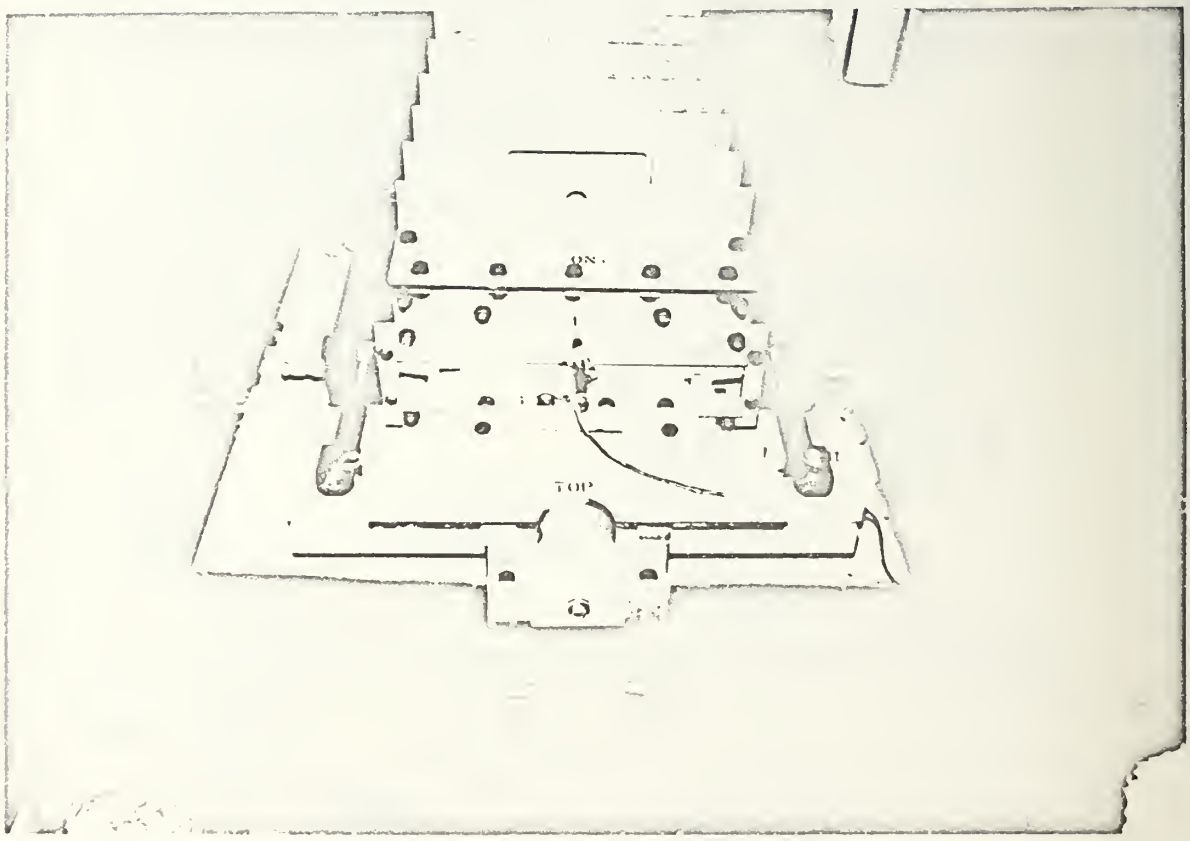

FIGURE 4-9P. PHOTOGRAPH OF THE CLAMP ASSEMBLY

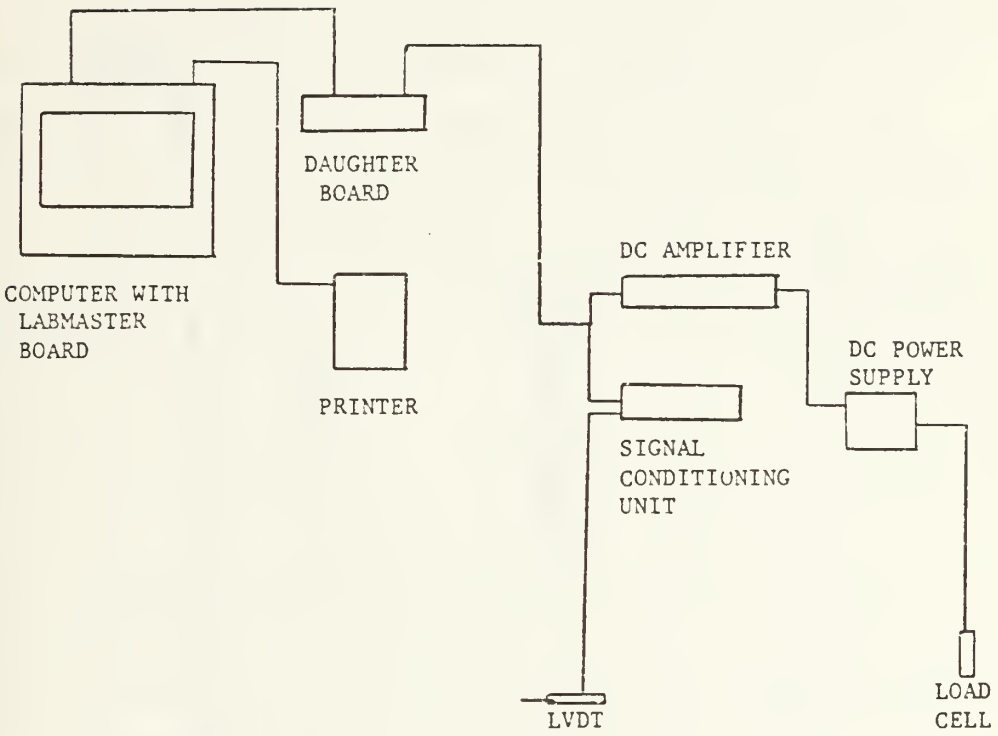

FIGURE 4-10. DATA ACQUISITION SYSTEM

Figure 7

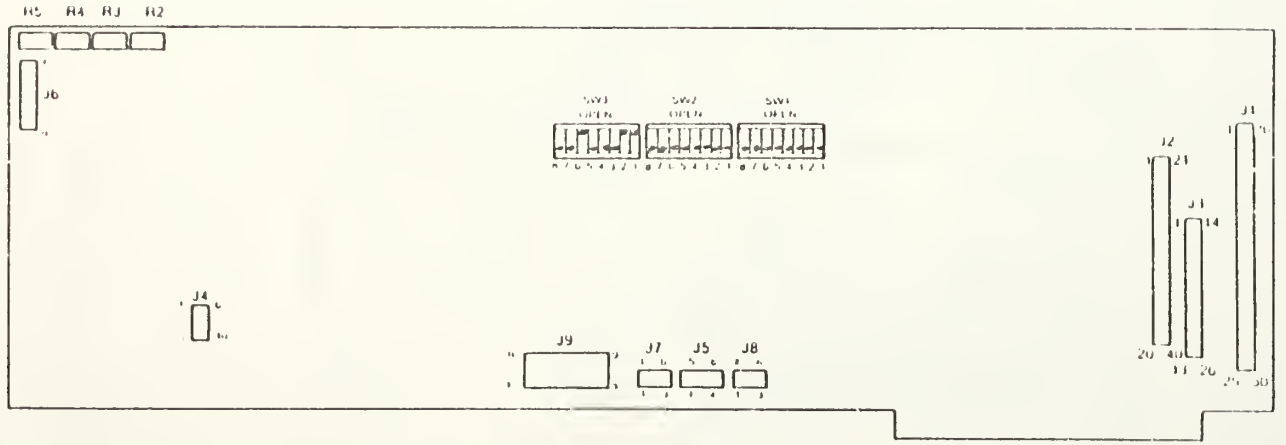

Mother Board Switch and Jumper Placement

ADDRESS 784:
SW1 - All closed
SW2 - All closed
SW3 - 1, 2, & 6 open
rest closed

FIGURE 4-11. SWITCH SETTING FOR MOTHER BOARD

METHODOLOGY

The operational procedures for the tensile pullout and tension creep analyses are desribed below. The methodology includes a description of the preparation of the geosynthetic, the soil/geosynthetic placement and compaction, application of normal load, placement of the clamp assembly, start-up of the DAS, and procedures for the tensile pullout and tension creep analyses. Problems encountered during initial test setup and those encountered subsequently are addressed.

Geosynthetic Preparation

Extreme care should be exercised in preparation of the reinforced section of the geosynthetic. Steel sheets are used to confine the epoxy laden reinforced system during cure. Procedural steps are outlined below:

(1) The geosynthetic is cut to the desired length of embedment plus 18 inches to allow for the reinforced section.
(2) Four pieces of TREVIRA 1120 nonwoven geotextile are cut; two 15 1/2 by 18 inch sections and two 3 by 15 inch strips.
(3) A 16 guage, 16 by 18 inch steel plate is placed in

the location desired for curing of the epoxy reinforced section. The plate is covered with a large sheet of PVC plastic sheet to prevent epoxy from bonding to the steel.

(4) Materials are arranged. Protective gear including rubber gloves and eye protection is worn. Ambient temperature is recorded.

(5) 125 cc of the epoxy is mixed with an equal portion of the curing agent in a large tin. Thorough mixing of the two agents is required.

(6) One of the large sheets and small strips of the Trevira are impregnated with the epoxy mix. To ensure saturation of the epoxy into the nonwoven, the cloth is kneaded by hand.

(7) The large sheet of epoxy impregnated Trevira is spread onto the plastic covered steel. The small strip is spread along the top end of the section to provide additional reinforcement.

(8) The impregnated nonwoven is covered with the geosynthetic.

(9) Steps (5) and (6) are repeated and the cloth is spread over the geosynthetic. Again, the strip is placed to reinforce the bolt hole locations.

(10) The specimen is covered with a plastic sheet and another 16 guage steel sheet. Approximately 20 to 30 pounds are placed over the steel sheet to confine the reinforced section.

(11) After curing for 24 hours, the specimen is trimmed with a band or saber saw and 11/16-inch diameter holes are drilled to fit the clamping plates.

(12) The two C 4 X 5.4 clamps are bolted to the sandwiched steel and reinforced section.

Curing time is temperature dependent for this epoxy. Stress concentrations develop in areas around the bolt holes, therefore, it is imperative that adequate time is provided for the complete curing of the system. One sample which had been prepared as above but cured at approximately 55 °F deformed a total of 3/16 inches during a pullout test. Longer curing times must be taken if temperatures fall below 70 °F. Temperatures should be kept above 75 °F if possible.

Soil-Geosynthetic Placement/Compaction

The soil may be placed and compacted using any means which assures placement at a uniform void ratio. For the concrete sand utilized in the tests run herein, two types of compaction methods were used; one involved the use of an air-driven compaction foot and the other, a manually operated drop ram.

The soil is brought to conditions of desired moisture content. The soil is then compacted in 2 1/2 to 3 inch loose lifts. The manually operated drop ram was utilized for most

of the analyses as it did not scatter the soil as much as the air driven foot. Slightly lower densities were obtained for the drop ram, but the void ratio and density were uniform.

After the soil is compacted to mid-height of the frame, the reinforced geosynthetic is placed through the slot in the front of the box. An 8 by 15 inch section of plywood is used to support the clamp. Care must be exercised in centering the specimen in the slot since loading is accomplished through the center of the box without regard to placement of the specimen. Soil is added to the top of the geosynthetic and compacted, again in 2 1/2 to 3 inch loose lifts. When the soil layer is level with the top of the box, a screed is used to level the soil at a height 1/4 inch below the top of the frame. This ensures equal application of normal pressure. Finger pressure is applied in the corners of the soil to ensure that the soil is of sufficient compaction to resist the bladder pressure. Additionally, soil is molded in the corners to provide a smooth transition for the otherwise sharp corners of the frame. If fine grained materials are to be used in the test, compaction method and water content would be altered to achieve the desired structure.

Normal Load Application

The rubber membrane is placed over the compacted soil and aligned over the bolt holes. The flanges should be free of any soil which would interfere with the seal of the membrane. The membrane is clamped on the ends with large document clamps to prevent slippage during placement of the top plate. After placement of the top plate the document clamps are removed and the top plate is aligned to the frame by installing the A325 bolts and washers. The bolts are tightened to a torque of 105 ± 05 foot-pounds.

After connection of the pressure hose to the top plate, the system is pressurized to the desired test level and checked for leaks. To ensure integrity of the bladder, the pressure is backed off from the regulator. Observation of the pressure gauge will indicate any leaks in the system. Pressure is then applied and bolts adjacent to the leak are given additional torque until leakage stops. The system is rechecked for additional leaks as necessary.

Clamp Assembly Placement

The hydraulic rams are extended to clear the clamping plates and accept the primary yoke. This is accomplished by applying slight pressure to the oil reservoir. Care should be taken not to overextend the rams as this would

necessitate the removal of the hose supplying normal load to retract the cylinders. The primary yoke is installed on the hydraulic ram clevis. Clearance between the primary yoke and the clamping plates should be about 1 inch. The secondary yoke is fitted with the load button and the connection bars. The bars are threaded through the opening in the primary yoke and supported by 1/8-inch diameter roller pins in the slot on the primary yoke. The bars are connected to the clamp by 5/8-inch diameter pins or bolts. Depending on the clamp placement, the bars may be adjusted by altering the bolt connection at the secondary yoke. The LVDT is then placed in the clamp and lightly secured.

Data Acquisition System Check

The procedures for the computer program operation are listed in Appendix A. After the program is installed and booted, the system electronic components may be tested by observing data output.

Once the components have been determined to be operating correctly, the load cell is seated and the LVDT is adjusted to the limit of its linear range.

Pullout Test

The tensile pullout test may be performed in one of two modes; stress control or strain control. In the stress control pullout test loads are gradually increased by applying pressure to the oil reservoir. The analyses in this paper were performed at a loading rate of approximately 150 lbs/min. This resulted in deflection rates which varied between 0.005 to 0.1 inches per minute. Force continues to be applied until rupture or pullout of the geosynthetic is observed.

Results are plotted as alpha versus deflection of the clamp. Alpha is the total load on the geosynthetic divided by the width of the specimen.

The reinforced section of the geosynthetic should be ckecked for signs of failure around the bolt holes.

Creep Test

The creep test, although not performed in this investigation, would be accomplished in the following manner. First, steady state conditions of temperature would be established in the environmental room. A tensile pullout test would be performed to evaluate the stress at failure, α_f, for the perscribed soil and boundary conditions. A load

would then be applied to the geosynthetic corresponding to a specified percentage of the failure load. This stress level would then be held constant and deflections would be monitored as a function of time. The time interval for sampling would be altered to a logrithmic interval for the creep test.

Shutdown Procedures

Pressure is released from the oil reservoir and top bladder at the conclusion of the test. The clamp assembly is disassembled and the hydraulic rams retracted into the cylinders. This is accomplished by attaching the pressure hose to the front of the cylinders and applying pressure. The top lid bolts are removed and top plate removed. A container is used to hold the soil as the specimen is removed from the box.

A cylinder is driven into the soil layer and a soil specimen is obtained. The void ratio, moisture content and relative density of the soil are then measured using standard test procedures.

Data Analysis

The data points may be stored on a floppy disk in a data file. The data file may be accessed by MICROSOFT Chart

software which is used to plot out the data. A subinterval is normally used for plotting due to the large number of points generated during the test.

Safety Precautions

Because of the high pressures and loads associated with the operation of the LSPCD it is important to exercise caution while operating the device.

The oil reservoir has been tested to 650 psi with a safety factor of four. Over time the connections may loosen due to fatigue. Therefore, the bolts should be tested for the proper torque of 40 foot-pounds. The O-ring seals may be expected to deteriorate over time and should be immediately replaced if any leakage is noticed. When servicing the vessel, the general condition of the steel should be noted. Any corrosion or damage reduces the factor of safety.

RESULTS

Introduction

Two sets of data were generated in this investigation. First, a series of standard soil tests were completed on the granular soil and second, pullout data were obtained from the LSPCD during tensile pullout tests at various boundary conditions.

Soil Analyses

The soil used in the investigation is a light tan fine concrete sand which was obtained locally. The soil is a limestone sand with a USCS classification of SW. The testing program included a sieve analysis, relative density determination, a standard Proctor test and a series of direct shear tests.

The gradation curve, shown in Figure 6-1, is the average of three tests performed on the sand. The sand is uniformly graded with a coefficient of uniformity of 3.1 and a maximum particle size of approximately 1 mm.

Results from the relative density determination (ASTM D2049) on the sand are summarized on Table 6-1. Minimum and maximum void ratios were determined as 0.652 and 1.09,

respectively. This corresponds to a maximum dry density of 100.0 pcf and a minimum dry density of 79.3 pcf.

The standard Proctor test (ASTM D698) results are provided in Figure 6-2. The moisture density curve exhibits the characteristic flat shape for sands for a range of moisture contents. One distinct advantage is apparent in the use of this material for the investigation. That being the large range of moisture contents for which approximately equal densities may be obtained.

A total of nine direct shear tests were performed. Three Mohr failure envelopes were developed representing the variation in strength properties as a function of void ratio. A comparison of the Mohr envelopes is provided in Figure 6-3. Individual plots of Mohr envelopes, shear stress versus strain and shear stress versus volumetric strain are provided for void ratios of 0.72, 0.86 and 0.99. The friction angles for the reported void ratios are 44.4 , 39.5 , and 35.0 , respectively. These plots are incorporated into Figures 6-4 through 6-6. Normal loads used for the direct shear analyses were; 20.50 psi, 51.25 psi and 102.50 psi (2952 psf, 7380 psf and 14760 psf).

Signode TNX-250 Geogrid

The material used in this investigation is a polyester (polyethylene Terephthalate) geogrid manufactured by Signode Industries, Inc. The trade name given the geogrid is TNX-250.

The grid is produced by overlapping strands 0.47 inches in width by 0.03 inches in thickness into a square pattern with nominal dimensions of 3 by 3 inches, center to center. The geometry is depicted in Figure 6-7.

The geogrid has a wide width tensile strength of 3000 pounds per foot and an elongation at break of 8 percent. Results of a wide width tensile test is presented in Figure 6-8. It is chemically stable, stabilized against UV degradation and is biologically inert.

These data were obtained from manufacturer literature which is included in Appendix D.

Pullout Tests

A total of eight pullout tests were performed. Early test data, where methodology for the test was being developed, were discarded. Data from five tests are presented herein. Three of the tests were performed at a

confining stress of 840 psf and two others at 1590 psf. Embedment length was varied in the testing program. Void ratios varied between 0.82 and 0.85 with one test being performed at a void ratio of 0.90.

Results are plotted as alpha, which is the force on the geosynthetic per foot of width, versus the horizontal deflection of the clamp. A comparison between the geosynthetics tested at various embedment lengths and equal confining stresses is presented in Figure 6-9. Figure 6-10 presents a similar comparison for the two specimens tested at a confining stress of 1590 psf. A comparison between the specimens at different confining stresses while maintaining equal embedment is provided in Figure 6-11 for the 15.19 inch embedment length. Figures 6-12 through 6-16 are individual plots of the five tests. Table 6-4 is a collection of the essential data achieved as a result of the analyses. Photographs were taken of the failed geogrids tested in the analyses and are provided in Figures 6-17P through 6-19P.

The alpha versus horizontal deflection curves exhibit the elasto-plastic behavior which would be expected for this material. The effects of both confining stress and embedment length are as expected. In the two specimens which failed by pullout the alpha/deflection curve flattens out and the shape is similar to that observed for soils. However, in

those specimens where the failure mode was by rupture, increasing values of alpha were observed with increasing rates of deflection until rupture finally occured.

Under different boundary conditions three modes of failure are possible.

If the geosynthetic is under high confining stress and/or is placed with long embedment lengths, large strains develop in the longitudinal strands adjacent to the clamp. Small translation prevent rotation of the nodes and ribs. The large strains result in rupture in the longitudinal strands adjacent to the clamp. This failure mode is depicted in Figures 6-17P.

Under moderate confining stresses and/or moderate embedment lengths, large translation occurs which results in both rib and node rotation. The rotation of the ribs coupled with the translation of the geogrid results in the development of passive pressures. The large translation of the nodes and rotation of the ribs leads to areas of high stress concentration in the area just to the front of the node. When this occurs either the longitudinal strand ruptures or the rib delaminates (peels away) from the longitudinal strands. Both mechanisms may be observed throughout the geogrid as shown in Figure 6-18P. A condition may exist whereby all of the ribs delaminate from the

structure without any rupture of the longitudinal strands, this mode is shown in Figure 6-19P.

In the third failure mode, which would occur at low confining stresses and/or small embedment lengths, a soil shear plane develops in an area adjacent to the ribs. In the geogrid, the stress and strain distribution are relatively constant over the length. Interface friction parameters may be determined for this failure condition. Large translations may result in the rotation of the nodes and ribs. Due to the small confining stress, however, the translation is insufficient to result in delamination of the grid. Hence, a yield plane develops within the soil outside of the ribs.

In summary, of the five geogrids examined in this investigation, two failed by the delamination mode and three by longitudinal strand rupture.

The unconfined tensile strength of the geogrid is 3000 pounds/foot (Appendix D). In the confined analyses where longitudinal rupture dominated the failure mode, the confined tensile strength was approximately 4500 pounds/foot. Frictional forces at the interface acccunt for the additional load carrying capacity of the geosynthetic. In the case where delamination was the predominant failure mode, the specimen under a confining stress of 840 psf

failed at 3110 psf while the specimen under 1590 psf of confining pressure failed at 4110 psf.

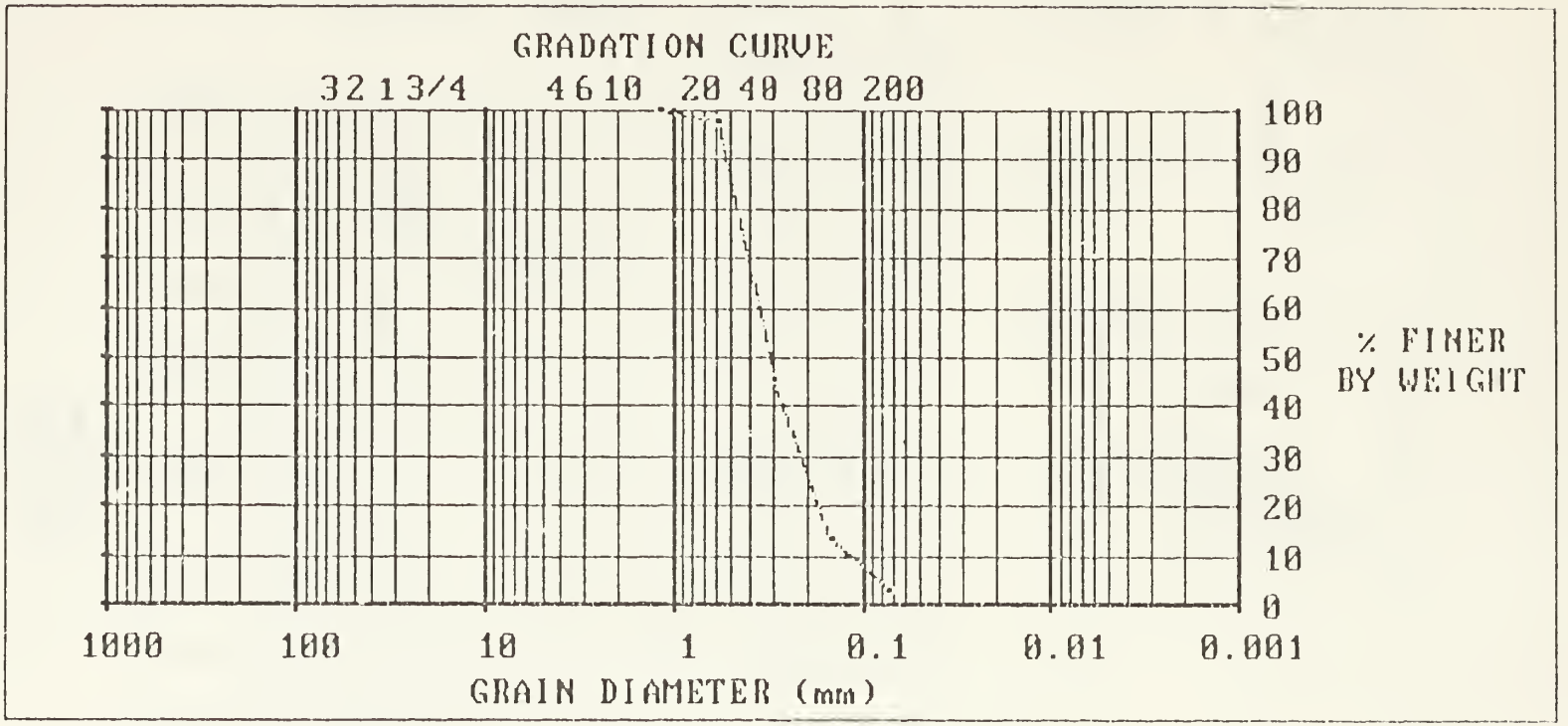

FIGURE 6-1. GRADATION CURVE FOR CONCRETE SAND (Cu = 3.1)

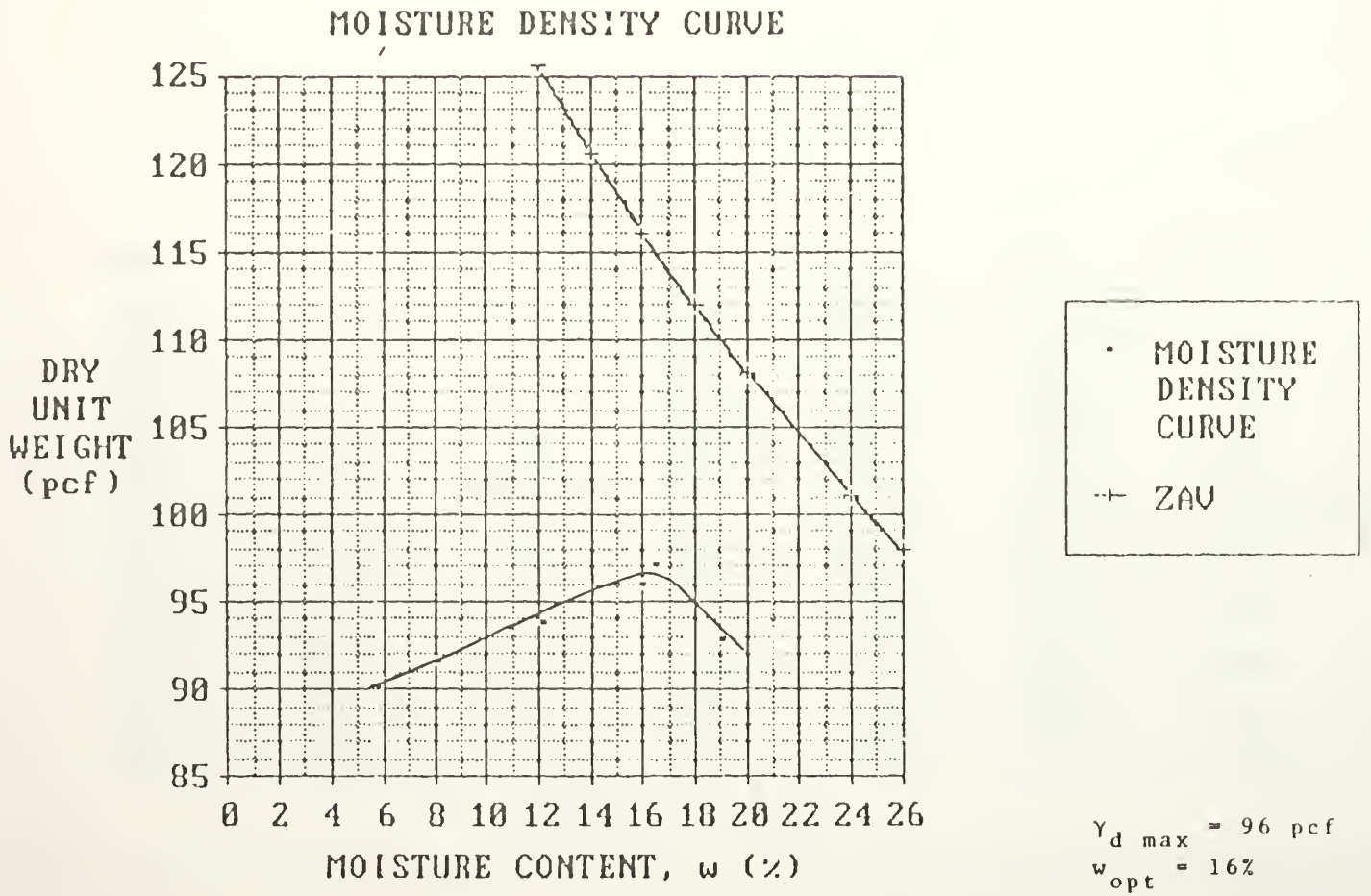

FIGURE 6-2. MOISTURE DENSITY CURVE FOR CONCRETE SAND

RELATIVE DENSITY

Mold Dimensions:
Dia (in): 6.022
Depth (in): 6.138
Vol (ft^3) 0.101

e (max) Determination:

Wt.Mold (g)	Wt.Soil & Mold (g)	Wt.Soil (g)	Void Ratio (e)	
3518	7178	3660	1.08	
3518	7158	3640	1.09	Dry Density (min) = 79.3 pcf
3518	7167	3649	1.08	

e (min) Determination:

Wt.Soil (g)	Defl. (in)	Vol. (ft^3)	Void Ratio (e)	
3660	1.244	0.0807	0.655	Dry Density (max) = 100.0 pcf
3640	1.279	0.0801	0.652	
3649	1.238	0.0808	0.662	

TABLE 6-1. RELATIVE DENSITY DETERMINATION FOR CONCRETE SAND

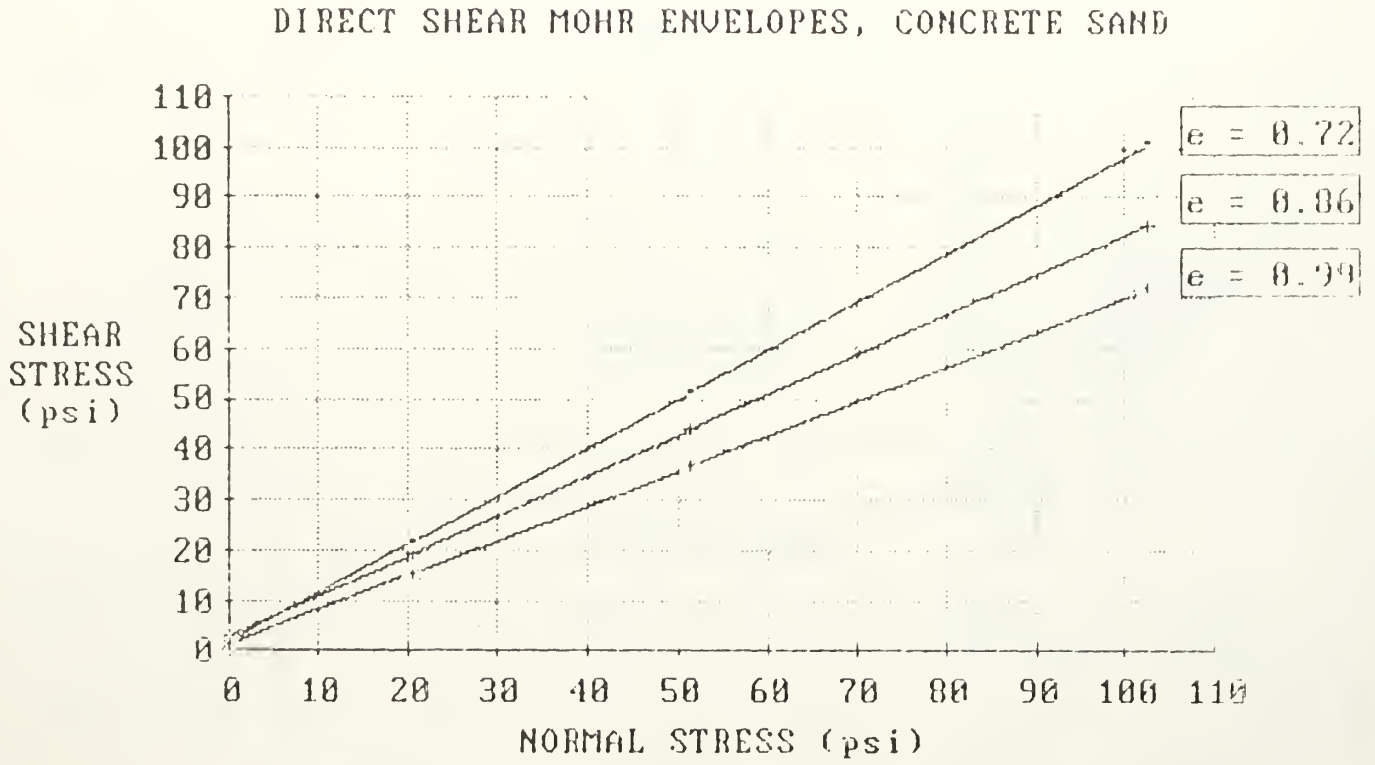

FIGURE 6-3. FAILURE ENVELOPES FOR CONCRETE SAND AT VARIOUS VOID RATIOS

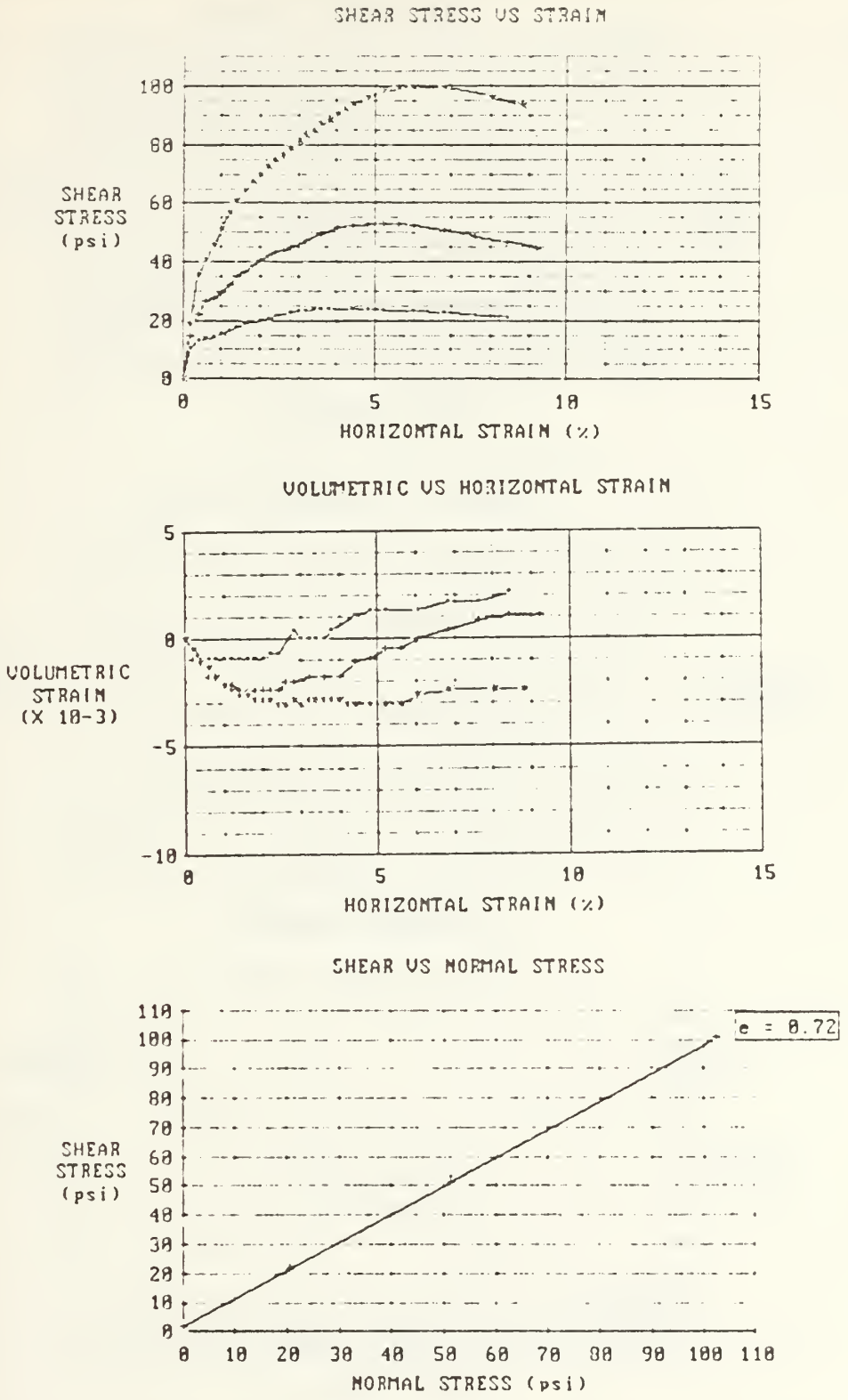

FIGURE 6-4. DIRECT SHEAR RESULTS FOR DENSE SAND (e = 0.72)

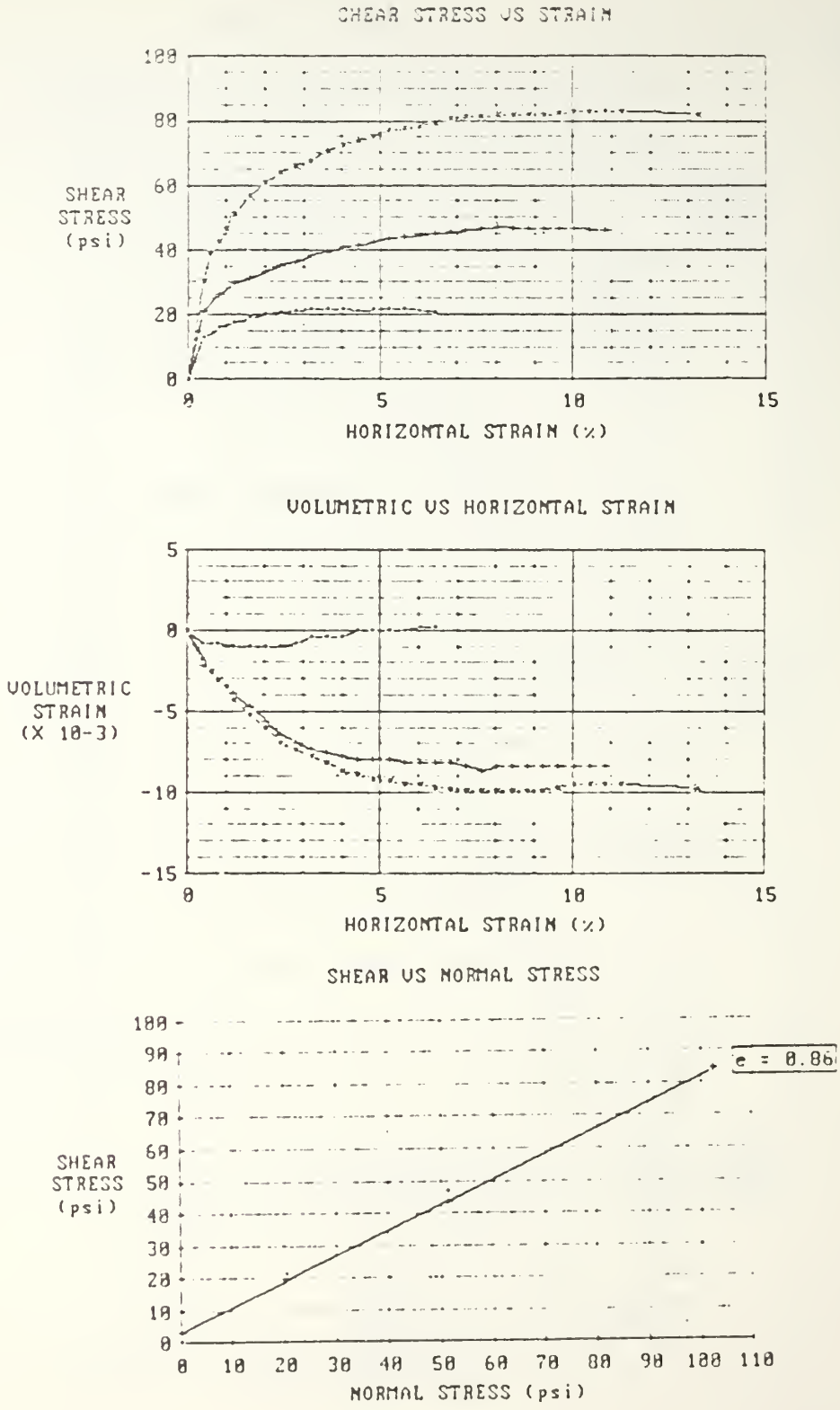

FIGURE 6-5. DIRECT SHEAR TEST RESULTS FOR MEDIUM CONCRETE SAND (e = 0.86)

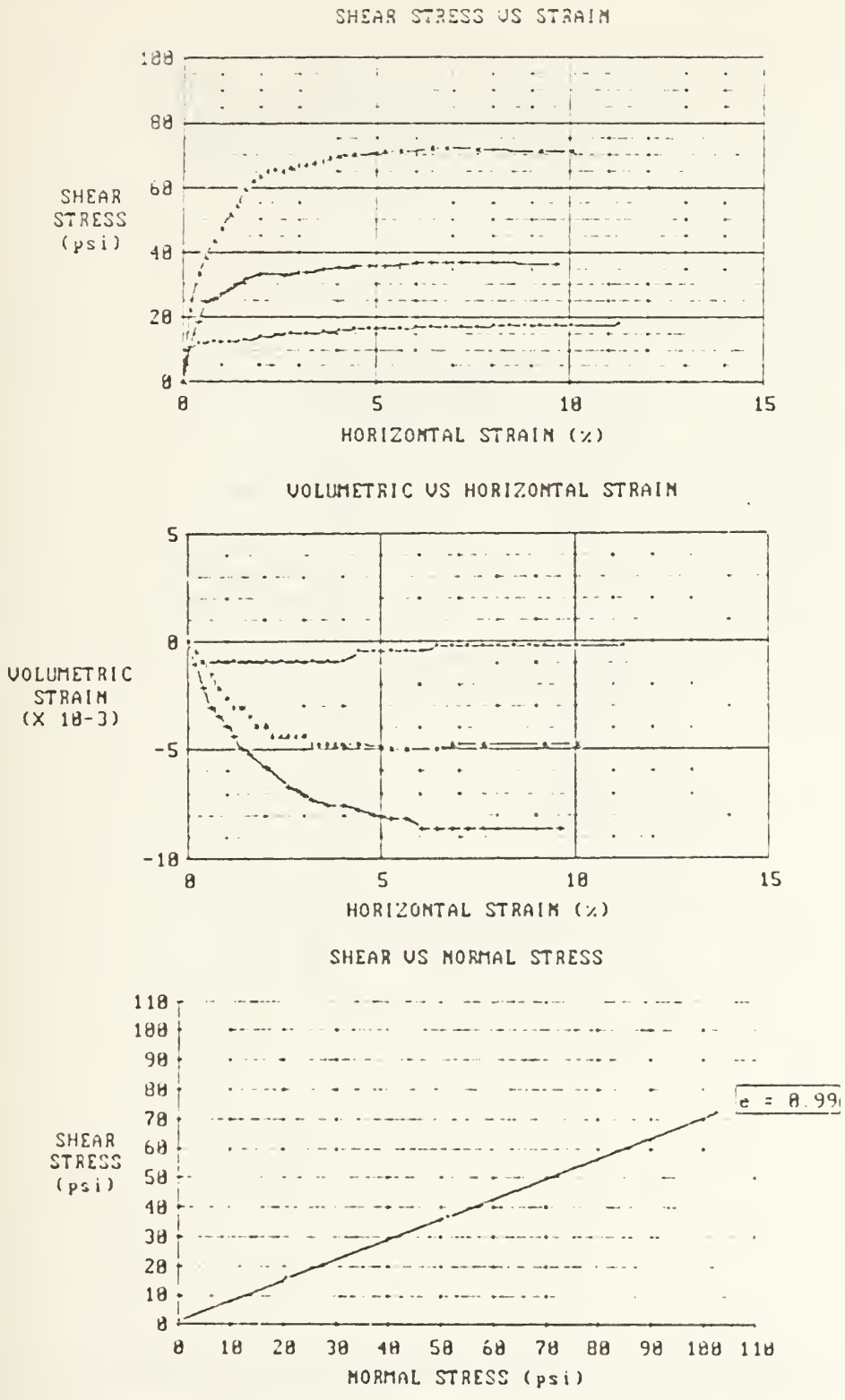

FIGURE 6-6. DIRECT SHEAR RESULTS FOR LOOSE SAND (e = 0.99)

TYPICAL STRESS-STRAIN CURVE
SIGNODE TNX-250 GEOGRID

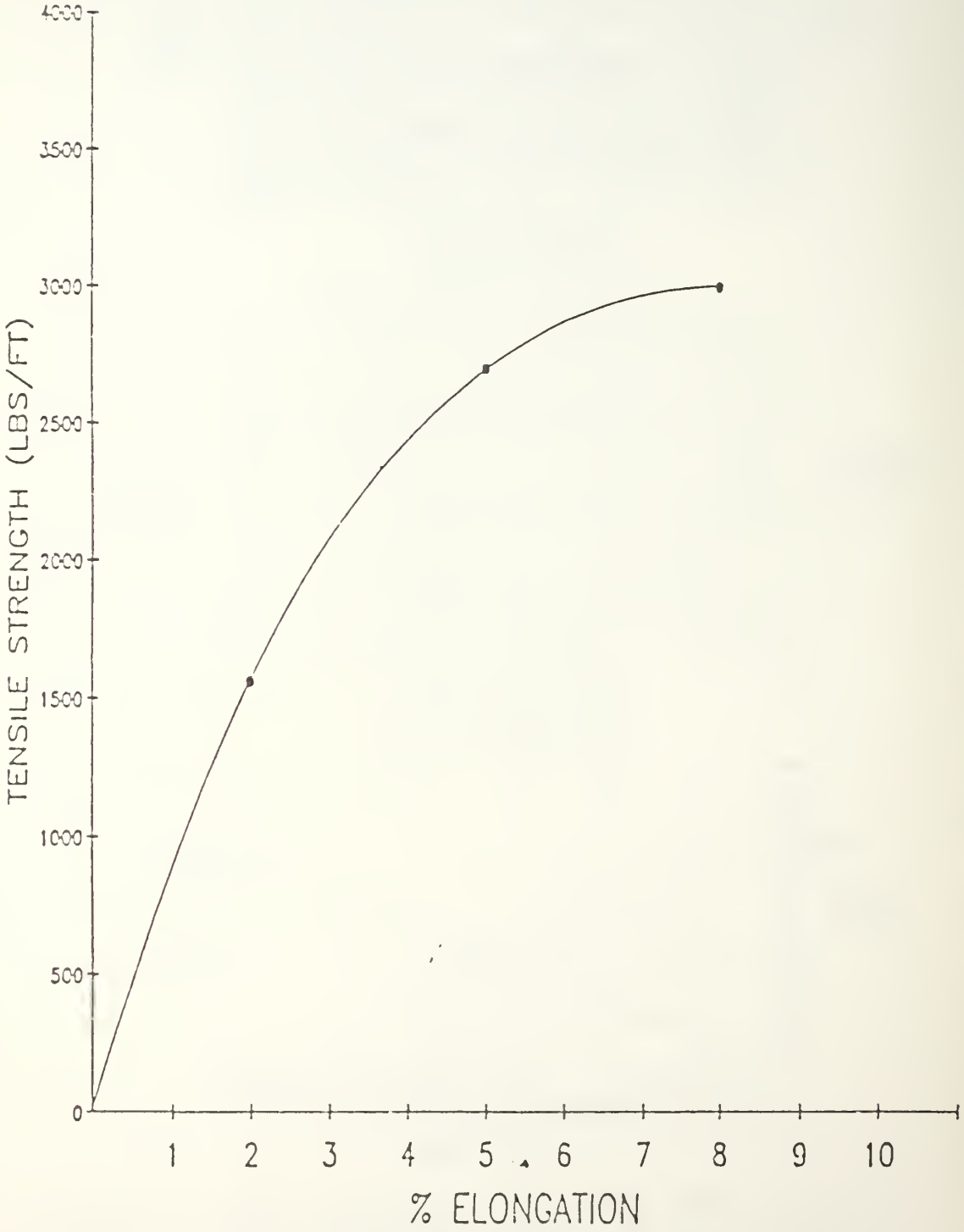

NOTE: WIDE WIDTH STRIP TENSILE STRENGTH TEST. STRAIN RATE - 10%/MIN

FIGURE 6-8. STRESS-STRAIN CURVE FOR UNCONF. TNX-250 1/27/86

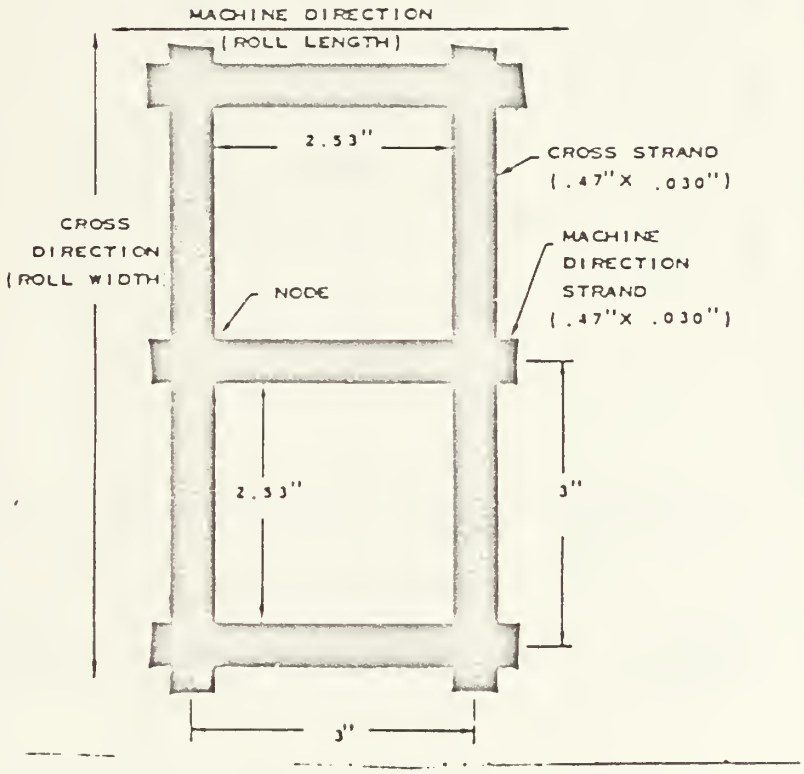

FIGURE 6-7. PHYSICAL CHARACTERISTICS OF SIGNODE TNX-250

TABLE 6-2

RESULTS OF PULLOUT ANALYSES

Test #	Embedment Length (in)	Confining Stress (psf)	Alpha (lbs/ ft)	w %	e	Dr %	Failure Mode
1	42.15	780	4520	8.0	.85	54.7	rupture
2	18.25	780	4666	14.4	.90	43.3	rupture
3	15.19	780	3030	14.6	.83	59.3	pullout
4	15.19	1530	4320	15.2	.82	61.6	rupture
5	12.25	1530	4110	15.3	.83	60.2	pullout

Notes:

1 - Confining stress equals weight of soil above geosynthetic layer plus bladder pressure.

2 - Pullout indicates delamination of all rib members.

3 - Rupture indicates failure of the longitudinal strands.

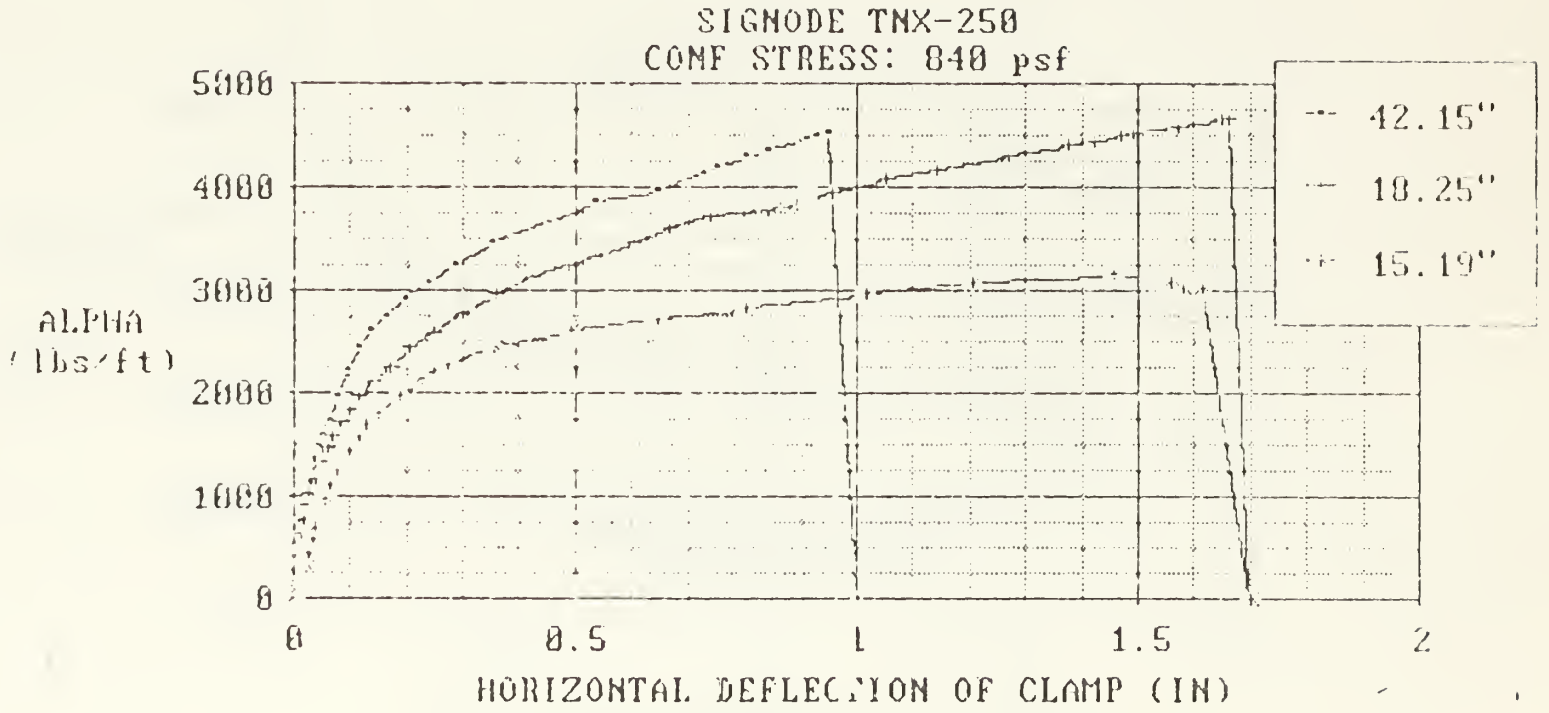

FIGURE 6-9. ALPHA VS HORIZONTAL DEFLECTION FOR THREE DIFFERENT EMBEDMENT LENGTHS AT A CONFINING PRESSURE OF 840 psf.

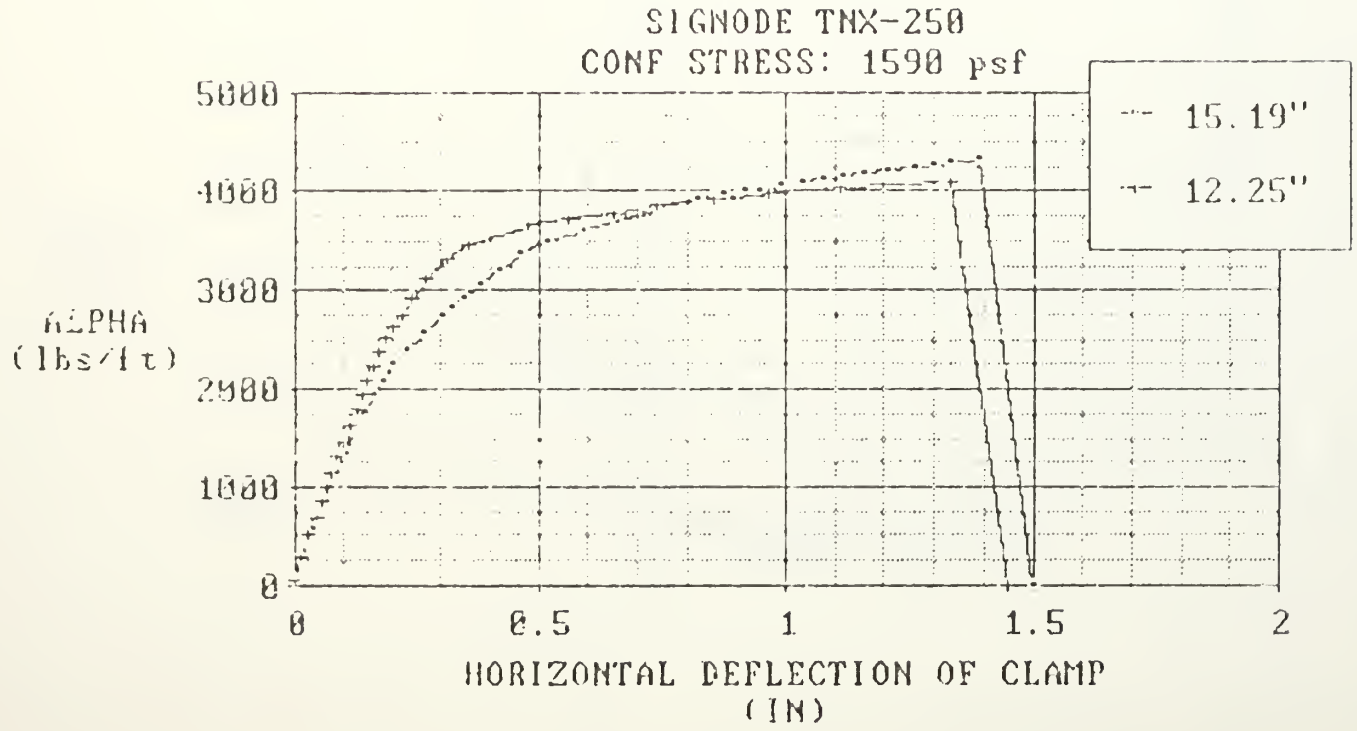

FIGURE 6-10. ALPHA VS HORIZONTAL DEFLECTION CURVES FOR TWO DIFFERENT EMBEDMENT LENGTHS AT A CONFINING PRESSURE OF [%() PSF.

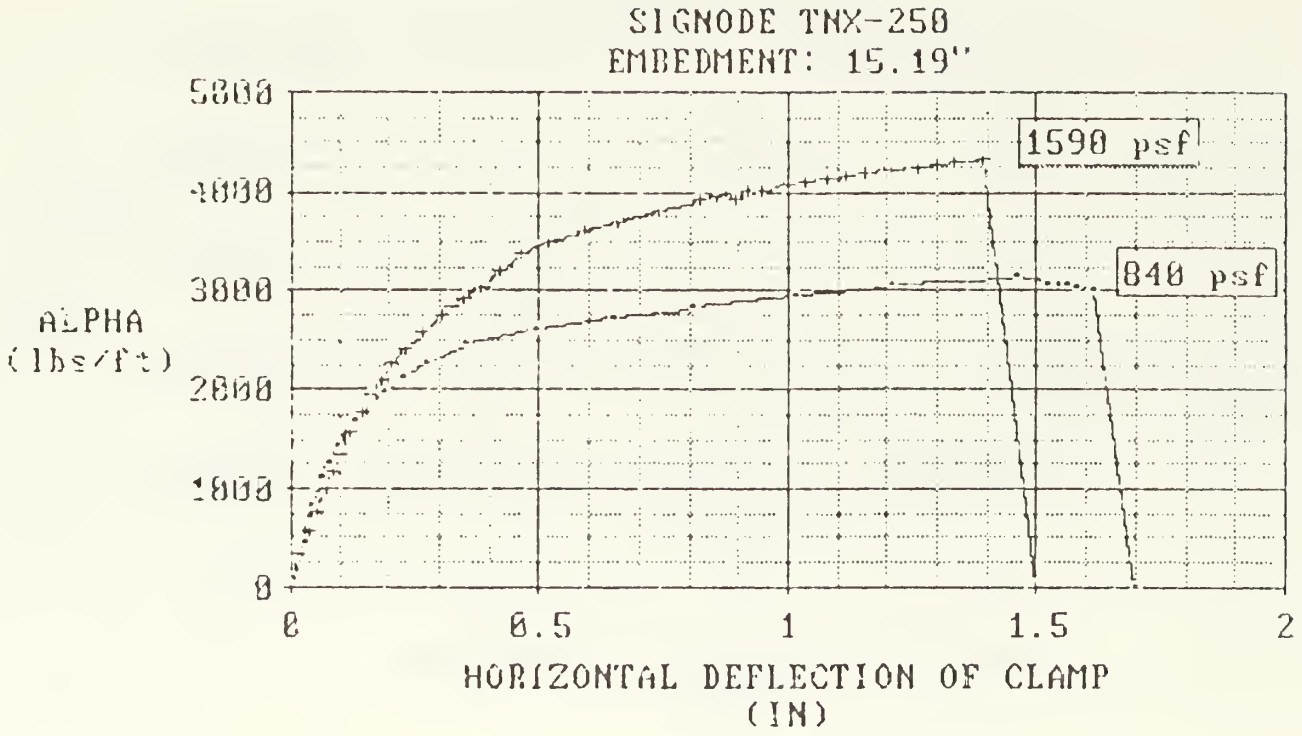

FIGURE 6-11. ALPHA VS HORIZONTAL DEFLECTION FOR SPECIMENS EMBEDDED AT 15.19" AT DIFFERENT CONFINING PRESSURES.

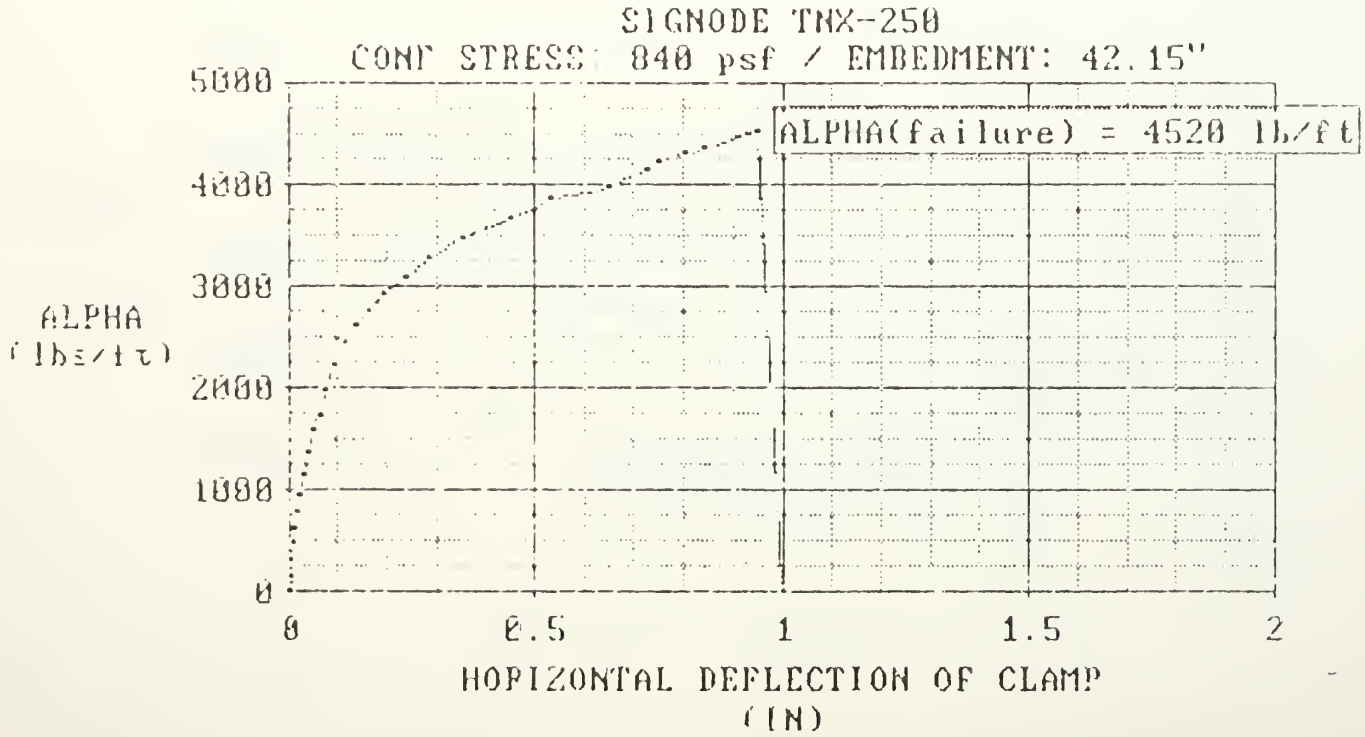

FIGURE 6-12. ALPHA VS HORIZONTAL DEFLECTION FOR AN EMBEDMENT OF 42.15" AND CONFINING STRESS OF 840 PSF.

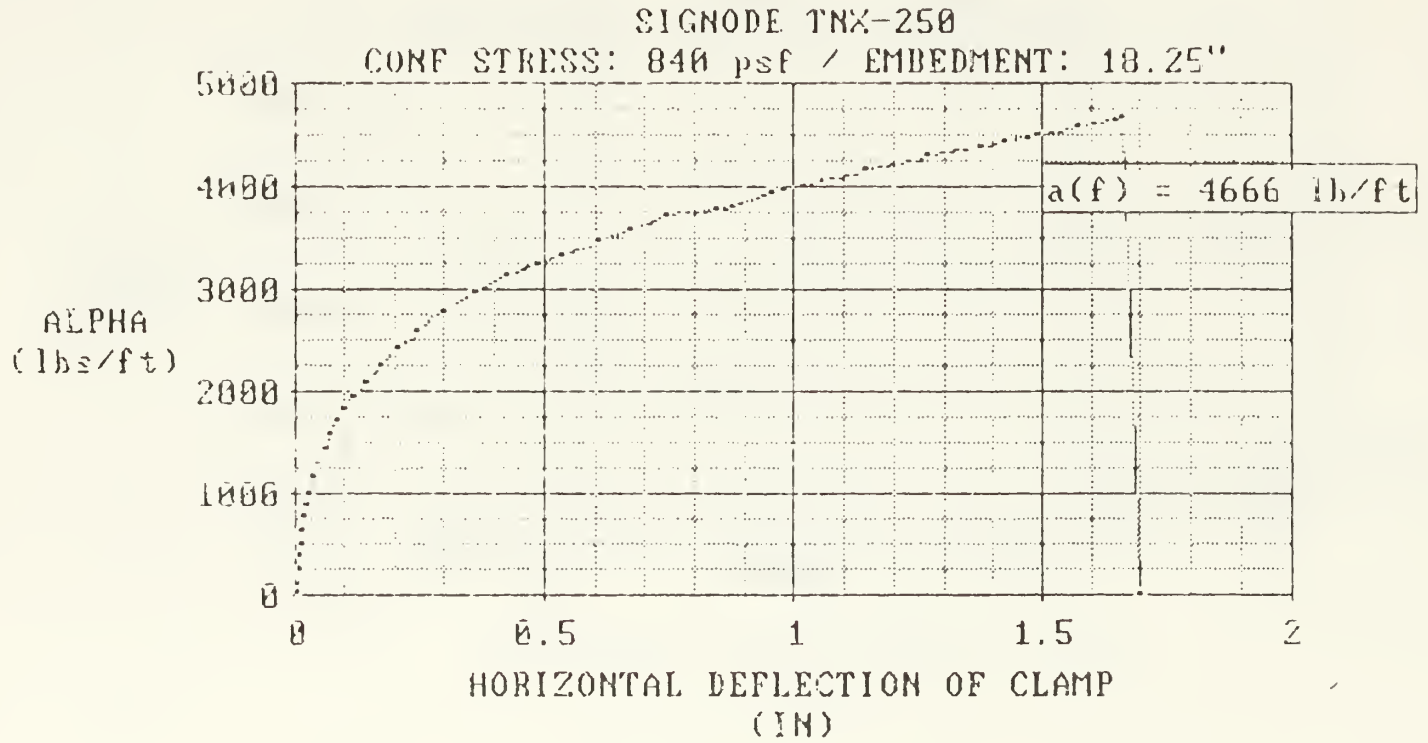

FIGURE 6-13. ALPHA VS HORIZONTAL DEFLECTION FOR 18.25" EMBEDMENT AND CONFINING STRESS OF 840 PSF.

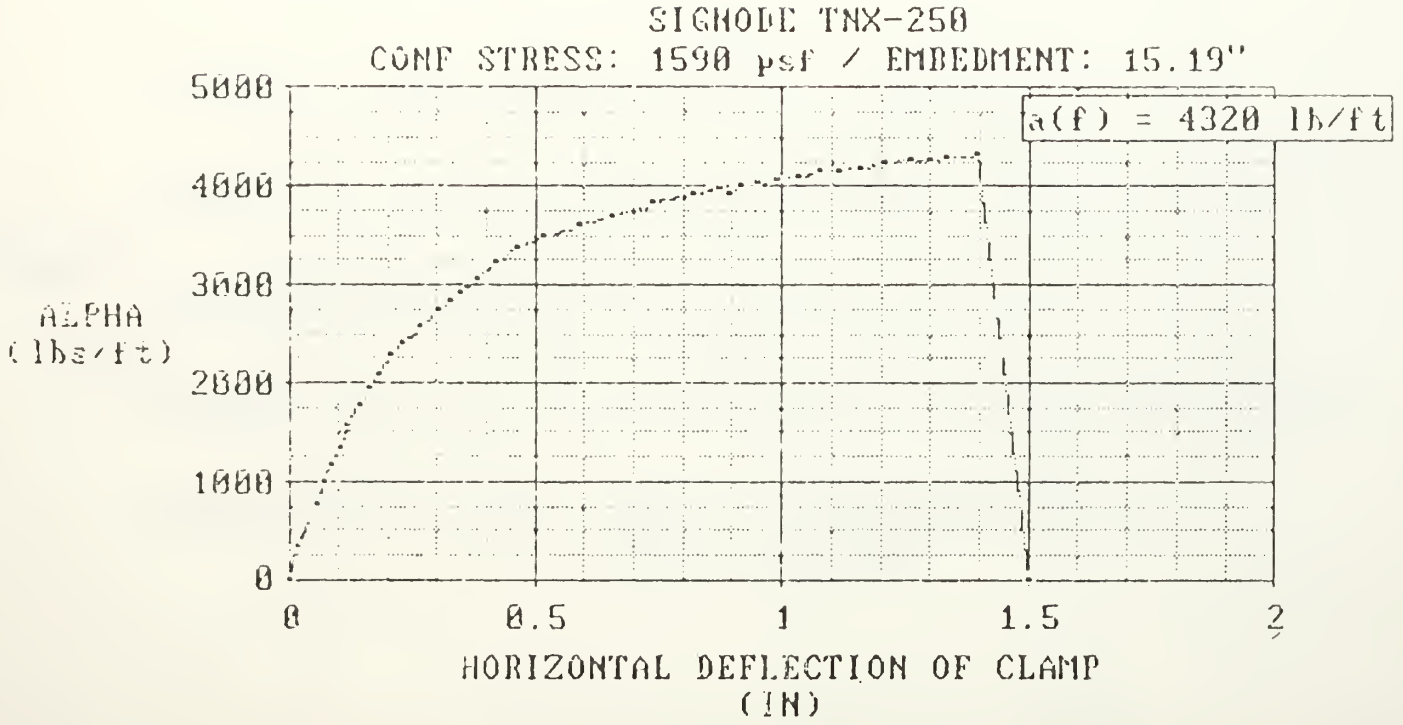

FIGURE 6-14. ALPHA VS HORIZONTAL DEFLECTION FOR EMBEDMENT OF 15.19 AND CONFINING STRESS OF 840 PSF.

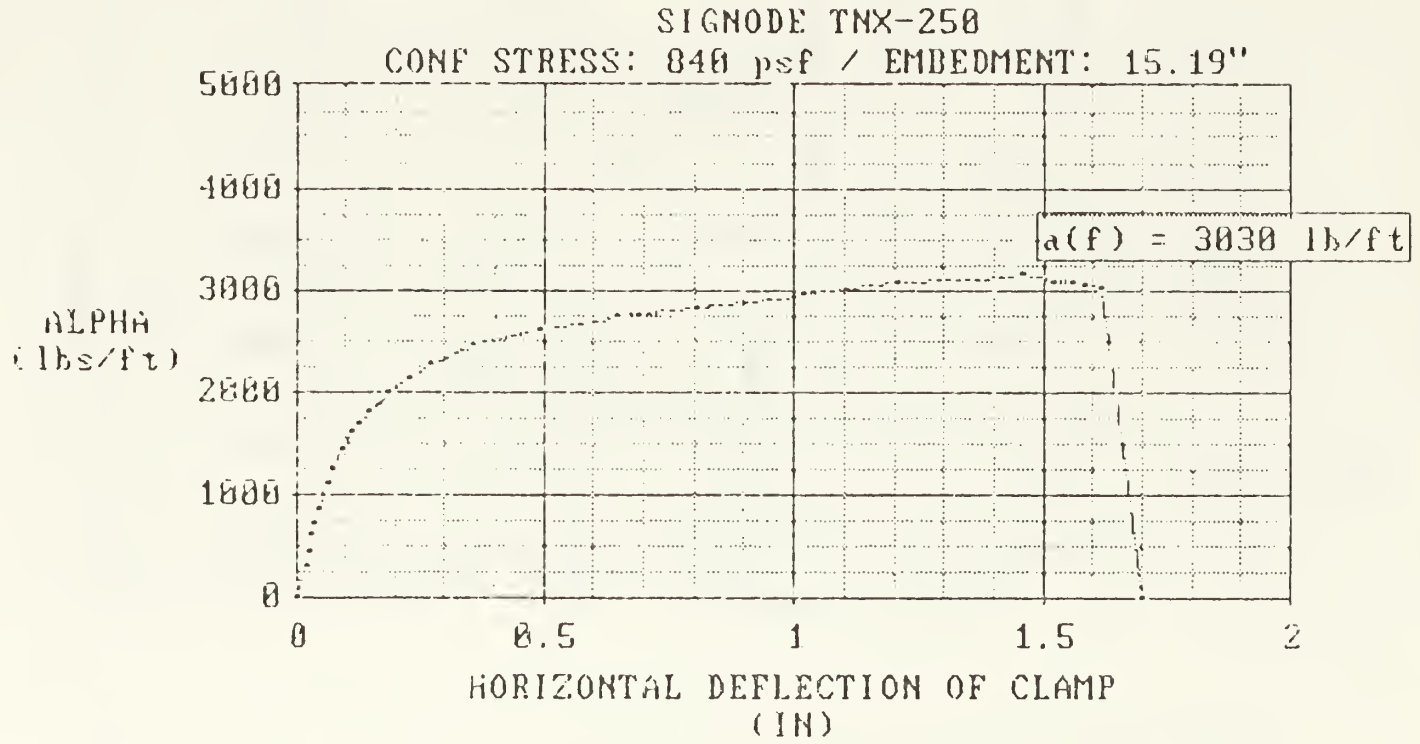

FIGURE 6-15. ALPHA VS HORIZONTAL DEFLECTION FOR AN EMBEDMENT OF 15.19" AND CONFINING PRESSURE OF 1590 PSF.

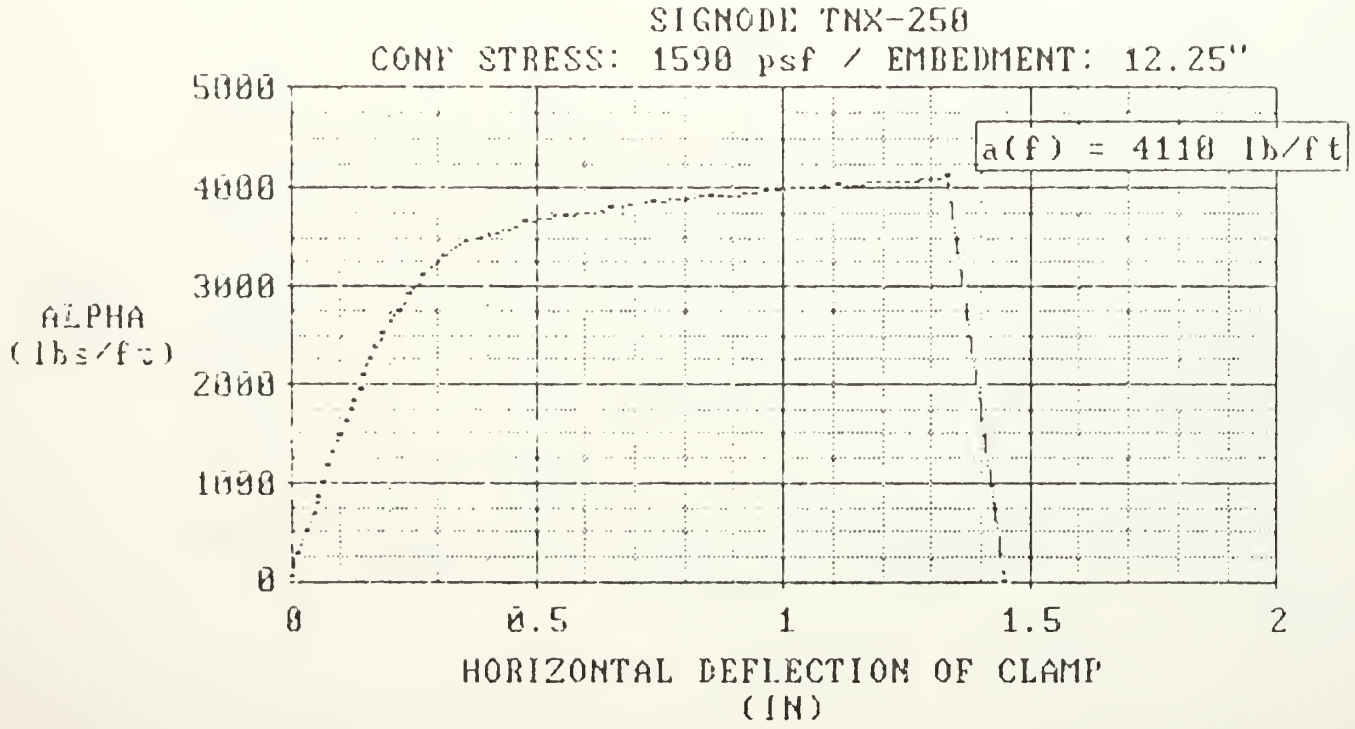

FIGURE 6-16. ALPHA VS HORIZONTAL DEFLECTION FOR EMBEDMENT OF 12.25" AND CONFINEMENT OF 1590 PSF.

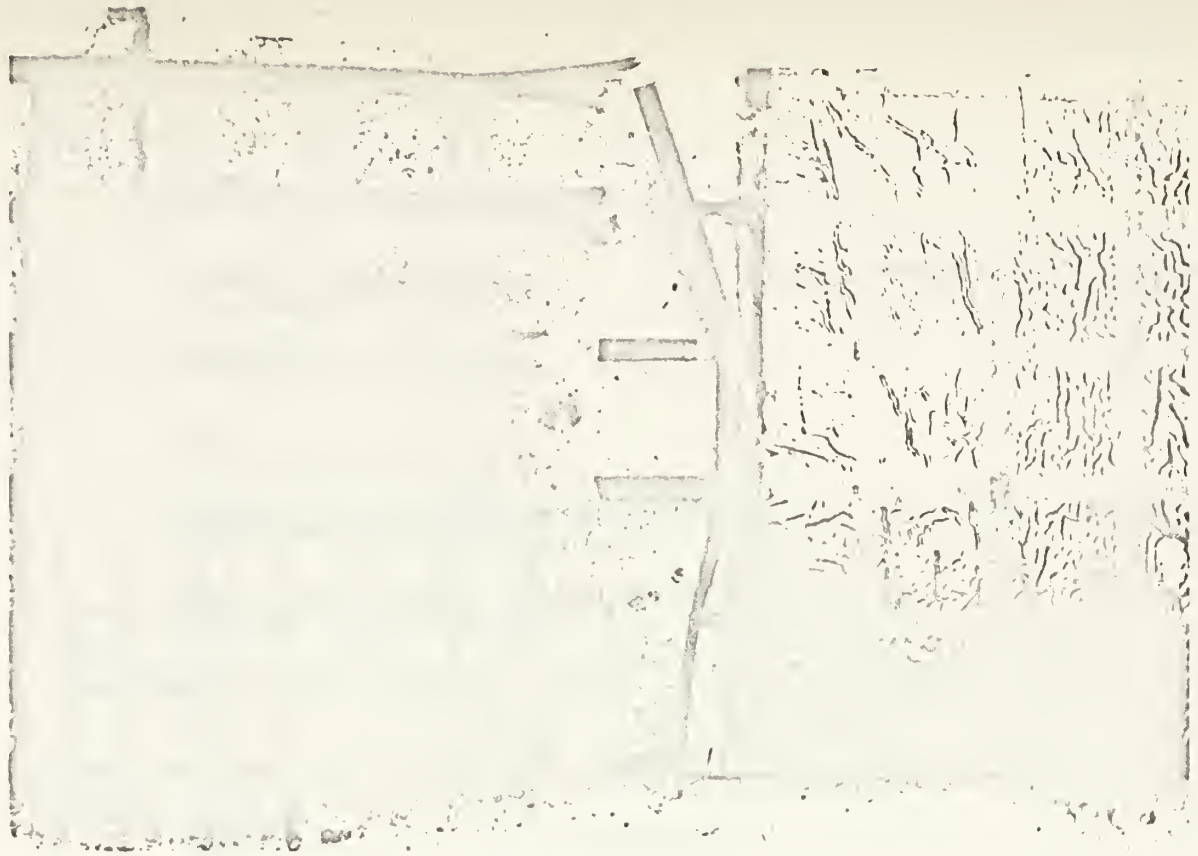

FIGURE 6-17P. PHOTOGRAPH OF GEOGRID EXHIBITING FAILURE OF LONGITUDINAL STRANDS ADJACENT TO CLAMP

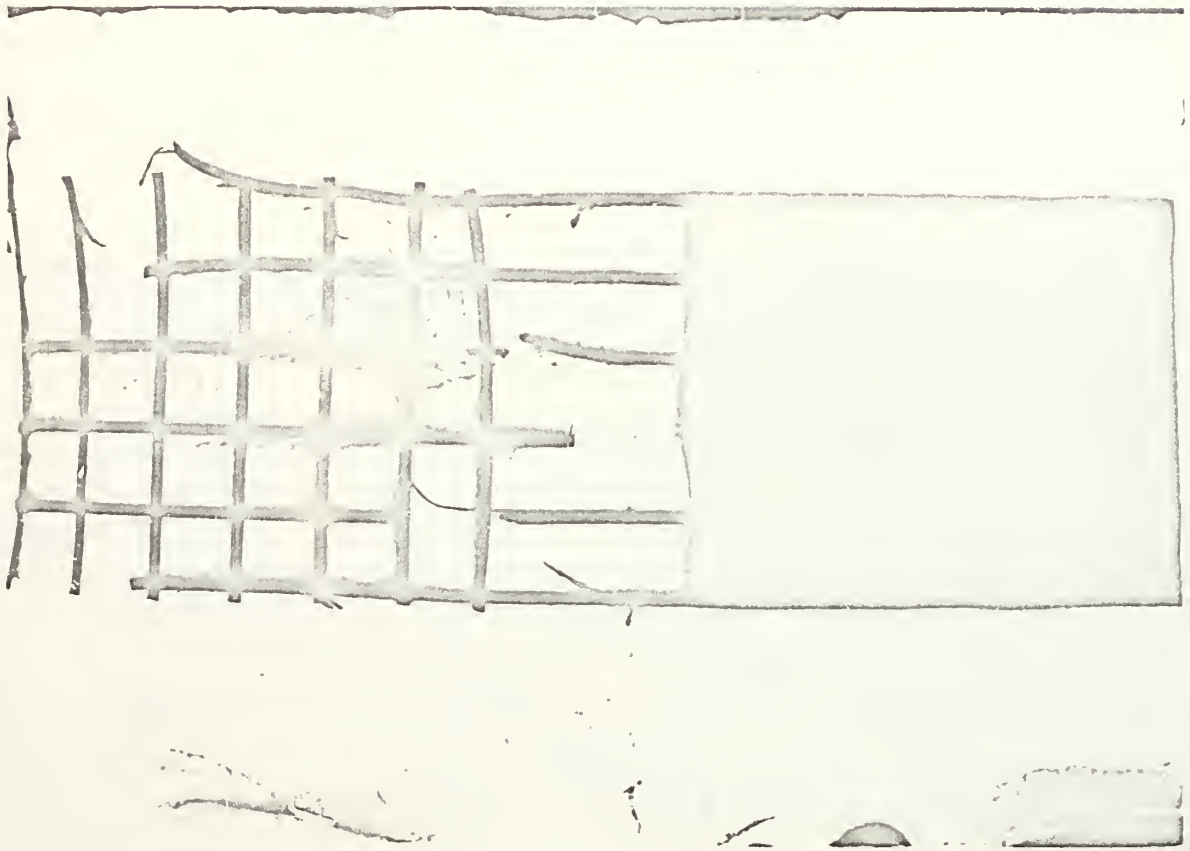

FIGURE 6-18P. PHOTOGRAPH OF GEOGRID EXHIBITING FAILURE DUE TO ROTATION OF THE RIBS

FIGURE 6-19P. PHOTOGRAPH OF GEOGRID EXHIBITING FAILURE BY DELAMINATION OF THE RIBS

CONCLUSIONS

The rate at which geosynthetics will be used in the construction industry will undoubtably continue to increase. One of the major unknowns in the design of geosynthetic reinforced structures is the creep and confined tension behavior of the composite structure. A better understanding of confined tensile strength and creep of geosynthetics will lead to better predictions and more cost effective designs.

Confined tensile strength and creep of geosynthetics are complex processes which are a function of several parameters. These parameters can be broken down into three broad areas: those pertaining to soil characteristics, those pertaining to the geosynthetic properties and, those pertaining to the environment.

Presently three methods have been developed for the analysis of confined tensile creep and confined tensile strength: a direct shear test, a pullout analysis and the triaxial test. Many of the devices used in the analyses, however, have severe limitations due to the boundary conditions imposed by the device. These boundary conditions may drastically affect results.

Numerical models have been proposed for the analysis of polymer creep in-isolation and for soils. No model,

however, has yet been developed for the two materials working as a composite.

A Large Scale Pullout / Creep Device (LSPCD) has been designed, fabricated and tested at various boundary conditions. The LSPCD has a broader range of loading capability than previous instrumentation. Confining stresses may range between 0 and 14400 psf. Pullout loads up to 16330 pounds may be attained with the device.

A concrete sand was utilized in this investigation. The void ratio of this sand was easily controlled through the use of either the manually operated ram or the pneumatic drop hammer. The manually operated ram was chosen for most of the tests as it did not scatter the soil as much as the pneumatic hammer.

For the geogrid tested in this investigation the following conclusions may be drawn:

1. The confined tensile strength of the geogrid is typically higher than the wide width tensile strength. For the boundary conditions evaluated, an increase in tensile strength of 150% was measured for the Signode TNX-250 geogrid.

2. Under conditions of equal confining stress, geogrids shorter in embedment length will fail at lower confined tensile strengths and with larger horizontal deflections.

3. Under conditions of equal confining stress, failure of the geogrid occurs at distances further away from the clamp until the geogrid is of such length to produce pullout. Therefore, embedment length may significantly affect stress and strain distribution in the geogrid.

4. Relatively small deflections were required for the material to achieve high confined strength. Therefore, the SIGNODE TNX 250 geogrid is an ideal material for use in retaining walls where large deflections would be intolerable.

5. Under conditions of equal embedment length, increased pressures will result in larger confined tensile strengths and decreased horizontal deflections.

6. The mechanisms of stress and strain vary under different boundary conditions. Three possible failure modes exist under different cases of boundary conditions:

- Mode I:

In this mode the geosynthetic is placed under a high normal stress (σ_n) and/or has a large embedment length (Le). The total force developed (α_f) in the geosynthetic is the result of two factors; the tensile strength (T_1) of the longitudinal strands and; the shear forces which are mobilized on the failure plane in the soil. Because of the confining stress and/or the anchoring mechanism provided by the embedment length, translation of the ribs is prevented. Thus, the longitudinal strands adjacent to the clamp are under high levels of strain. The increasing stress results in rupture of the longitudinal members adjacent to the clamp.

- Mode II:

Moderate confining stresses and/or a moderate embedment length characterized this mode. The total force developed within the geosynthetic is the result of the delamination strength of the nodes and the shear strength mobilized on the failure plane in the soil. The geogrid translates due to the moderate confining pressures and/or the shortened embedment length. This translation results in a rotation of the ribs. When translation continues, the ribs delaminate

from the longitudinal stands. However, prior to delamination, stress concentrations develop in the area adjacent to the node which may result in failure of the longitudinal member prior to delamination. The failure mode is characterized by a large translation of the nodes, deflection and rotation of the ribs, stress concentrations at the nodes and delamination of the ribs.

- Mode III:

Low confining stresses and/or small embedment lengths characterize this mode. The shear stress at he interface is the only component which results in the development of force in the geogrid. Due to the low level of confinement large translations may be expected with small deflections of the ribs. The grid would be expected to distort very litle in this mode. The conclusions regarding Mode III have not been confirmed by analyses, however.

LSPCD RECOMMENDED MODIFICATIONS

The following improvements are recommended to provide either more efficient operation of the device and more accurate data which may be duplicated in other laboratories.

1. Modify the pressure system to provide strain rate control. Presently the system is stress controlled. More consistent results will be obtained with the introduction of strain control.

2. The LSPCD is presently manually operated by altering regulator pressure. In conjunction with strain control, a control panel would greatly facilitate operation of the device. The control panel would integrate all mechanisms for the device.

3. If geosynthetics continue to be tested which are of lengths substantially shorter than the LSPCD, a channel should be attached to the side panels and a shorter lid constructed. This would facilitate lid removal, extraction and recompaction of the soil.

RECOMMENDATIONS FOR FURTHER RESEARCH

Several avenues of approach may be taken using the LSPCD as either a design or research tool. These recommendations are listed below.

1. Creep experiments were not conducted in this investigation. Creep studies should be carried out and comparisons made to Rate Process Theory, the Mitchell-Singh model and other numerical relationships.

2. Much work remains in the development of constitutive relationships for confined geosynthetic creep. These relationships would both benefit in the physical and chemical design of the geosynthetic and in the design of structures utilizing geosynthetics.

3. Tests conducted in this investigation were conducted on one geogrid in a particular soil. In practice, a variety of soils and conditions will be encountered. Pullout and creep behavior of geosynthetics encapsulated in these other materials should be investigated.

4. In the pullout device, stresses and strains are maximum at the clamp and progress to zero at the free end. Presently, no method has been developed which can accurately measure these varying strains. Work is

presently underway at the Georgia Institute of Technology to utilize a plexiglass pullout box and X-ray analyses to monitor the strains of a geosynthetic impressed with lead beads.

5. Only a limited range of pressures was used in this investigation. Void ratios were kept approximately constant. Properties and conditions need to be varied over a larger range in order to develop meaningful relationships between these parameters.

6. To verify Mode III, the condition of low confining stress and/or short embedment length, pullout tests should be conducted at low pressures.

REFERENCES

Bell, J.R. and R.G. Hicks, "Evaluation of Test Methods and Use Criteria for Geotechnical Fabrics in Highway Applications", Federal Highway Administration Report No. FHWA/RD-80/021 Contract No. DOT-FH-11-9353, June 1980.

Bonaparte, R., R.D. Holtz and J.P. Giroud, "Soil Reinforcement Design Using Geotextiles and Geogrids", Report presented at Geotextile Testing and the Design Engineer, June, 1985.

Casagrande, A., "Characteristics of Cohesionless Soils Affecting the Stability of Slopes and Earth Fills", Contributions to Soil Mechanics, 1925-1940, Boston Society of Civil Engineers, Oct. 1940.

Christensen, R.W. and T.H. Wu, "Analysis of Clay Deformation as a Rate Process", Journal of the Soil Mechanics and Foundations Division, ASCE, SM6, Nov. 1964.

Christopher, B.R. and R.D. Holtz, Geotextile Engineering Manual, Federal Highway Administration, National Highway Institute, Contract No. DTF61-83-C-00150, Washington D.C., 1984.

Christopher, B.R., R.D. Holtz and W.D. Bell, "New Tests for Determining the Stress Strain Properties of Geotextiles", Proceedings of the Third International Conference on Geotextiles, Vienna, 1986.

Coleman, B.D. and A.G. Knox, "The Interpretation of Creep Failure in Textile Fibers as a Rate Process", Textile Research Journal, May 1957.

El-Fermaoui, A. and E. Nowatzki, "Effect of Confining Pressure on the Performance of Geotextiles in Soils", Proceedings of the Second International Conference on Geotextiles, Las Vegas, 1982.

Findley, W.N., J.S. Lai and K. Onaran, Creep and Relaxation of Nonlinear Viscoelastic Materials, North Holland Publishing Co, Amsterdam, 1976.

Finnie, I. and W.R. Heller, Creep of Engineering Materials, McGraw Hill Book Co., Inc. New York, 1959.

Glasstone, S., K.D. Laidler and H. Eyring, The Theory of Rate Processes, McGraw Hill Book Co., Inc. New York, 1941

Holtz, R.D. and W.D. Kovacs, An Introduction to Geotechnical Engineering, Prentice Hall, New Jersey, 1981.

Holtz, R.D., W.R. Tobin and W.W. Burke, "Creep Characteristics and Stress Strain Behavior of a Geotextile Reinforced Sand", Proceedings of the Second International Conference on Geotextiles, Las Vegas, 1982

LaFeber, D., "Soil Structural Concepts", Engineering Geology, Vol. 1, No. 4, 1966.

Lambe, T.W. and R.V. Whitman, Soil Mechanics, John Wiley and Sons, Inc., New York, 1969.

Lee, Kenneth L., "Mechanisms, Analysis and Design of Reinforced Earth, State-of-the-Art Report", Proceedings of a symposium on Earth Reinforcement, ASCE, New York, 1978.

Martin, J.P., R.M. Koerner and J.E. Whitty", "Experimental Friction Evaluation of Slippage between Geomembranes, Geotextiles and Soils", Proceedings of the International Conference on Geotextiles, Denver, USA, 1984.

McGown, A., K.Z. Andrawes and M.H. Kabir, "Load Extension Testing of Geotextiles Confined in Soil", Proceedings of the Second International Conference on Geotextiles, Las Vegas, 1982.

Mitchell, J.K., "Shearing Resistance of Soils as a Rate Process", Journal of the Soil Mechanics and Foundations Division, ASCE, Vol. 90, SM1, Jan. 1964.

Mitchell, J.K., Fundamentals of Soil Behavior, John Wiley and Sons, Inc., New York, 1976.

Myles, B., "Assessment of Soil Fabric by Means of Shear", Proceedings of the Second International Conference on Geotextiles, Las Vegas, 1982.

Onaran, K. and W.N. Findley, "Combined Stress-Creep Experiments on a Nonlinear Viscoelastic Material to Determine the Kernel Functions for a Multiple Integral Representation of Creep." Transactions of the Society of Rheology, 9:2, 299-327, 1965.

Rowe, P.W., "The Stress Dilancy Relations for Static Equilibrium of an Assembly of Particles in Contact", Proceedings, Royal Society, London, Series A, Vol. 269, 1962.

Shrestha, S.C. and J.R. Bell, "Creep Behavior of Geotextiles

Under Sustained Loads", Proceedings of the Second International Conference on Geotextiles, Las Vegas, 1982.

Singh, A. and J.K. Mitchell, "General Stress-Strain-Time Function for Soils", Journal of the Soil Mechanics and Foundations Division, ASCE, SM1, Jan. 1968.

Skempton, A.W., "Effective Stress in Soils, Concrete and Rocks", Selected Papers on Soil Mechanics, Thomas Telford, London, 1984.

Sowers, G.F., Introductory Soil Mechanics and Foundations: Geotechnical Engineering. MacMillan Publishing Co., Inc., New York, 1979.

Terzaghi, Karl, Theoretical Soil Mechanics, John Wiley and Sons, New York, 1948.

Terzaghi, Karl, From Theory to Practice in Soil Mechanics. John Wiley and Sons, New York, 1960.

Vidal, M.H., "The Development of Reinforced Earth, Earth Reinforcement, Proceedings of a Symposium, ASCE, New York, Apr. 1978.

Williams, N.D., Personal communication, 1986.

Williams, N.D. and M. Houlihan, "Evaluation of Friction Coefficients Between Geomembranes, Geotextiles and Related Products", Proceedings of the Third International Conference on Geotextiles, Vienna, 1986.

Williams, N.D. and M. Houlihan, "Interface Friction Parameters", Report to be published at New Orleans International Geotextile Conference, 1987.

APPENDIX A: DATA2.BAS USER'S MANUAL

DATA2 is a basic program which is used to:

1. Assign the starting address of the LABMASTER board,
2. Receive input parameters of specimen geometry and time,
3. Provide flexibility to the user with regard to testing interval,
4. Retreive digital data from the A/D converter,
5. Mathematically convert the digital data to force or displacement and,
6. Print the results.

Variables utilized in the program are listed on Table A-1.

Program Operation

After the computer is booted with the MS-DOS systems disk the proceedures listed below are followed:

1. Replace the DOS systems disk with the LABPAC 2.1 disk, at the A prompt type:

   A> Labpac

2. When the A prompt reappears type:

A> Basica

3. Load the DATA2 program by depressing the F3 function key and typing:

load"DATA2

4. Hit the F2 function key to execute the program.

5. The program will request two input parameters, specimen width and time. Enter the specimen width in inches and the time in the format HH:MM:SS.

6. Values for the LVDT, ALPHA, load and time are displayed on the screen. The LVDT is adjusted to the limit of its linear range.

7. Ctrl-PrtSc is depressed to send results to the printer.

8. Selected data points are entered onto disk for access by MICROSOFT CHART software.

TABLE A1

VARIABLES FOR DATA2

Computer Variable	Description	Units
W	Specimen Width	Inches
T$	Time	HH:MM:SS
VOLTAGE	Voltage reading from A/D Converter	mV
DEFL	Deflection at the Clamp	Inches
LBS	Force measured at the Clamp	Pounds
ALPHA	Force per unit width at the Clamp	lbs/ft

```
LIST
11 REM
12 CLS
20      INPUT "SPECIMEN WIDTH (IN.)";W
40      INPUT "DELAY IN SECONDS BETWEEN SAMPLINGS";S
51      ADDRESS = 784
52      S=S*5.6
53      A=0
65      INPUT "TIME(HH:MM:SS) =";T$
66      TIME$=T$
70 FOR I=0 TO 1 STEP 1
72      IF A=0  THEN GOSUB 1000
74      A=A+1
80 REM disable auto-incrementing, external start conversions, and all
90 REM interrupts.  panel.
100 OUT ADDRESS+4,128
110 REM output channel number
120 OUT ADDRESS+5,I
130 REM start a conversion.
140 OUT ADDRESS+6,0
150 REM wait until bit 7 of status byte is a 1 signaling done converting
170 REM read in the data .
180 LOW = INP( ADDRESS + 5 )
190 HIGH = INP( ADDRESS + 6 )
200 REM convert from twos complement to a number between -10 and 10
210 X = 256*HIGH + LOW
220 IF X > 32767 THEN X = X-65536!
230 VOLTAGE = X/204.8
240     IF I = 1 GOTO 270
250     DEFL = 1/10*VOLTAGE +1
270     LBS = [illegible] = VOLTAGE
280     NEXT I
290     ALPHA=LBS*12/W
300     F$="               #####.####     #####.###      #####.###       \
   \"
310     PRINT USING F$;DEFL,LBS,ALPHA,TIME$
320     FOR I = 1 TO S*1000:NEXT I
340     IF A=104 THEN A=0
380     GOTO 70
1000    REM SUBROUTINE SPACE
1040    PRINT CHR$(15)
1050    PRINT
1060    PRINT
1250    PRINT "                    UNIT (IN)      LOAD LBS      ALPHA (G/FT)       T
IME"
1260    PRINT
1280    RETURN
0
```

	δ(in)				δ̇(in/m)
	0				
	.002				
	.008				.004
	.007				.001
	.011				.001
	.013				.001

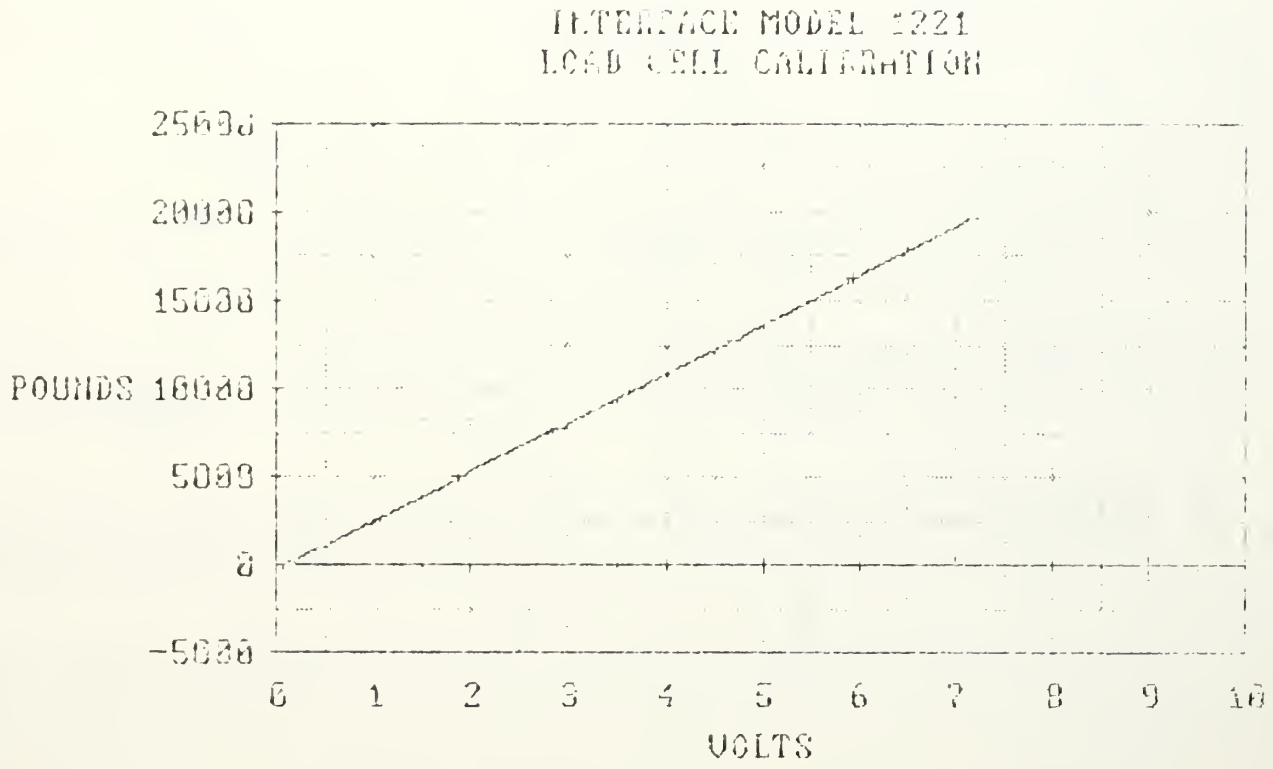
INTERFACE MODEL 1221
LOAD CELL CALIBRATION
25000
20000
15000
POUNDS 10000
5000
0
-5000
0
1
2
3
4
5
6
7
8
9
10
VOLTS

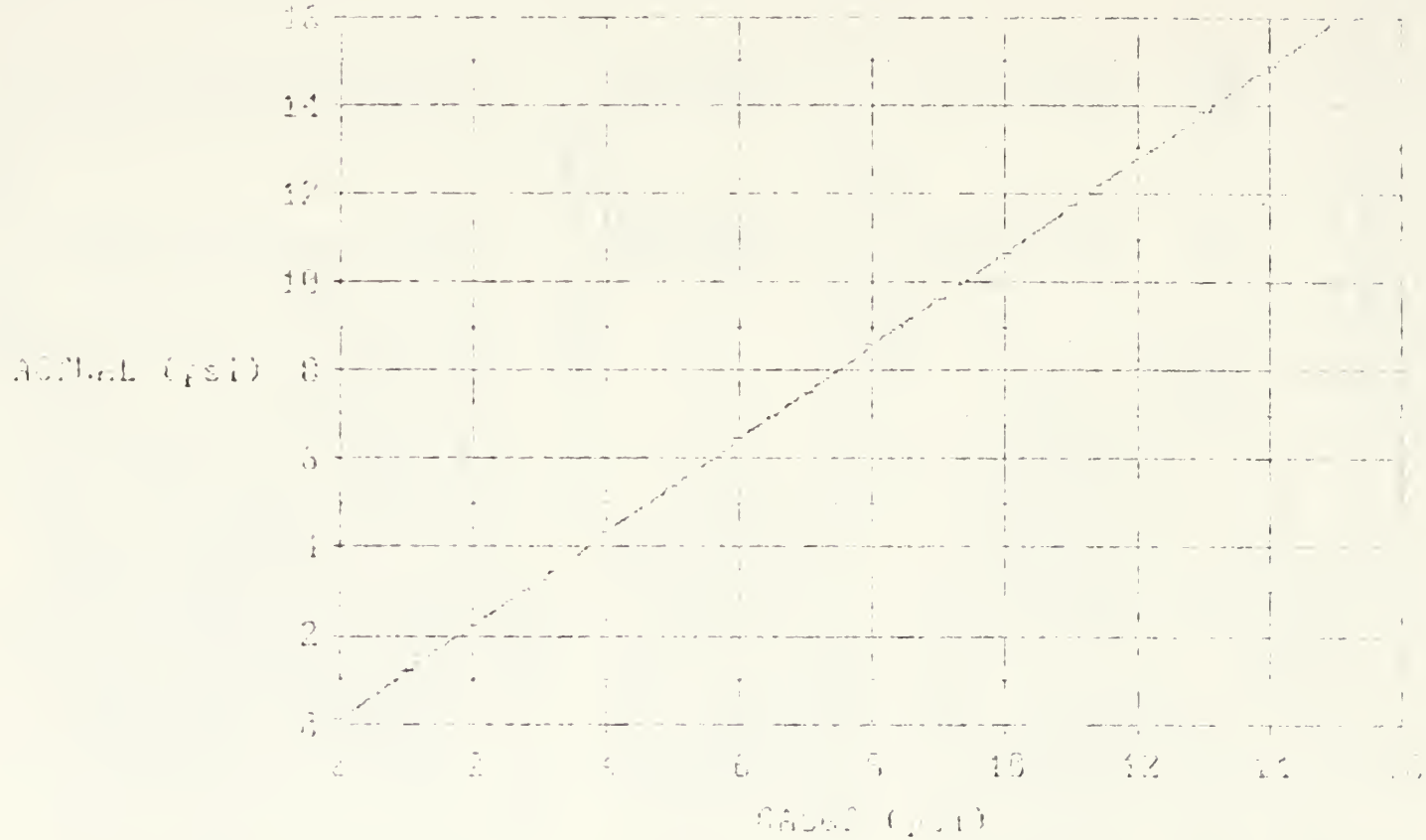
16
14
12
10
8
6
4
2
0
2
4
6
8
10
12
14
16

APPENDIX C. LSPCD MATERIALS LIST

Items listed are those purchased in the fabrication of the LSPCD. Vendor codes as noted below are attached following this appendix.

ITEM, SIZE		QUAN	VENDOR	COST
I. PULLOUT BOX				
Steel Channel	C 8 X 18.75	20'	GI	120
Steel Plate	58 X 24 X 1/2	2	GI	190
Steel Plate	6 X 18 3/8 X 1/2	4	T	51
Steel Bar	1/2 X 1 X 12	12'	T	12
Angle Iron	L 3 1/2 X 2 1/2 X 1/4	20'	T	22
Bolts, nuts A 325	5/8 X 2"	100	F	65
Channel Washers 5/8"		100	F	40
		Subtotal, box:		500
II. CLAMP ASSEMBLY				
Steel Channel	C 3 X 4.1	28"	GI	10
Steel Channel	C 6 X 8.2	78"	GI	20
Steel Channel	C 4 X 7.25	22"	T	18
Steel Bar	1/2 X 2	12'	T	17
Epoxy, Magnobond 2014		5 gal	MP	115
Curing Compound 346		5 gal	MP	100
		Subtotal, Clamp:		280
III. PRESSURE SYSTEMS				
Hydraulic Cylinders, Dayton Z196A		2	G	300
Valve, HP, Speedaire		2	G	15
Hose, Flexible, HP, 4Z217 3/8 X 60		3	G	68
Hose, Flexible, HP, 4Z218 3/8 X 96		2	G	80
Adapter, 6X834		10	G	15
Adapter, Hydr 90, 1A164-1, 1/2 X 3/8		4	G	12
Pipe, Male 90 elb, 6X836-7, 3/8		4	G	10
Regulator, Oxweld 998335		1	M	13
Regulator, Smith H1883-580		1	M	220
Nitrogen Tanks 2250 wp		4	H	50
Pipe, sched 40, 10" ID X 12"		1	T	80
Steel plate, 3/4 X 12 X 12		2	T	40
Rod, Threaded, 5/8-13		12'	F	14
Rubber, Neoprene, 1/8 X 30 X 60"		1	GR	75
O-ring, 10" ID, neoprene, 1/8" dia		6	DP	21
		Subtotal, Press Sys:		1135

ITEM, SIZE	QUAN	VENDOR	COST
IV. DATA ACQUISITION SYSTEM			
Load Cell, Interface Model 1221	1	I	605
LVDT Schaevitz, 3000 HR	1	S	320
Signal Conditioner, ATA 101	1	S	415
Subtotal, DAS:			1340
SYSTEM COST, TOTAL:			3255

VENDOR LISTING

Code	Company	Phone
F	Fasteners of Georgia 4777 Fulton Industrial Blvd Atlanta 30336	691-8301
G	W.W. Grainger, Inc. 2255 NW PKWY SE Marietta 30067	955-8758
M	Miller Arc Welding Equip Pye Barker Welding Supply Co 871 Wheeler St NW	875-7561
GR	Georgia Rubber 1643 Chattahoochee Ave NW Atlanta	355-0830
T	Tull Metals Co 6058 Bunt Roc Blvd SW Atlanta	449-1611
H	Holox Co 600 Northside Dr NW Atlanta	524-0242
I	Interface c/o Electro South 1009 Sun Valley Dr Roswell 30076	993-6245
S	Schaevitz US Route 130 & Union Ave Pennsanken, NJ	(609) 662-8000
GI	Gainesville Iron Works (Charles Davis) 890 Main St SW Gainesville, GA 30501	521-3356
DP	Dixie Packaging Co 1009 Marietta NW Atlanta, GA 30318	874-6026
MP	Magnolia Plastics 5547 Peachtree Ind Blvd Chamblee, GA	451-2777

TWO YEAR WARRANTY

Interface, Inc hereby warrants all products of its manufacture as follows: Commencing with the date of shipment of each load cell to the original purchaser, and for a period expiring two years from said date, Interface, Inc. warrants that each unit shall remain free from defects in parts, materials, and workmanship.

The warranties herein shall not obligate Interface, Inc, in any manner whatsoever with respect to, and shall not be applicable to, any defects which after inspection by Interface, Inc are not to Interface, Inc.'s reasonable satisfaction demonstrably the result of defective parts, materials or workmanship. Interface is not liable for consequential or contingent damages and its liability is strictly limited to the original purchase price of the product or its repair or replacement at Interface's option. The factory should be immediately notified of suspected warranty claims. All transportation and insurance charges for returned merchandise are to be prepaid and borne by customer.

The foregoing warranty is in lieu of any and all other warranties or guaranties expressed or implied and of all other obligations on the part of Interface product which has been repaired or altered by persons unauthorized by Interface, has been subject to misuse, negligence or accident, or has been installed, adjusted or used otherwise than in accordance with the instructions furnished by Interface, Inc.

CERTIFICATION

Interface, Inc. certifies that this load cell was thoroughly tested and inspected and found to meet its published specifications when shipped from the factory. Interface, Inc. further certifies that its calibration measurements are traceable to NBS.

INSTALLATION

The load cell should be mounted on a surface which is flat and parallel within 0.0002 T.I.R. for Universal, and within 0.0005 T.I.R. for compression units. It should be mounted to the surface with grade 8 bolts evenly tightened to the following torques:

Bolt Size	1/4-28	1/4-28	5/16-24
Installation Torque (ft.-lbs.)	5 (Alum Load Cell)	10 (Steel Load Cell)	25

Bolt Size	3/8-24	7/16-20	1/2-20	5/8-18
Installation Torque (ft.-lbs.)	45	80	120	250

The load cell mating thread should be class 3.

interface

Load Cell

CALIBRATION CERTIFICATION

WARRANTY

INSTALLATION INFORMATION

Customer (illegible)

Model 1221-1K-25K

CALIBRATION

Bridge*	Date	9-2-86
Range 25,000 lbs.	Serial No.	35680
Input Resistance	351.1	ohms
Output Resistance	351.1	ohms
Recommended Excitation		10 VDC or VAC
Maximum Excitation		20 VDC or VAC
Non-linearity (terminal) (Above 2K refer to NOTES)	—	%FS
Hysteresis (Above 2K refer to NOTES)	—	%FS
Compensated Temp. Range	+15 °F to +115	°F
Thermal Zero Shift	0.0008	%FS/°F
Zero Balance	0.45	%FS
Tension Output	—	mV/V
Compression Output	4.234	mV/V

*For multiple bridge load cells

WIRING

Function	Pin		Pigtail	
	Tens.	Comp	Tension	Compression
+Excitation	A	A	Red-Wht/Red	Red-Wht/Red
+Output	B	C	Green	Wht-Wht/Yel
−Output	C	B	Wht-Wht/Yel	Green
−Excitation	D	D	Blk-Wht/Blk	Blk-Wht/Blk
Shield				

Polarity shown results in positive output

SHUNT CALIBRATION

— ohms −Exc. to −Out. — lbs.

59K ±0.01% ohms @ 10V −Exc. to +Out. 12134.7 lbs.

Calibrated by DS

NOTES:

STATIC ERROR BAND — The band of maximum deviations of the calibration curve from the best fit line through zero including the effect of Non Linearity, Hysteresis and Non-Repeatability, expressed as a percentage of Rated Output.

± — In Tension

± 0.019 In Compression

For Universal model load cells, use of a jam nut is recommended in order to reproduce conditions of calibration and to achieve best performance. See Installation Information for jam nut installation instructions.

NOTES:

INTERFACE, INC.
7401 EAST BUTHERUS DRIVE • SCOTTSDALE, ARIZONA 85260
TLX 825-882 TELEPHONE (602) 948-5555 USA

engineering

LINEAR VARIABLE DIFFERENTIAL TRANSFORMERS
TEST AND INSPECTION DATA

Type 1000 HR Serial No. 3634 Range ± 1.000"

PLEASE READ BEFORE USING THIS TRANSDUCER

This measurement device is manufactured to high precision standards. Our factory checks prior to shipment assure its performance. To obtain the optimum performance in your application, handle and install with care. Do not machine, grind or tap core and coil assembly. Core and coils are matched sets; for best performance do not interchange cores.

TEST CONDITIONS

Primary Connections: yel/black and yel/red
☒ grounded ☐ not grounded

Secondary Connections: black and red
☒ grounded ☐ not grounded

Secondary Midpoints: (a) green (b) blue
☒ (a) tied to (b) ☐ (a) not tied to (b)

Case Connections: ☐ grounded ☒ not grounded

Primary Excitation: 3 volts at 2500 Hz

Secondary Load: 0.5 Meg ohms (in parallel with ___ mfd)

TEST DATA

Displacement: ± 1.000 inches

Output: _____ volts
_____ volts/input volts

Linearity: ± _____ % of full range output

Null (Combined Quadrature and Harmonics): _____ mv (rms)

Output-to-Input Phase Angle: _____ degrees ☐ leading (+) ☐ lagging (−)

Special Tests: _____

INSPECTION

☒ Workmanship ☒ High Voltage Test
☒ Completeness of Assembly

REMARKS

_____

ACCEPTANCE

1-29-86 (O.A. S.E. F17)

Tested by ST 56 Date 1-29-86
Inspected by _____ Date _____
Military Inspection _____ Date _____
(When Required)

SCHAEVITZ engineering

01/29/86

MODEL 1000-HR S N 3634
SCHAEVITZ PART NO.2560395-000

EXCITATION = 3 000 VAC @ 2500Hz

NULL = 1.187 mVrms

INCHES	AC VOLTS	CALC VOLTS	DEVS
-1 00000	-1.156	-1.156	+0 001
-0 80000	-0.925	-0 925	-0 000
-0.60000	-0.694	-0.693	-0 001
-0 40000	-0.460	-0 461	+0 001
-0 20000	-0.229	-0 230	+0 001
+0.20000	+0.231	+0 233	-0 002
+0 40000	+0.464	+0 465	-0 001
+0 60000	+0 697	+0.696	+0 001
+0 80000	+0.928	+0 928	+0 000
+1.00000	+1.160	+1 159	+0 000

LINEARITY = 0.11%

SENS = 0.386 mV/V/.001"

1 of 1

engineering

LINEAR VARIABLE DIFFERENTIAL TRANSFORMERS
TEST AND INSPECTION DATA

Type 3000 HR Serial No. 3023 Range ± 3.000"

PLEASE READ BEFORE USING THIS TRANSDUCER

This measurement device is manufactured to high precision standards. Our factory checks prior to shipment assure its performance. To obtain the optimum performance in your application, handle and install with care. Do not machine, grind or tap core and coil assembly. Core and coils are matched sets; for best performance do not interchange cores.

TEST CONDITIONS

Primary Connections	yel/black and yel/red ☒ grounded ☐ not grounded
Secondary Connections	black and red ☒ grounded ☐ not grounded
Secondary Midpoints	(a) green (b) blue ☒ (a) tied to (b) ☐ (a) not tied to (b)
Case Connections	☐ grounded ☒ not grounded
Primary Excitation	3 volts at 2500 Hz
Secondary Load	0.5 Meg ohms (in parallel with ___ mfd)

TEST DATA

Displacement	± 3.000 inches
Output	_____ volts _____ volts/input volts
Linearity	± _____ % of full range output
Null (Combined Quadrature and Harmonics)	_____ mv (rms)
Output-to-Input Phase Angle	_____ degrees ☐ leading (+) ☐ lagging (−)
Special Tests	_____ _____

INSPECTION

☒ Workmanship ☒ High Voltage Test
☒ Completeness of Assembly

REMARKS

ACCEPTANCE

Q.A. S.E. F 22

OCT 27 '86

Tested by ST 71 Date OCT 27 86
Inspected by _____ Date _____
Military Inspection (When Required) _____ Date _____

SCHAEVITZ engineering

10/24/86

MODEL HR 3000 S/N 3023
SCHAEVITZ PART NO 2560398-000

EXCITATION = 3.000 VAC @ 2500Hz

NULL = 3.4 mVrms

INCHES	AC VOLTS	CALC VOLTS	DEV's
-2.9998	-2.099	-2.100	+0 001
-2.4008	-1.682	-1.681	-0 001
-1.8003	-1.267	-1.262	-0 005
-1.2007	-0.842	-0.843	+0 001
-0 6006	-0.418	-0.424	+0 006
+0 5998	+0.418	+0.414	+0 --
+1.1993	+0.830	+0.834	-0 004
+1.7990	+1.250	+1.253	-0 003
+2.3988	+1.670	+1.672	-0 002
+2.9993	+2.094	+2.091	+0 003

LINEARITY = 0 14%

SENS = 0.233 mV/V/.001"

INSTALLATION INSTRUCTIONS & PARTS LIST

HYDRAULIC CYLINDERS

MODELS 4Z189A THRU 4Z196A, 4Z448A & 4Z449A

FORM
SS1539
07084

DAYTON ELECTRIC MANUFACTURING CO. CHICAGO 60648

0985/2527

READ INSTRUCTIONS CAREFULLY BEFORE ATTEMPTING TO INSTALL, OPERATE OR SERVICE DAYTON HYDRAULIC CYLINDERS. FAILURE TO COMPLY WITH INSTRUCTIONS COULD RESULT IN PERSONAL INJURY AND/OR PROPERTY DAMAGE!

RETAIN INSTRUCTIONS FOR FUTURE REFERENCE.

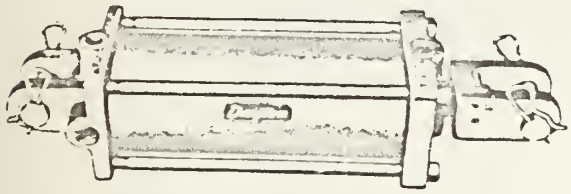

Figure 1

Description

These Dayton double-acting tie rod hydraulic cylinders are designed for heavy duty applications in agricultural, transportation, and construction equipment. The cylinders have a maximum operating pressure of 2500 PSI. Units have SAE O-ring ports to eliminate leakage. NPTF adapter fittings are included with cylinder.

Unpacking

Inspect contents for possible shipping damage. Make sure port plug (1), pins (2), SAE to NPTF adapters with O-ring (2) and clips (4) are included.

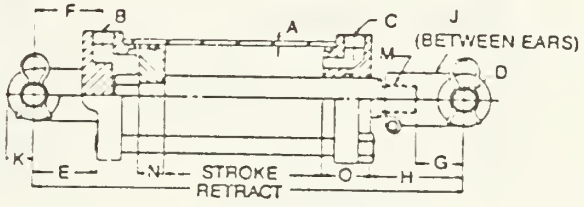

Figure 2 — Dimensions

Specifications

AREA & FORCE CHART FOR 2½ to 5" BORE CYLINDERS

BORE DIA	PUSH FORCES					PULL FORCES				
	EFFECTIVE AREA	FORCES IN LBS. @ PSI 1000	1500	2000	2500	EFFECTIVE AREA	FORCES IN LBS. @ PSI 1000	1500	2000	2500
2½"	4.91	4,910	7,365	9,820	12,275	3.68	3,680	5,520	7,360	9,200
3	7.07	7,070	10,605	14,140	17,675	5.84	5,840	8,765	11,680	14,600
3½	9.62	9,670	15,430	19,240	24,050	8.40	8,400	12,590	16,800	21,000
4	12.56	12,560	18,840	25,120	31,400	10.16	10,160	15,240	20,320	25,400
5	19.63	19,630	29,445	39,260	49,075	17.23	17,230	25,845	34,460	43,075

HYDRAULIC CYLINDERS DIMENSIONS

MODEL	BORE DIA.	STROKE LENGTH	RETRACT	ROD DIA.	A	B* + C*	D	E	F	G	H	J	X	M	N	O	SHPG. WT.
4Z189A†	2½"	18"	20¼"	1⅛"	1/8"	3/4"-16	1.015"	2 7/16"	2 3/8"	1 13/16"	5¼"	1.06"	15/16"	1⅛-12"	1"	2⅜"	23
4Z190A†	3	8	20¼	1⅛	3/16	3/4"-16	1.015	2 7/16	2 7/16	1 13/16	5¾	1.06	15/16	1⅛-12	1	1 13/16	26
4Z194A	3	16	31½	1⅜	3/16	3/4"-16	1.015	2 7/16	2 7/16	1 13/16	9	1.06	15/16	1⅛-12	1	1 13/16	39
4Z191A†	3½	8	20¼	1⅛	3/16	3/4"-16	1.015	2⅜	2 7/16	1 13/16	5¾	1.06	15/16	1⅛-12	1	1 13/16	31
4Z195A	3½	16	31½	1⅜	3/16	3/4"-16	1.015	2⅜	2 7/16	1 13/16	9	1.06	15/16	1⅛-12	1	1 13/16	43
4Z448A	3½	24	34¼	1⅜	3/16	3/4"-16	1.015	2⅜	2 7/16	1 13/16	3¾	1.06	15/16	1⅛-12	1	1 13/16	54
4Z192A	4	8	20¼	1½	3/16	3/4"-16	1.015	2 9/16	2 7/16	1⅞	5¼	1.06	1	1½-12	1	1 13/16	43
4Z196A	4	16	31½	1¾	3/16	3/4"-16	1.015	2 9/16	2 7/16	1⅞	8½	1.06	1	1½-12	1	1 13/16	61
4Z449A	4	24	34¼	1¾	3/16	3/4"-16	1.015	2 9/16	2 7/16	1⅞	3¼	1.06	1	1½-12	1	1 13/16	74
4Z193A	5	8	20¼	1¾	1/4	7/8"-14	1.265	2¾	2⅝	2⅛	4	1.06	1¼	1½-12	1	2½	64

(*) SAE O-ring ports
†Built in accordance to American Society of Agricultural Engineers specifications.

ORDER REPLACEMENT PARTS THROUGH DEALER FROM WHOM PRODUCT WAS PURCHASED

Please provide following information
- Model Number
- Serial Number (if any)
- Part Description and Number as shown in parts list.

If dealer cannot supply, order from:
Dayton Electric Mfg. Co.
Parts Department
5959 W. Howard St.
Chicago, Illinois 60648

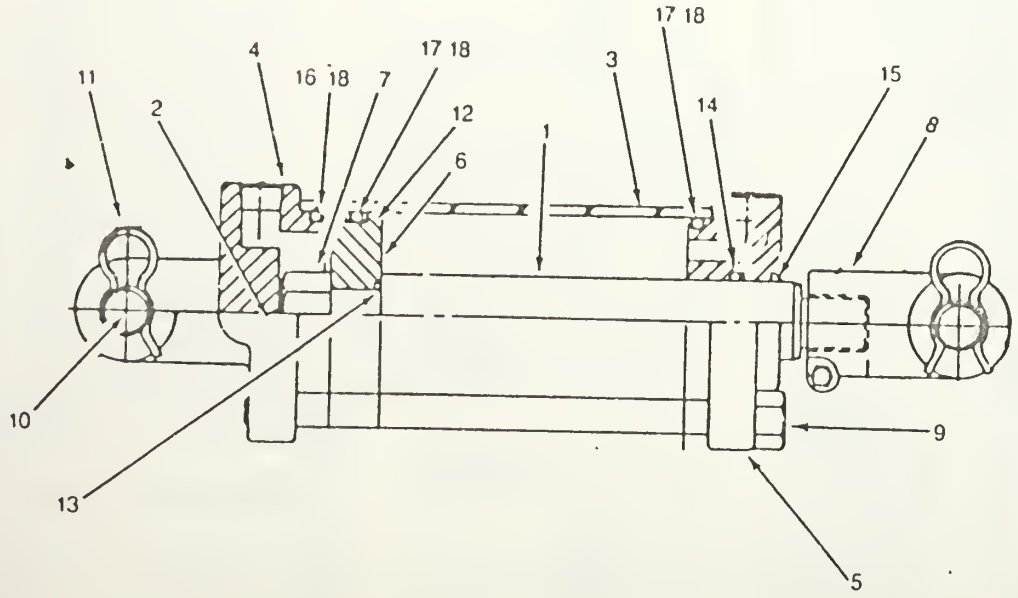

Figure 3 — Replacement Parts Illustration

LIMITED WARRANTY

Dayton hydraulic cylinders, Models 4Z1824 [illegible] 4Z449A, are warranted by Dayton Electric Mfg. [illegible] nal user against defects in workmanship or [illegible] (rental use excluded) for one year after date of purchase. [illegible] is determined to be defective in material or workmanship and returned to an authorized service location, as Dayton designates, shipping costs prepaid, will be repaired or replaced at Dayton's option. For warranty claim procedures, see "Prompt Disposition" below. This warranty gives purchasers specific legal rights, and purchasers may also have other rights which vary from state to state.

LIMITATION OF LIABILITY. To the extent allowable under applicable law, Dayton's liability for consequential and incidental damages is expressly disclaimed. Dayton's liability in all events is limited to, and shall not exceed, the purchase price paid.

WARRANTY DISCLAIMER. Dayton has made a diligent effort to illustrate and describe the products in this literature accurately; however, such illustrations and descriptions are for the sole purpose of identification, and do not express or imply a warranty that the products are merchantable, or fit for a particular purpose, or that the products will necessarily conform to the illustrations or descriptions.

Except as provided below, no warranty or affirmation of fact, expressed or implied, other than as stated in "LIMITED WARRANTY" above is made or authorized by Dayton, and Dayton's liability in all events is limited to the purchase price paid.

Certain aspects of disclaimers are not applicable to consumer products, e.g.: (a) some states do not allow the exclusion or limitation of incidental or consequential damages, so the above limitation or exclusion may not apply to you; (b) also, some states do not allow limitations on how long an implied warranty lasts, consequently the above limitation may not apply to you; and (c) by law, during the period of this Limited Warranty, any implied warranties of merchantability or fitness for a particular purpose applicable to consumer products purchased by consumers may not be excluded or otherwise disclaimed.

PROMPT DISPOSITION. Dayton will make a good faith effort to provide correction or other adjustment with respect to any product which proves to be defective within warranty. For any product believed to be defective within warranty, first write or call dealer from whom product was purchased. Dealer will give additional directions. If unable to resolve satisfactorily, write to Dayton at address below, giving dealer's name, address, date and number of dealer's invoice, and describing the nature of the defect. If product was damaged in transit to you, file claim with carrier.

PRODUCT SUITABILITY. Many states and localities have codes and regulations governing sales, construction, installation, and/or use of products for certain purposes, which may vary from those in neighboring areas. While Dayton attempts to assure that its products comply with such codes, it cannot guarantee compliance, and cannot be responsible for how the product is installed or used. Before [illegible] of a product, please review the product application and [illegible] cal codes and regulations, and be sure that the product information or use will comply with them.

DAYTON ELECTRIC MFG. CO., 5959 W. HOWARD ST., CHICAGO, ILLINOIS 60648

Replacement Parts List

REF. NO.	DESCRIPTION	PART NUMBERS FOR MODEL:									
		4Z189A	4Z190A	4Z191A	4Z192A	4Z193A	4Z194A	4Z195A	4Z196A	4Z448A	4Z449A
1	Piston rod	010500005	010500005	010500005	010800005	011000039	010700015	010700015	011000009	010700018	011000012
2	Pipe plug	200200021	200200021	200200021	200200021	200300028	200200021	200200021	200200021	200200021	200200021
3	Tube	051300014	051500007	051700009	051900008	052100010	051500007	051700013	051900012	051700016	051900015
4	Bolt	141300022	141500043	141700023	141900037	142100035	141500043	141700023	141900037	141700023	141900037
5	Gland	081300146	081500230	081700182	081900231	082100184	081500227	081700178	081900230	081700178	081900230
6	Piston	071300004	071500004	071700005	071900006	072100002	071500003	071700005	071900003	071700005	071900003
7	Locknut	220000208	220000208	220000208	220000210	220000212	220000208	220000208	220000212	220000208	220000212
8	Clevis	100000018	100000018	100000018	100000043	100000021	100000018	100000018	100000043	100000018	100000043
9	Tie-rod	170201121	170201121	170201121	170301133	170301135	170201201	170201201	170301213	170201281	170301293
10	Clevis pin	190400001	190400001	190400001	190400004	190600001	190400001	190400001	190400004	190400001	190400004
11 ▸	Hair-pin clip	190400002	190400002	190400002	190400002	190600003	190400002	190400002	190400002	190400002	190400002
12	B/U washer	▲	▲	▲	▲	▲	▲	▲	▲	▲	▲
13	O-ring	▲	▲	▲	▲	▲	▲	▲	▲	▲	▲
14	Polyurethane U-cup rod seal	▲	▲	▲	▲	▲	▲	▲	▲	▲	▲
15	Wiper	▲	▲	▲	▲	▲	▲	▲	▲	▲	▲
16	O-ring	▲	▲	▲	▲	▲	▲	▲	▲	▲	▲
17	O-ring	▲	▲	▲	▲	▲	▲	▲	▲		
18	Back-up washer	▲	▲	▲	▲	▲	▲	▲	▲	▲	▲
▲	Packing kit	PMCK-7000	PMCK-7100	PMCK-7200	PMCK-8600	PMCK-8200	PMCK-9200	PMCK-9300	PMCK 9400	PMCK-9300	PMCK 9400
△	Adaptor w/O-ring	200200093	200200093	200200093	200200093	200300112	200200093	200200093	200200093	200200093	200200093

△Not shown.

General Safety Information

1. Do not exceed 2500 PSI operating pressure.
2. Overpressure may cause sudden failure.
3. Make sure pressure has been relieved in hydraulic lines before installing cylinder.
4. Keep cylinder rod from contacting any object which may damage the rod.
5. Do not overtighten fittings. Apply only enough torque for proper sealing.
6. After installing clevis pins, make sure locking clips are secure.
7. Consult specifications and make sure the hydraulic cylinder size is appropriate to the application. Do not use an undersized cylinder.
8. Use petroleum based hydraulic oils only.

Assembly

The cylinder has two hydraulic line connections at the base end. Select the connection location that best fits the application and plug the other with the pipe plug supplied. Use supplied adaptors if connections are NPT fittings.

Installation

CAUTION: Use petroleum based hydraulic oils only.

1. Relieve all pressure in hydraulic lines before installing the cylinder.
2. Adjust rod length to fit the application and tighten the rod clevis lock bolt.
3. Select the hydraulic connection at the base of the cylinder that best fits the installation and plug the other with the pipe plug supplied.
4. Clevis should be unthreaded no further than to the point where rod threads are flush with the inside of the clevis throat.

Operation

1. Air must be removed from the cylinder to ensure smooth operation.
2. If there is air in the cylinders, loosen the hydraulic fittings slightly while operating the cylinder at a light load. When a steady stream of hydraulic oil is seen from the fitting, retighten the connection.
3. Do not operate cylinder at pressures higher than 2500 PSI.

Maintenance

To repair the cylinder, the following procedures should be followed:

1. Be sure you have the proper replacement packing kit.
2. Relieve all pressure and loads on the cylinder and remove from equipment. Plug all hydraulic connections.
3. Drain oil from cylinder.
4. Loosen and remove the four tie-rod bolts.
5. With a soft-head mallet tap off the gland and butt castings from the tube. Pull the piston rod assembly from the tube.
6. Clamp piston rod in vise with soft jaws and remove locknut. Pull gland off rod from piston and clean all parts.
7. Remove and replace all seals, making sure the two hardest large diameter O-rings are used on the gland and butt castings and the one softer O-ring is used on the piston.
8. Slide gland and piston on piston rod. Install locknut and tighten securely.
9. Slide tube over piston and tap gland into tube. Tap butt into other tube end and align so tie-rods can be installed.
10. Install tie-rods and wrench tighten evenly.

TORQUE REQUIREMENT CHART

2½-3½" BORE — 50±5 Ft. lbs.
4-5" BORE — 100±10 Ft. lbs.

11. Reinstall cylinder per installation instructions.

Trouble Shooting Chart

SYMPTOM	POSSIBLE CAUSE(S)	CORRECTIVE ACTION
Leakage around piston rod.	1. Rod seal worn out from extensive use. 2. Seal has been cut from knick in rod.	1. Repack cylinder. 2. Repack cylinder and replace damaged rod.
Cylinder will not hold up load.	1. Piston seal worn out from extensive use. 2. Seal has been cut from score on tube walls.	1. Repack cylinder. 2. Repack cylinder and replace scored tube. Check for contamination in hydraulic oil.

MAGNOLIA
PLASTICS, Inc.

TECHNICAL BULLETIN

5541 PEACHTREE INDUSTRIAL BOULEVARD AREA 404
CHAMBLEE, GEORGIA 30341 451-2777

MAGNOBOND 2014 &
MAGNOBOND 2014-1

DESCRIPTION

Magnobond 2014 and Magnobond 2014-1 are epoxy resins which find many areas of application in laminating, casting, and adhesives. For your convenience Magnolia has charted the most popular curing agents for use with these systems. Selection of a curing agent will depend on use, working time, and possible cure times.

Epoxy systems based on 2014 will be lower in viscosity than those systems based on 2014-1.

MIXING

Carefully select a curing agent for your needs because the hardener dictates the type and kind of cured epoxy system you will have. All mix ratios are by weight. Carefully weigh each component, A and B, and thoroughly mix for 3-5 minutes by hand or 2-3 minutes by power stirrer. Immediately after mixing you must be concerned with your working time. Check the chart to see how much time you have to use the mixed material. CAUTION: Working times given in the chart are based on 3 ounces of mixed material at 77°F. Epoxy systems are mass and temperature dependent. The higher the temperature, the shorter the working time and vice versa. Large volumes of material should not be mixed at one time due to the short working time and violent exotherm. Limitations for mixed material by volume are indexed in the chart.

COLORING

Epoxy systems cure compatible with most universal tints available at paint stores everywhere.

SURFACE PREPARATION

Epoxy systems are tenacious adhesives to all but a few surfaces. Best adhesion can be achieved through proper surface preparation and non-adhesion is possible through use of a release agent.

CURE

MAGNOBOND 2014 and MAGNOBOND 2014-1 will cure at room temperature with any of the hardeners in the chart. Cure may be accelerated by heat. Consult a Magnolia Technical Representative for technical assistance. The 2014 and 2014-1 systems will cure sufficiently for handling after an overnight cure at room temperature and achieve full strength after 3 days at 77°F.

(OVER)

CURING AGENTS FOR MAGNOLIA COMPOUNDS 2014 & 2014-1

	230	235	249-2	232-C	346
USES	Fast cure in thin sections	General Purpose Good Chemical Resistance Laminating	Adhesive Laminating	Bonding Low Viscosity	Bonding Casting Boat Repair Laminating
MIX RATIO pbw	100:25	100:25	100:35	100:50	2:1 by vol.* 1:1 by vol.
WORKING TIME 3-oz.@77°F	7 minutes	20-25 min.	28-38 min.	80-90 min.	4 hours
SET TIME 77°F	2-3 hours	3-6 hours	12 hours	24 hours	18 hours
THICKNESS LIMITATION	1/4 inch	1/4 inch	1/2 inch	1 inch	1 inch

*Use 2 to 1 for best water and high temperature resistance. Use 1 to 1 for added flexibility.

At all time wear protective gloves and clothing while using these epoxy systems and always use in a well ventilated room. Although these systems are relatively non-toxic, sensitivity to these thermosetting compounds varies from individual to individual.

DANGER	FIRST AID
May cause severe irritation. Do not get into eyes, on skin or clothing. Do not inhale vapors. Use with adequate ventilation. Wash thoroughly after handling. For Industrial Use Only. Keep container closed. Do not re-use this container.	Eyes - Immediately flush eyes with plenty of water for at least 15 minutes. Get medical attention. Skin - Wash immediately with soap and water. Clothing - Remove clothing and wash before re-use. Destroy shoes that cannot be decontaminated.

8/8/85

PRELIMINARY TECHNICAL DATA

PRODUCT TNX-250 Geogrid

POLYMER Polyester (Polyethylene Terephthalate)

COLOR Black

MECHANICAL PROPERTIES	Machine Direction	Cross Direction
Ultimate Wide Width Tensile Strength:	3000 lbs/ft	3000 lbs/ft
% Elongation At Break:	8%	8%
5% Secant Modulus:	54,000 lbs/ft	54,000 lbs/ft
2% Secant Modulus:	78,000 lbs/ft	78,000 lbs/ft

Creep: Polyester inherently exhibits superior resistance to creep than many other polymers.

Soil Pullout: Preliminary results indicate pullout resistance exceeds the shear strength of the soil.

ENVIRONMENTAL PROPERTIES

Chemically stable - Unaffected by naturally occurring soil conditions

Stabilized against U.V. degradation

Remains elastic with no brittleness to - 50°F

Biologically Inert

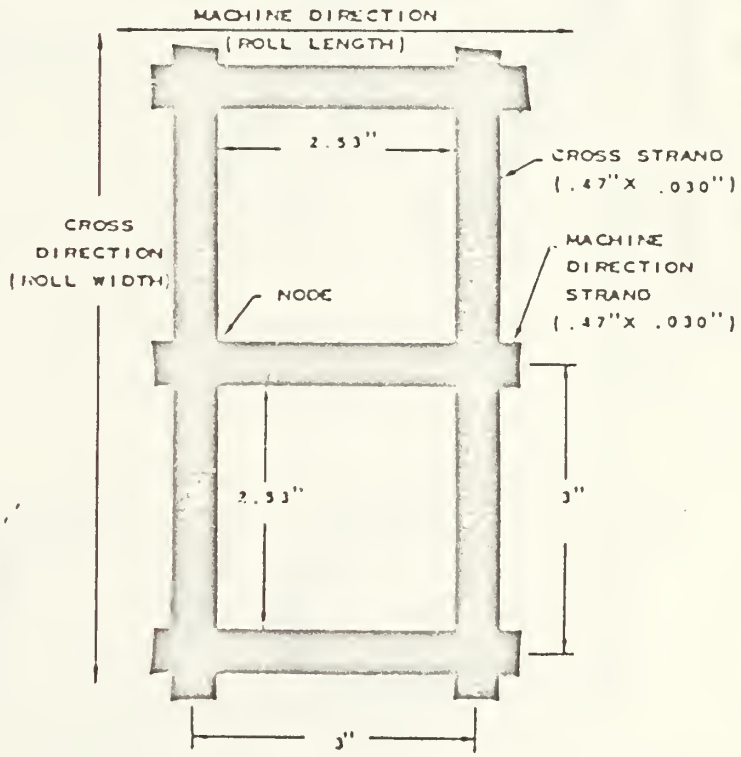

AVAILABLE ROLL SIZES

Width(s):	5.8 ft	11.8 ft
Length(s):	155 ft	155 ft
Weight:	81 lbs	162 lbs
Area:	100 yds^2	200 yds^2

te: Reported grid tensile strength and modulus based on test procedures which were in general cordance with proposed ASTM Committee D-35 method for Wide Width Strip Tensile Strength Test. mple size: 3 strands wide X 4" gauge length. Strain Rate - 10%/min.
e data presented is preliminary and subject to change without notification. Rev. 1/27/86

TYPICAL STRESS-STRAIN CURVE
SIGNODE TNX-250 GEOGRID

NOTE: WIDE WIDTH STRIP TENSILE STRENGTH TEST. STRAIN RATE - 10%/MIN

1/27/86

END

2-87

DTIC

DEFENSE TECHNICAL INFORMATION CENTER

DTIC
Acquiring Information -
Imparting Knowledge

DEFENSE LOGISTICS AGENCY
Cameron Station
Alexandria, Virginia 22304-6145

Thesis
N4637 Newman
c.1 Pullout and creep of geosynthetics in a soil matrix.